CORTICAL STATE DYNAMICS DURING SENSORY DECISION-MAKING

Elina Alexandra Katariina Jacobs

A thesis presented for the degree of
Doctor of Philosophy

UCL
Institute of Neurology

Supervisors:
Profs Kenneth D Harris & Matteo Carandini

September 2018

I, Elina Alexandra Katariina Jacobs, confirm that the work presented in this thesis is my own. Where information has been derived from other sources, I confirm that this has been indicated in the thesis.

Acknowledgments

First and foremost, thank you to my supervisors, Kenneth Harris and Matteo Carandini, for creating not just an incredibly stimulating scientific environment, but equally a fun and safe environment that made coming to the lab an enjoyable experience no matter what. Sometimes life throws the craziest curve balls at the most unexpected times, and I have no words for how grateful I am that I had a supportive environment to come to that allowed me to keep doing what I love.

Thank you especially to Kenneth, my primary supervisor, for the lessons and his advice, from how to think about data analysis and ask the right questions to obtain meaningful answers, to how to survive in academia. Equally, thank you to Matteo for teaching me to always think about the big picture, and for instilling in me the importance of clear presentation; both written and verbal.

Thank you to Jennifer Linden, who welcomed me to her lab meetings and who became an unofficial additional advisor to me throughout my PhD, and thank you to Sarah-Jayne Blakemore, who continued to be available as a mentor even after my rotation year had ended.

Thank you to Aman Saleem, who was there in the early days of my PhD and offered his guidance and advice when I was trying to find my way into a new field.

A big thank you to Michael 'Mush' Okun, who volunteered to advise me on my experiments and data analysis, and who taught me many of my quantitative skills.

Thank you to Nick Steinmetz, whom I can only describe as a force of nature, for all his help and advice, from deciding on experimental parameters to data analysis to how to cope with PhD stress.

Thank you to Chris Burgess, who patiently helped a novice learn how to code, for providing the groundwork for the behavioural tasks I developed, and for many lively discussions about science.

Thank you to Charu Reddy for being an incredibly capable lab manager and for not just keeping the lab organised, but also such a social and fun place to be. Thank you to Andy Peters and Pip Coen for helping out with experiments and troubleshooting, and to Miles Wells and Laura Funnell who

helped with a lot of training.

A big thank you to all the lab members for not just being colleagues but travel buddies and friends, for all the fun times not just in the lab, but for all the trips we have taken together - to conferences, to the windy beaches of England, to Iceland, the Isle of Skye, Romania, and India.

Thank you to my family for always believing in me, and a big thank you to my friends, particularly Eva Merina and Noelia, without whom I wouldn't have kept my sanity through all these years, and my flatmate Misun; I am fortunate to have lived with such a kind and smart fellow PhD student.

Thank you to the Wellcome Trust, who provided the funding and made this work possible.

Lastly, thank you to all the Latin dancers; the Bachateros and Bachateras, the Salseros and Salseras, and all the other countless dancers in London. You don't know how much your energy and relentless joy of life has meant to me, and how much you have helped me stay sane and grounded when times were stressful.

Mirun muistolle,

äidille,

ja perheelleni.

Abstract

Cortical states, defined as the dynamics of cortical neural activity on the timescale of seconds or more, vary during different behavioural states. Originally associated mainly with the sleep-wake cycle, it is now recognised that cortical states present subtle changes during waking that reflect the cognitive and behavioural demands an individual is pursuing. Therefore, it has been suggested that attention leads to a desynchronised cortical state, characterised by the absence of low frequency oscillations, which is thought to improve the information processing of the object of interest and thereby improve performance in attention demanding tasks. To maximise the beneficial effects of desynchronisation, it has been proposed that this state should occur locally, as this may spot-light the attended feature.

I investigated this hypothesis by asking whether attending to a specific sensory modality leads to local desynchronisation of the sensory cortex of the modality being used. I trained mice to perform visual and auditory decision making tasks, and assessed cortical state through spectral analysis of widefield calcium signals. Genetically encoded calcium indicators were expressed in cortical excitatory neurons, and their activity was imaged simultaneously across cortex while the animals were performing the different tasks.

Cortical states correlated with task engagement rather than with task performance, and this effect was global. Unexpectedly, the biggest desynchronisation was seen in somatosensory cortex in all tasks, and there was a long lasting effect of reward. These effects could not be explained by movement or pupil diameter, a commonly used measure of arousal. Furthermore, desynchronisation correlated with reaction time.

Thus, variations in cortical state closely relate to changes in task engagement, demands and outcome. This suggests that desynchronization is not a causal effect of attention that improves performance, but instead may be a cognitive state related to preparing rapid and coordinated responses to sensory stimuli.

Impact Statement

The work presented in this thesis has contributed to two publications, Burgess et al. (2017) and Steinmetz et al. (2017), and will also contribute to a first author publication of my own. In addition, this work was selected for short talks at two conferences, in April 2016 at the FENS Brain Conference "The Brain in Focus" and in November 2016 at the "Visual Cognition - Decision Making" nanosymposium at the Society for Neuroscience Annual Meeting. This work was also selected for the Society for Neuroscience 2016 'Hot Topics' booklet, which is distributed to the media. Lastly, this work has been presented as posters at the Okinawa Institute of Science and Technology Computational Neuroscience Summer School in 2016, and at the UCL Neuroscience Symposium 2017.

The method I employed for investigating cortical states is novel and therefore comprises a methodological innovation that can be used in future research. The auditory task I developed is also unique and novel and may be adapted by future work wishing to employ auditory decision making tasks that use tonal discrimination.

The findings from this work challenge the currently prevailing hypothesis in systems neuroscience that desynchronisation is related to performance accuracy. As this is a controversial result, it is likely to fuel further discussion and research into the question, which will lead to furthering our understanding of cortical states and how the brain processes sensory information and produces coordinated behavioural responses.

Finally, insights into cortical states and their role in sensory processing represent an important part of our understanding of neural physiology. In the long term, this will be of medical benefit as neurological disorders such as autism and schizophrenia for instance are known to be affected at early sensory processing stages. Knowledge of how a healthy brain functions will be key to deciphering what goes wrong during disease and for developing therapeutic strategies. Additionally, understanding of cortical states may help in the development of brain-machine interfaces: a machine capable of detecting subtle fluctuations in cortical states may for example be used for various applications; from controlling robots, prosthetic limbs, virtual environments to controlling the administration of drugs that enhance cognition.

Table of contents

List of Abbreviations

2AFC	Two alternative forced choice
2AUC	Two alternative unforced choice
A	Anterior
ACh	Achetylcholine
AP	Action Potential
au	arbitrary unit
AUD	Auditory Cortex
BRF	Brainstem Reticular Formation
CaM	Calmodulin (calcium modulated protein)
DA	Dopamine
EEG	Electroencephalogram
FS	Fast Spiking (neuron)
G6f	GCaMP6 fast
G6s	GCaMP6 slow
GCaMP6f	GCaMP6 fast
GCaMP6s	GCaMP6 slow
GECI	Genetically Encoded Calcium Indicator

GFP	Green Fluorescent Protein
GLM	Generalised Linear Model
ie	id est (Latin for "in other words")
ITI	Inter Trial Interval
LFP	Local Field Potential
LGN	Lateral Geniculate Nucleus
M	Medial
MO	Motor Cortex
NaN	Not a Number (Matlab abbreviation)
NE	Norepinephrine; Noradrenaline
PSI	Population Synchrony Index
QP	Quiescent Period
REM	Rapid Eye Movement (sleep)
RF	Receptive Field
ROI	Region Of Interest
RT	Reaction Time
RS	Regular Spiking (neuron)
RSP	Retrosplenial Cortex
SEM	Standard Error of the Mean
SR	Stimulus Response
SS	Somatosensory Cortex
SVD	Singular Value Decomposition
SWS	Slow Wave Sleep

TO	Time-out
TRN	Thalamic Reticular Nucleus
V1	Primary Visual Cortex
V4	Visual area V4 (in extrastriate cortex)
VIS	Visual Cortex
Vm	Membrane potential
VSD	Voltage Sensitive Dye
WN	White noise

Chapter 1

Introduction

Overview

I will begin by providing a brief overview of the historical landmark studies that set the stage for modern investigations in the field of cortical states. I will go through the regulatory mechanisms of cortical states, and then proceed to discussing recent work investigating the function of cortical states during waking, specifically during behavioural and attentional tasks.
In addition, I will introduce widefield imaging and why this was the method of choice in this work. I will finish with stating the specific hypothesis and aims addressed in this thesis.

1.1 Cortical states

Historical background

In humans, cortical states were first observed by Berger in 1929 when in a landmark study, he introduced a method sensitive enough for picking up the electrical activity of the brain through the skull: the electroencephalogram (EEG). Up until then, the electrical activity generated by the cortex had been surgically measured in other species such as cats, dogs, rabbits and monkeys, and Berger and others had also recorded human brain activity in patients who had undergone brain surgery (Berger, 1929). But it was the demonstration that the activity from a healthy, intact brain could be surveyed via electrodes placed on the scalp that paved the way for research on cortical states.

Consequently, cortical states were first mostly studied as patterns of EEG activity. It was quickly noted that the biggest differences in activity occur between equally different behavioural states: waking and sleeping. Sleep states are characterised by high amplitude low frequency oscillations that disappear upon waking, and become particularly prominent during deeper sleep stages (Davis et al., 1937; Blake, 1937). In contrast, waking and REM (rapid eye movement) sleep, which is why it is also sometimes called paradoxical sleep, are characterised by higher frequency oscillations. Furthermore, anesthesia induces similar low frequency oscillations as deep sleep. Since both sleep and anesthesia are associated with behavioural inactivity and a loss of consciousness, the cortical state during waking became termed the active or activated state, and the view that cortical states are primarily

a function of the sleep cycle became dominant (Vanderwolf, 2003; Harris, 2005).

This idea was further fortified by a landmark study by Moruzzi and Magoun (1949), who discovered the reticular activating system. Using the "encéphale isolé" preparation, where the brainstem is cut at the level of the medulla, they showed that stimulation of the reticular formation leads to a transition from the sleep associated state of high-amplitude slow wave activity to the activated state associated with waking, despite the subjects being anesthetised. They further showed that this effect was mediated by ascending projections towards cortex, which is how the term reticular ascending/activating system was coined.

Subsequent research invested much effort into establishing the anatomical substrates of this system, and has demonstrated the existence of several distinct nuclei within the reticular system that play key roles in controlling cortical states. This identified two main pathways to the cortex: one via projections to the thalamus, which in turn widely projects to the cortex and exerts an effect on cortical state, and another via projections to neuromodulatory systems which provide widespread innervation of the cortex (Starzl et al., 1951). The following section will elaborate further on these two systems.

1.1.1 Regulatory mechanisms

Neuromodulatory control

Several nuclei of the reticular formation, including the deep mesencephalic nucleus and the nucleus pontis oralis which are situated in the core of the brainstem, as well as the parabrachial and periaqueductal gray nuclei in the upper brainstem, project to the basal forebrain, which in turn sends cholinergic projections across the cortex. Stimulation of the basal forebrain as well as its cholinergic axons leads to widespread cortical activation (Goard and Dan, 2009; Pinto et al., 2013; Eggermann et al., 2014), as does systemic administration of cholinergic agonists, while cholinergic antagonists abolish cortical activation (Vanderwolf, 2003). These experiments clearly implicated acetylcholine (ACh) as a key regulator of cortical states, which can be modulated by reticular nuclei.

In addition, many nuclei of the reticular formation send direct neuromodulatory projections to the cortex. The locus coeruleus for example sends noradrenergic projections across the cortical mantle (Chandler et al., 2014), and electrical stimulation as well as optogenetic activation of the noradrenergic cells in locus coeruleus also lead to widespread cortical activation (Carter et al., 2010). This nucleus also receives input from other reticular nuclei, for example the nucleus paragigantocellularis. Similarly, the rostral raphe complex sends serotonergic projections to the cortex, which also modulate cortical state (Parvizi and Damasio, 2001; Vanderwolf, 2003). On top of sending direct projections to the cortex, many of these nuclei also project to the basal forebrain and can thus exert additional indirect effects on cortical state.

Furthermore, dopamine has also been implicated in the modulation of cortical states. The ventral tegmental area and substantia nigra send dopaminergic projections to the thalamus and basal forebrein (Smiley et al., 1999), and although there are also dopaminergic projections to the cortex, these have been shown to modulate rather than induce cortical activation (Vanderwolf, 2003).

Thalamic control of cortical activation

The "classical reticular nuclei" of the reticular formation, which includes the cuneiform nucleus, the deep mesencephalic nucleus, and the pedunculopontine tegmental nucleus, send glutamatergic projections to the intralaminar nuclei of the thalamus as well as the basal ganglia (Hallanger et al., 1987; Pare et al., 1988; Parent et al., 1988). In fact, it was originally thought that the effects of stimulating or lesioning of the reticular formation were mediated by thalamocortical projections from the thalamic intralaminar nuclei (Parvizi and Damasio, 2001). In addition, several neuromodulatory systems also project to the thalamus: there are cholinergic projections from the laterodorsal tegmental nucleus which also project to the reticular thalamic nucleus, noradrenergic projections from the locus coeruleus, serotonergic input from the raphe nuclei, and histamine projections from the hypothalamus (McCormick and Bal, 1997).

The thalamus has long been considered the main relay station to the cortex, primarily transmitting sensory information (Sherman and Guillery, 1996). During sleep and anesthetized states, the thalamus functionally disconnects from the cortex, and enters a bursting firing pattern, which is incompatible with sensory information processing, and thus the cortex is

'cut off' from sensory input (Steriade, 2000). Upon waking, thalamic neurons enter a tonic firing mode, which can also be induced by application of neuromodulators and activation of the reticular ascending system. This activation of the thalamus renders it capable of sensory information processing and transfer again, and drives the cortical state transition from inactivated to activated (Steriade, 2000; Hirata and Castro-Alamancos, 2010).

The global nature of cortical states

It is thus clear that cortical state is under control of a complex interplay of different systems. Many of the nuclei within the reticular formation are not just interconnected, but project to other brain regions that exert global effects, and in some cases several of them. Thus, by stimulating or inhibiting one of them, it is likely that one affects several systems simultaneously, which makes it difficult to discern the exact function of each. For a long time, there was a debate whether cortical states were under thalamic (Steriade, 2000) or neuromodulatory Vanderwolf (2003) control; however it is likely that both make distinct but equally important contributions that may differ in functional ways that have yet to be understood.

The feature in common between these systems is that they have broad influences over cortical activity, which led to the idea that cortical states were inevitably global, which also fit with the observation that transitions between behavioural states such as sleep and waking tended to be abrupt.

Given the marked differences in oscillatory patterns between the different states, it was clear that there would be corresponding differences in local cortical processing features. These will be the subject of the next section.

Physiological basis

The activity picked up by an EEG constitutes a composite of the neural activity of the underlying cortical tissue. As technology advanced, it became possible to record the activity of populations as well as individual cortical neurons and to investigate how their firing patterns related to the observed oscillatory patterns.

This lead to the observation that during the slow, high amplitude oscillations of sleep states, nearby neuronal populations fire with increased temporal synchrony (Steriade et al., 1993). This temporal synchrony disappears as the slow oscillations decrease in amplitude and are replaced by higher frequency oscillations during waking. Therefore, the state associated with sleep and slow high amplitude oscillations became termed a "synchronised cortical state", while the state associated with waking and higher frequency oscillations became termed a "desynchronised cortical state" (Harris and Thiele, 2011).

The oscillatory patterns obtained through EEG can also be observed in the local field potential (LFP) of electrophysiological recordings. The LFP is produced by the transmembrane currents of the surrounding neurons and glial cells and depends on the spatiotemporal profile of their activity (Taub et al., 2013). Thus, the LFP provides a more local signal than the superficial EEG measurements. As tools became available that allowed the measurements of cellular membrane potentials (Vm) in-vivo, it became apparent that these oscillatory patterns are also a signature of the Vm and reflect the synaptic barrage onto the neuron (Haider and McCormick, 2009). During the synchronised state, the membrane potential of a neuron oscillates be-

tween a hyperpolarised state, when it receives little synaptic input, and a depolarised state when it receives increased and highly correlated synaptic input. These states are also called "down" and "up" phases, respectively (Figure 1.1, Harris and Thiele 2011). In contrast, during the desynchronised state, the membrane potential remains at a steady depolarised state and receives more continuous, uncorrelated synaptic input.

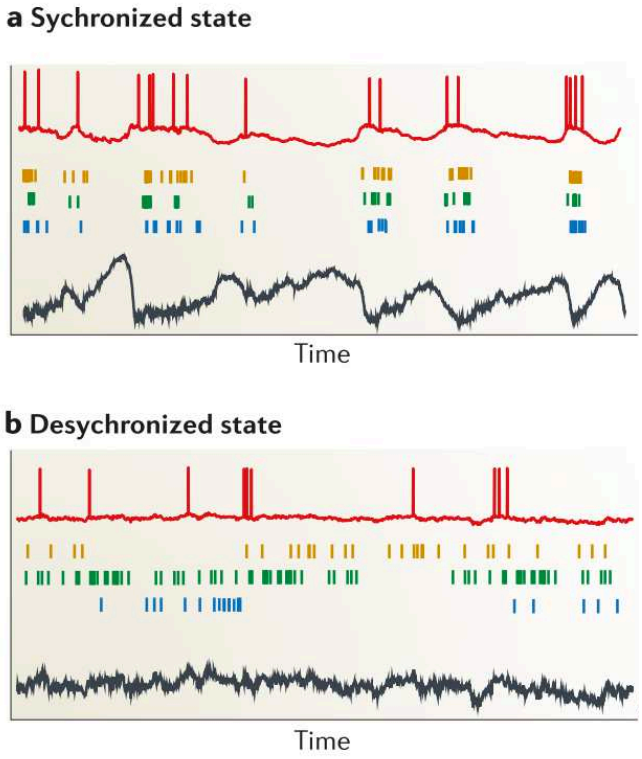

Figure 1.1: Distinct population activity patterns in different cortical states.
a) In synchronised states, cortical populations show synchronous fluctuations in firing rate. During the up phase, neurons show increased firing, during the down phase spiking is reduced or absent. The red trace shows the corresponding depolarisation and hyperpolarisation of the membrane potential in an intracellular recording. The black trace represents the local field potential (LFP), which shows the low frequency oscillation. b) In a desynchronised state, coordinated slow fluctuations in population activity are absent, and low frequency fluctuations in the LFP and membrane potentials are suppressed.
Reproduced from Harris and Thiele (2011).

1.1.2 Behavioural modulation

Although Berger himself already noted in his original report of his EEG findings in humans that mental effort had an effect on the oscillatory patterns he was recording (Berger, 1929), investigations into the relationship between behavioural and cortical states during waking have only recently begun to be undertaken. Notably, it has been observed that during quiet wakefulness, when the individual is awake but not engaged in a physical or mental activity, some low frequency (<10Hz) oscillations remain. It is therefore increasingly recognised that the awake state is not a single homogeneous state but that within the activated state, different degrees of synchronisation and desynchronisation are possible which likely constitute different substates (Figure 1.2, Zagha and McCormick 2014).

Movement related cortical state changes

One of the most easily distinguishable behavioural states is movement, for example running or whisking, which reliably desynchronises the cortex (Crochet and Petersen, 2006; Poulet and Petersen, 2008; Zagha et al., 2013; Bennett et al., 2013; Reimer et al., 2014; Vinck et al., 2015; Scholvinck et al., 2015; Zhou et al., 2014; McGinley et al., 2015). In visual cortex, running is associated with increased evoked responses and decreased interneuronal correlations (Niell and Stryker, 2010; Keller et al., 2012; Ayaz et al., 2013; Erisken et al., 2014; Dipoppa et al., 2018), while in auditory cortex running suppresses evoked responses (Zhou et al., 2014; Schneider et al., 2014). In somatosensory cortex, whisking onset is associated with a switch from a synchronised to more desynchronised state (Poulet et al., 2012), which

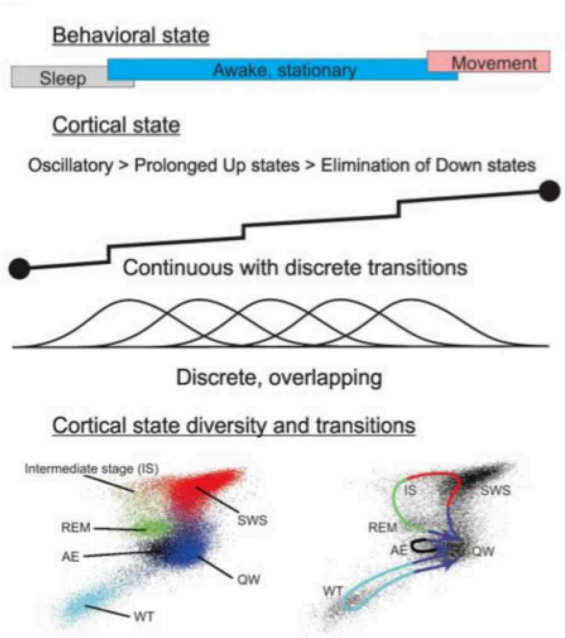

Figure 1.2: Cortical states during different behavioural states.
Abbreviations: AE: active exploration; IS: intermediate stage; REM: rapid eye movement sleep; SWS: slow wave sleep; QW: quiet wake; WT: whisker twitching. Reproduced from Zagha and McCormick (2014).

increases the signal to noise ratio in neural responses. In addition, such a transition does not dependent on sensory feedback, as deaffarentation of the sensory nerves did not abolish the desynchronisation, suggesting that the state switch was internally generated (Poulet and Petersen, 2008). Interestingly, there is a further difference between free whisking and active touch (whisking without and with touching another object, respectively): responses are largest during active touch (Crochet et al., 2011). Finally, in somatosensory cortex at least, these transitions require thalamic input, as pharmacological inactivation of thalamus abolishes normal desynchronisation characterised by depolarised membrane potentials, but instead leads to a desynchronised-like hyperpolarised state (Poulet et al., 2012).

Large observable movements such as running or whisking are not the only

conditions for state transitions, as desynchronised states can occur in their absence as well. Interestingly, state transitions correlate with pupil diameter, whether or not they are accompanied by movement (Reimer et al., 2014; Vinck et al., 2015; McGinley et al., 2015). Reimer et al. (2016) showed that pupil dynamics are closely related to the neuromodulatory activity of acetylcholine (ACh) and noradrenaline (NA) in cortex. Therefore, pupil diamater is frequently used as an indicator of behavioural arousal and a non-invasive measure of brain state, and it has been shown that periods of increased arousal in the absence of movement equally affect cortical processing and stimulus evoked responses (Vinck et al., 2015; Reimer et al., 2014; McGinley et al., 2015).

Attention

Attention is another classical cognitive state that can occur in the absence of overt behaviours such as movement.

Spatial attention

Attention has been studied extensively in the visual system using spatial attention. The studies typically require monkeys to fixate on a central cross whilst two or more visual stimuli are presented, and a cue indicates a spatial location in which a change in stimulus is likely to occur. If a change happens, the monkeys are trained to report this either by making a saccade or pressing a lever or button. The cue reliably leads to attention to the cued spatial location as monkeys are significantly more likely to detect a change in the cued versus uncued locations. Spatial attention is associated with several changes in cortical processing, including increased firing rates, decreased

variability and inter-neuronal correlations, and increased gamma (40-100Hz) synchrony between neurons selective for the same attended feature (Moran, 1985; Spitzer et al., 1988; McAdams and Maunsell, 1999, 2000; Cohen and Maunsell, 2009; Mitchell et al., 2009; Engel et al., 2016; Beaman et al., 2017; Fries et al., 2001, 2002; Bosman et al., 2012). It is thought that these changes in neural processing underlie the improvements in performance associated with increased attention. Interestingly, mental effort has equally been shown to correlate with pupil size (Kahneman and Beatty, 1966; de Gee et al., 2014, 2017).

Attending rhythmic stimuli

In contrast to these results from spatial attention, it has been shown when stimuli are rhythmic, low frequency oscillations can become more pronounced (Schroeder and Lakatos, 2009). Specifically, oscillations become entrained to match the rhythm of the presented stimuli so that stimulus onset coincides with the most excitable phase of the oscillation: when neurons are more depolarised and therefore more likely to fire in response, which in turn is thought to maximise the stimulus response. This has been shown in auditory cortex, when monkeys were trained to attend to one of two different tone trains that were presented simultaneously but consisted of different tonal frequencies and were offset from each other: the attended but not the ignored stream reset the phase of the oscillation (Lakatos et al., 2013). Similarly, when visual and auditory stimuli were presented concurrently but with offset phases, the attended modality determined the phase of the oscillation, in both visual and auditory cortex (Lakatos et al., 2008, 2009; O'Connell et al., 2014). Moreover, these studies suggest that the low-excitability phase of the

oscillation coincides with the unattended stimulus, which can have a suppressive effect. In auditory cortex, this can also occur in the areas that are outside the tonotopic area that matches the presented stimulus (O'Connell et al., 2015). Altogether, these studies suggest that attention can utilize low frequency oscillations, and thus increase synchronisation, to maximise the responses to attended stimuli and suppress responses to irrelevant stimuli. However, this requires stimuli to be rhythmic, as else the oscillatory entrainment may lead to the low excitability phase to coincide with the stimulus. It has therefore been suggested that low frequency entrainment only occurs when stimuli are predictable, and when stimuli are unpredictable, low frequency oscillations are abolished to maintain the cortex in a more constant state of high-excitability: the desynchronised state (Schroeder and Lakatos, 2009; Lakatos et al., 2016). It is this latter scenario that this thesis aims to investigate.

Behavioural relevance

Given all these behavioural modulations on cortical states and sensory responses, this raises the question whether these manifestations are also causally involved. If desynchronisation improves information processing, then this should manifest in improved task performance. Few studies have directly assessed this so far. The majority of spatial attention studies for example have investigated the associated changes in neural properties in great detail, but have not compared them with performance on a trial by trial basis. Recently, Engel et al. (2016) and Beaman et al. (2017) showed that local desynchronisation was associated with increased task performance in change detection tasks. Pinto et al. (2013) showed that increasing desyn-

chronisation by optogenetic stimulation of basal forebrain projections in V1 improved performance in a visual discrimination task on a trial by trial basis, and McGinley et al. (2015) found a strong correlation between performance in an auditory discrimination task and cortical state. In somatosensory cortex in contrast, Sachidhanandam et al. (2013) showed that both synchronised and desynchronised states were compatible with good performance in a whisker deflection detection task. Outside sensory cortices, Vyazovskiy et al. (2011) found that local bursts of synchronised activity in frontal cortex negatively affected performance in a sugar-pellet reaching task.

Altogether, there is some evidence to suggest that desynchronisation is associated with improved performance, but the precise nature of this relationship remains unclear.

Local modulation

It is clear now that cortical states are not just a function of the sleep-wake cycle, but that changes can occur during different behavioural states during wakefulness as well. Similarly, it was thought initially that cortical states were always global, but given that we now know that behavioural demands can shape cortical states, it is possible that the assumption about the global nature of cortical processing is equally mistaken. Despite the global projections of most neuromodulatory systems, it has been shown that there are afferents targeting specific cortical regions for example (Zaborszky et al., 2015; Chandler et al., 2014).

The studies by Vyazovskiy et al. (2011); Engel et al. (2016); Beaman et al. (2017) provide some initial evidence that cortical states can indeed occur locally. Given the important role of thalamic input in cortical desyn-

chronisation, differences in thalamic drive to different cortical areas provide one possible mechanism for local cortical differences (Sherman and Guillery, 1996). Two recent studies investigating cross-modal attention showed that switching attention between visual and auditory stimuli is associated with differences in firing rates in the corresponding sensory thalamic nuclei, and that this modulation is required for successfully switching attention (Ahrens et al., 2015; Wimmer et al., 2015). Both studies implicated the thalamic reticular nucleus (TRN) in this modulation, but the effects on cortical state remain unknown.

1.2 Widefield imaging

In this last section, I will introduce the method of choice in my experiments, and explain why it is suitable for investigations of cortical state. I will begin with providing a brief overview of voltage sensitive dyes, as this was the first widefield method that provided some insights into cortical state dynamics and laid the foundation for the future work using calcium indicators.

Voltage sensitive dyes

The pioneering method for widefield imaging of in-vivo neural activity was the use of voltage sensitive dyes (VSD). VSDs intercalate into the cell membranes of neurons and act as molecular transducers: they increase or decrease their fluorescence with changes in membrane potential (Shoham et al., 1999). Typically, the dye consists of a conjugated molecule with a dipole that consists of a hydrophobic tail at one end and a fixed charge at the other hydrophilic end. The hydrophilic dye permits intercalation into the cell membrane, while the fixed charge prevents the dye from crossing the membrane (Grinvald et al., 1999). Importantly, the dipole renders the dye sensitive to changes in electric field across the neuronal membrane. The resulting changes in optical signal are linearly correlated with the membrane potential changes and occur within microseconds. This method thus provides submillisecond temporal resolution, and a spatial resolution of up to 50-100 microns.

In preparations with single cell resolution, the optical signal from VSDs matches the signal obtained by intracellular electrical recording (Grinvald et al., 1999). In recordings from in-vivo cortical tissue however, single cell

activity is not resolved and a pixel contains the blurred signal of several neural components, including dendritic signals, axons and cell somas (Grinvald and Hildesheim, 2004). More precisely, the signal represents the sum of membrane potential changes in both pre- and postsynaptic neurons as well as potential contamination from surrounding glial cells. Given a resolution of 50 microns for example, the VSD signal contains the activity contribution from 250-500 neurons and their processes. As dendritic processes extend over a much larger area than cell somas, the VSD signal in cortical tissue represents dendritic activity more than spiking. Therefore, this method allows the detection of slow subthreshold synaptic potentials that cannot be detected using methods that primarily measure spiking activity, such as multi-unit electrophysiology.

Finally, the VSD signal primarily reflects activity in superficial layers. The dye can penetrate up to a depth of 1.5mm, however the upper cortical layers are stained more thoroughly than the lower ones (Grinvald et al., 1999). In practice, a given pixel contains neural signals from the upper 400-800 microns. Nevertheless, this does not mean that the activity originates predominantly from layer I, as apical dendrites from deeper layers reach the upper layers and therefore also contribute to the signal. However, the exact contribution of different cortical layers remains unknown.

Applications

In the following paragraphs, I will go through selected example studies to illustrate how VSD widefield imaging has provided insights into cortical states.

One of the first examples of how VSD imaging could be applied to study-

ing cortical dynamics was by Arieli et al. (1996). They investigated the dynamics of ongoing activity during spontaneous and stimulus evoked conditions in anaesthetised cat visual cortex. The dynamics of ongoing activity are strongly influenced by cortical state, and Arieli et al. (1996) showed that the trial to trial variability in response to visual stimuli could be attributed to the ongoing activity, in other words: the cortical state preceding the stimulus presentation. This was one of the first demonstrations that cortical state also affects the spatial response pattern in cortex. Indeed, the spatiotemporal visual response in a given trial could be predicted through an additive effect of the ongoing activity on the average stimulus evoked activity.

Similar observations have been made in somatosensory cortex. By combining VSD imaging with simultaneous whole-cell recordings in rodents, Petersen et al. (2003a,b) showed that the local VSD signal closely followed the membrane potential fluctuations in layer 2/3 pyramidal cells. They then used the combination of methods to investigate how cortical state affects stimulus responses at the level of single cells (by whole-cell electrophysiological recordings) and population activity (by VSD imaging). This revealed that whisker deflections evoked smaller responses during up phases, when the membrane potentials were more depolarised and closer to threshold, than during the hyperpolarised down phases. Specifically, they showed that the responses not only differed in terms of amplitude, but also in terms of spatial spread: during up phases, the responses were locally confined, whereas during down phases, the sensory responses spread as waves to adjacent cortical columns. This revealed how local cortical state related to the surrounding cortical activity in a way that electrophysiology had not been able to reveal.

More recently, Mohajerani et al. (2010, 2013) have explored the spatiotemporal dynamics of travelling waves across large areas of cortex. Traveling waves are readily observed with widefield imaging; in the case of VSD the peak of the wave corresponds to a traveling font of depolarisation (Benucci et al., 2007), and it has been proposed that this corresponds to the up phase in the synchronised state. The authors showed that fluctuations in spontaneous activity were mirrored and synchronous in both hemispheres, and that slow traveling waves occurred across large regions of cortical space. In addition, evoked depolarisations using visual, auditory, whisker and tactile stimuli, produced traveling waves that followed stereotyped trajectories, starting in their respective sensory cortical area, but interestingly all ending in a common sink. This provided insights into how cortical states spread across cortex, and how different stimuli interact with and influence the spatiotemporal spread of cortical activity.

These examples show that widefield imaging enables the observation of state dependent spatial dynamics of cortical activity that was previously not possible. However, the VSD method still posed several caveats: firstly, the application of the dye requires an acute preparation, which limits the time during which data can be obtained to hours after the application and make investigations during wakefulness very limited. Secondly, VSDs have a much weaker signal than another type of fluorescent indicators: calcium indicators. Since neuronal firing is associated with increases in intracellular calcium, fluorescent indicators that change their level of fluorescence depending on the intracellular calcium concentration can provide an indirect readout of neuronal activity. The recent advent of genetically encoded calcium indicators (GECIs) has overcome both of these limitations of VSD. Nowadays, there

are GECIs whose signals are strong enough to be imaged through an intact skull and still retain a high signal to noise ratio. The following section will elaborate further on the generation and utility of these indicators.

1.2.1 Genetically encoded calcium indicators

Nowadays, the most widely used calcium indicators are GCaMPs. GCaMP consists of an enhanced circularly permutated GFP (green fluorescent protein) molecule (cpEGFP) that has been fused to CaM (calmodulin) in its C-terminus and the M13 fragment of the myosin light chain kinase in its N-terminus (Nakai et al., 2001). Calmodulin is an intracellular calcium sensor with four E-F hands. Each E-F hand consist of a N-terminal helix (the E helix), a central calcium sensitive loop and a C-terminal helix (the F helix) (Chin and Means, 2000). Upon increases in intracellular calcium levels, calmodulin undergoes a conformational change which produces alterations in the interhelical angles of the E-F hands and results in a more open conformation that enables interactions with calmodulin's targets. One such target is M13. Thus, upon increases in calcium levels, the conformational change of CaM and interaction with M13 translates into a conformational change in cpEGFP, which changes the fluorescence intensity of GCaMP (Nakai et al., 2001).

The first generations of GCaMP still suffered from low sensitivity, slow kinetics and therefore low signals. However, subsequent mutagenesis experiments have generated GCaMPs with highly increased sensitivity and faster kinetics (Akerboom et al., 2012; Chen et al., 2013). This produced the GCaMP6 sensors, which includes GCaMP6s and GCaMP6f (Chen et al., 2013). All have the purported ability to report single action potentials (AP).

GCaMP6s (s for slow) has the highest sensitivity and shows the biggest increase in fluorescence, but has the slowest kinetics, with a rise and decay time of 0.4s and 1s, respectively. GCaMP6f (f for fast) has slightly decreased sensitivity compared to GCaMP6s but still vastly improved sensitivity to prior sensors, and it provides the fastest kinetics: 0.2s and 0.4s rise and decay times, respectively.

Because GCaMP is a reporter that has been engineered from molecules than can be genetically expressed in living cells, this made it possible to create transgenic animals that endogenously express GCaMP. Indeed one of the great advantages of GECIs is the ability to target them to specific cell populations (Huang and Zeng, 2013). More and more driver lines have been developed that allow strong expression levels in select cortical neuron populations (Madisen et al., 2010, 2015).

An initial hurdle in the application of widefield imaging in GCaMP expressing transgenic mice was that the GCaMP fluorescence signal overlapped with endogenous activity dependent autofluorescence and was prone to hemodynamic artefacts (Vanni and Murphy, 2014; Ma et al., 2016). However, the recent development of tools for correcting for these factors (Ma et al., 2016) has enabled the first longitudinal studies of neural dynamics across large areas of cortex (Silasi et al., 2016; Murphy et al., 2016; Wekselblatt et al., 2016; Makino et al., 2017; Rossi et al., 2017; Musall et al., 2018; Pinto et al., 2018).

Assessing cortical states from GECIs

The most commonly used lines for widefield imaging express GCaMP in cortical excitatory neurons. The signal from a single pixel during widefield

imaging of calcium indicators reflects a population signal from the neural tissue the pixel comes from. In contrast to the VSD signal, which contains a large portion of subthreshold activity, the calcium signal predominantly reports suprathreshold spiking activity (Vanni and Murphy, 2014). Although GCaMP is expressed in the entire neuron, which includes axons and dendrites in addition to cell soma, the widefield signal is dominated by local spiking activity: local application of pharmacological agents that suppress action potentials abolishes most of the calcium signals, suggesting that long range axonal projections contribute a minor proportion to the signal (Berger et al., 2007). In addition, experiments using simultaneous widefield calcium imaging and electrophysiology have shown that the widefield signal reliably correlates with local spiking activity (Xiao et al., 2017). Furthermore, Xiao et al. (2017) also produced "spike triggered maps", for which they triggered the widefield images on spikes at different depths in cortex and showed that there is a high overlap (90% on average) between the maps obtained from different layers, suggesting that the widefield signal is not layer specific but reflects an amalgamation of activity from different layers.

By comparison, LFP or EEG signals reflect the population activity of the local neural tissue and underlying cortical tissue, respectively. Although the widefield signal reflects excitatory activity only, while the LFP and EEG are affected by both excitatory and inhibitory activity, the widefield signals and LFP and EEG signals are similar in nature. This should make it possible to apply similar spectral analysis techniques to widefield signals in order to make inferences about cortical states but with higher spatial resolution than is possible with LFP and EEG signals. Although the rise and decay times of GCaMP6 pose an upper limit to what oscillations can be observed

with widefield imaging, synchronised and desynchronised states should be assessable since they can be inferred from low frequency fluctuations, which GCaMP6 can track. Indeed, experiments performing simultaneous GCaMP6 widefield imaging and electrophysiology have shown that the widefield signal has high coherence with the LFP at up to 15Hz (Rossi et al. 2017; Xiao et al. 2017; unpublished observations from our group).

1.3 Hypotheses and aims of this thesis

By virtue of being determined by the synaptic activity of the underlying neural tissue, measuring cortical states thus provides a powerful tool for gaining a glimpse into the mode of operation of the cortex without the need of measuring the activity of populations of neurons and their synaptic activities. Therefore, cortical states can reflect the behavioural and attentional demands that an individual is facing. Desynchronisation is frequently associated with engaged and attentive states, suggesting it may facilitate the information processing required in those states (Harris and Thiele, 2011). If a desynchronised cortical state corresponds to an optimal information processing state, then attention may indeed induce this state and drive an improvement in task performance. In addition, in order to spot-light the feature of interest, one might expect the desynchronisation to occur locally where the information of interest is being processed.

These are the hypotheses at the base of the work presented in this thesis. (Note however that this thesis did not aim to assess sensory or information processing directly, but instead focused on cortical state dynamics, for the reasons outlined above.) In particular, I asked whether attending a specific sensory modality locally increases desynchronisation in the cortex of the modality in use. I therefore needed tasks that used two different sensory modalities; I chose visual and auditory decision-making tasks for this purpose. In addition, I needed a method that had a high enough spatial resolution to reveal localised differences in cortical states whilst being able to monitor neural activity across a large area; for this I chose widefield imaging of GECIs. The following chapters will further detail the development of

these methods, but first I will clarify the main aims of this thesis:

1. Establish whether desynchronisation is correlated with performance.
2. Assess whether desynchronisation can occur as a localised cortical state.
3. Determine whether local desynchronisation is associated with the sensory modality that is attended. Specifically, I asked:
    - Does visual cortex become desynchronised in a visual task whilst unrelated sensory cortices like auditory and somatosensory cortex remain more synchronised?
    - Does auditory cortex become desynchronised in an auditory task, whilst visual and somatosensory cortex remain more synchronised?

Chapter 2

Methods

2.1 Animals

All experiments were conducted according to the UK Animals Scientific Procedures Act (1986). All animals were on a normal daylight cycle (8am - 8 pm), and co-housed whenever possible.

Behavioural pilot animals were C57B/L6 wild-type animals (n = 3 females; EJ001, EJ002, EJ003). Two male GCaMP3 x Emx1 (EJ004, EJ005) double transgenic mice were also briefly used to pilot auditory behaviour.

All animals used for widefield imaging during behaviour were offspring of double or triple transgenic crosses (males: n = 7, females: n = 9), expressing either GCaMP6f or GCaMP6s in cortical excitatory neurons under the following drivers:

- Ai93; Emx1-Cre; Camk2a-tTa
  ⇒ GCaMP6f in all cortical excitatory neurons
  (n = 7; EJ007, EJ009, EJ011, EJ012, EJ013, EJ015, FR053)

- Ai94; Emx1-Cre; Camk2a-tTa
  ⇒ GCaMP6s in all cortical excitatory neurons

(n = 1; EJ010)

- Ai94; Rasgrf-Cre; Camk2a-tTa

  ⇒ GCaMP6s in layer 2/3 cortical excitatory neurons

  (n = 1; EJ006)

- Ai95; VGlut1-Cre

  ⇒ GCaMP6f in all cortical excitatory neurons

  (n = 2; Muller, Theiler)

- tetO-G6s; Camk2a-tTa

  ⇒ GCaMP6s in all cortical excitatory neurons

  (n = 3; Cori, Hench, Reichstein)

- Snap25-G6s

  ⇒ GCaMP6s in all cortical neurons

  (n = 2; Chain, Radnitz)

The pilot animals as well as the animals from the crosses above whose names start with "EJ" were animals that I implanted and conducted experiments on myself.

FR053 was implanted with a 2-photon imaging window over visual cortex by Luigi Federico Rossi, and trained by Chris Burgess who performed 2-photon imaging in this animal. When those experiments were finished, the animal was passed on to me for widefield imaging.

The remaining animals belonged to Nick Steinmetz, who performed the surgeries and experiments and whose data I analysed and included in my results.

2.2 Surgery

All animals underwent surgery at the age of 8-10 weeks. Animals were anesthetized with 2% isoflurane in oxygen, body temperature was kept at 37°C, and analgesia was provided by subcutaneous injection of rimadyl (1ml/0.1kg). The eyes were protected with ophthalmic gel (Viscotears Liquid Gel, Alcon).

The animal's head was first shaved to expose the skin above the cranium, onto which iodine ointment was applied as an antiseptic. The cranium was immobilised with ear bars on the stereotax. A subcutaneous injection of 0.01ml of lidocaine was injected at the site of incision. The skin on top of the cranium was then cut and removed to expose the dorsal surface of the cranium and the periosteum was carefully removed.

In the surgeries I performed for unilateral imaging, the temporalis muscle was detached unilaterally to expose auditory cortex on the left hemisphere. The skull was thinned above visual, auditory and posterior somatosensory cortex using a scalpel until the external table and diploe of the bone were removed. A metal headplate with a circular opening above posterior cortex was fixed to the cranium at an angle of -30° with dental cement (Sun Medical), and a 8mm coverslip was then secured above the thinned skull using UV cement (Norland Optical Adhesives #81, Norland Products Inc., Cranbury, NJ).

In the surgeries performed by Nick Steinmetz for bilateral imaging, the skull was left intact and a clear skull cap implantation following the method of

Steinmetz et al. (2017) was used. A light-isolation cone was 3D-printed and implanted surrounding the frontal and parietal bones and attached to the skull with cyanoacrylate (VetBond; World Precision Instruments, Sarasota, FL). Gaps between the cone and skull were filled with L-type radiopaque polymer (Super-Bond C&B). The exposed skull was covered with thin layers of UV cement, and a metal headplate was attached horizontally to the skull over the interparietal bone with Super-Bond polymer.

A saline injection of 0.2ml per hour was provided throughout the surgery. Post-surgical care was provided by placing the animal in an incubator or a heated mat for the first hour post-surgery. 0.16ml of rimadyl was provided in 200ml of drinking water for the first three days after surgery, and animals were given a high-fat diet during their recovery.

2.3 Behaviour

Behavioural training started 1-2 weeks post-surgery, and all animals were handled for habituation for several days prior to head-fixation and training on the tasks.

Mice were trained to sit head-fixed in front of an LCD monitor (refresh rate 60Hz), at the bottom of which a MF1 speaker (TDT) was placed for auditory or auditory distractor experiments. The paws of the mice were resting on a steering wheel, which the animals could turn to provide a response in the task (Burgess et al., 2017). The angle of the wheel was measured using a rotary encoder.

The software controlling the behavioural tasks was developed by a former PhD student in the lab, Christopher Burgess. This software has two variations: one called "ChoiceWorld" and another called "Signals". Both fulfil the same purpose of allowing synchronisation between stimulus presentation, animal behaviour and neural recordings. Both softwares allow the user to make choices concerning task parameters in the visual task, but only Signals allowed for the presentation of auditory stimuli (either alone or concurrent with visual stimuli). Mice trained on the visual tasks were trained on a combination of both softwares, while the mice performing the auditory or auditory distractor task were trained using Signals.

All animals were water-deprived, and received a drop of water (between 2-3.5ml, calibrated for each mouse) as a reward in correct trials. Licks were measured with a thin-film piezo sensor attached to the lick spout.

2.3.1 Tasks

Visual 2AFC Task

In the visual two-alternative forced choice (2AFC) task, a visual stimulus consisting of a Gabor patch of varying contrasts appeared randomly on the left or the right visual field. The movement of the steering wheel was coupled to the movement of the stimulus, and the aim of the task was to centre the visual stimulus. The animals had to make their choice within a given response window (1.5-5 seconds), else a neglect response was recorded. Correct choices were rewarded with water, and incorrect or neglect responses resulted in either a white noise burst or a time-out.

Visual 2AUC Task

A subset of mice were trained on a two-alternative unforced choice (2AUC) version of the task, which contained zero contrast trials in which the animals were required to keep still during the response window in order to receive a reward.

Similarly, another subset of mice trained by Nick Steinmetz were trained on a contrast-comparison task, in which two contrasts were presented, one on the left and right side of the visual field, and the animals had to move the higher contrast stimulus to the centre. Trials with equal contrasts on both sides required the animals to make a random choice.

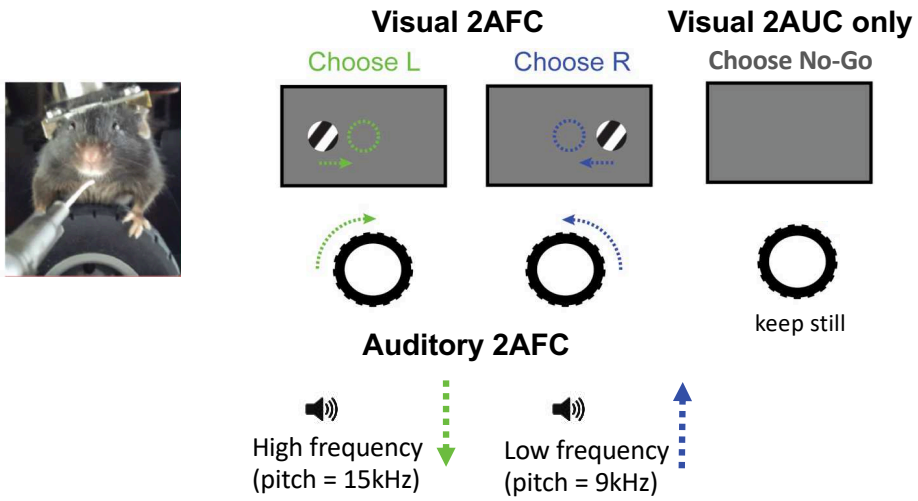

Figure 2.1: Behavioural tasks.
Left: Example of a head-fixed mouse with its paws resting on the steering wheel. Top middle: illustration of the stimulus presentation in the 2AFC task, top right: illustration of the no-go condition which was only used in the 2AUC task. Bottom: stimuli used in the auditory tasks. Turning the wheel changes the position of the visual stimuli, or the tonal frequency of the auditory stimuli.
Adapted with permission from Burgess et al. (2017)

Auditory Task

In the auditory 2AFC task, low or high frequency tone pips were presented from the speaker directly in front of the mice, and the movement of the wheel was coupled to changes in the tonal frequency of the tone pips. The aim of the task was to bring the tone frequency to the mid-frequency, which was also presented as a go-cue.

In the first pilot version of the auditory task, I used the same frequency range that another PhD student in the lab, Chris Burgess, had used in some of his early experiments which had presented visual and auditory stimuli simultaneously. I modified this task to be auditory only, and the auditory stimuli consisted of 8 and 32 kHz stimuli. The animals had to bring the

stimuli to a middle frequency of 16kHz.

In the second pilot version of the auditory task, the stimuli had a tonal frequency of 11.3 and 22.6 kHz, and the target (middle) frequency remained at 16kHz.

In the final version of the auditory task, the stimuli had a tonal frequency of 8 and 15kHz, and the target frequency was 11kHz. This range was chosen as the optimal one because mice should be able to comfortably hear the stimuli as they aged (Zheng et al., 1999; Kurt and Ehret, 2010; Ison et al., 2007), and sound calibrations performed inside the training rigs showed that there were minimal changes in amplitude within this range (Appendix A).

Auditory distractor task

The auditory distractor task consisted of the visual 2AFC task in which irrelevant auditory stimuli were presented simultaneously with the visual stimuli. The auditory stimuli consisted of the same auditory pips as in the final auditory task, and low and high frequency tones were randomly associated with either side of visual stimuli (but consistently within a given session; such that low was paired with left and high with right, or vice-versa).

Trial structure

All tasks shared the same basic trial structure. Trials started with a baseline of 1-5 seconds, and in order for a stimulus to appear, the animals had to remain quiescent (keep the wheel still) for 0.5-2 seconds; early movement lead to a delay in stimulus appearance.

In some cases, the stimulus was preceded by an auditory tone cue which

signalled the imminent appearance of a stimulus. In this case, movement during the baseline delayed the cue onset. Only the pilot animals (EJ001, EJ002, EJ003, EJ004 and EJ005) and the first imaging animals (EJ006, EJ007 and EJ009) were trained on this variant.

In all other cases, the stimulus appeared first and remained fixed until the onset of a go cue. Some animals (EJ010, FR053, EJ011, EJ012, EJ013 and EJ015) were also trained to keep still for 0.3-0.8 seconds when the stimulus appeared, otherwise the onset of the go cue was delayed.

In the visual tasks, the go cue consisted of either a tone or a visual gabor stimulus at the centre of the screen in the visual task. (The animals trained with a visual go cue were EJ011, EJ012, EJ013 and EJ015.) The modality of the cue did not affect the behaviour, therefore these tasks were analysed together. In the auditory and audio-visual tasks, the go cue consisted of a tone (consisting of the target frequency in the auditory task).

After the go cue, the interactive response window started, during which the movement of the wheel translated to the movement of the stimulus. In the visual tasks, changing the wheel position changed the position of the visual stimulus on the screen. In the auditory task, changing the wheel position changed the tonal frequency of the auditory stimulus.

The trial ended either when the animal provided a choice, or when the response window ended. The only exception to this were the first behavioural pilot animals, who were trained with an infinite response window, in which case a trial only ended when a response was provided.

Correct choices ended with a reward period (0.5-1 second), incorrect choices

(when the wheel was turned in the wrong direction) or neglect responses (when the mice failed to respond within the allowed time window) resulted in a time-out (2 seconds). This time-out was also signalled with a white noise burst in some mice (10/16), however, this was later dropped as it was found to not be necessary for good performance.

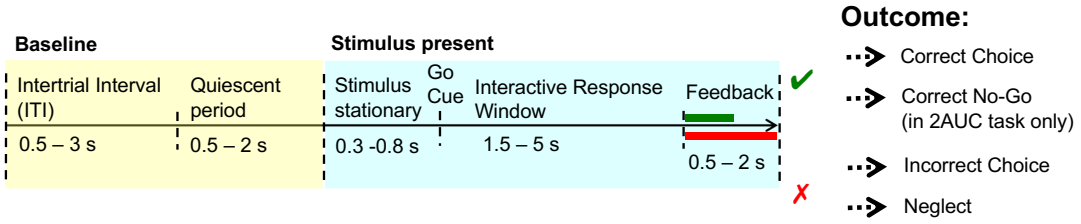

Figure 2.2: Trial structure.

2.3.2 Training procedure

All animals were trained in dedicated training rigs which were coated in acoustic foam (type: convoluted, thickness: 40mm, AnyFoam Ltd), which served to minimize acoustic resonances in the auditory task, and to provide some sound insulation.

Animals were first trained on the visual 2AFC task in dedicated training rigs, starting with easy, high-contrast stimuli. Once animals had learned the association between wheel and stimulus movement, and that moving the stimulus to the centre of the screen resulted in a reward (this took between 1-3 weeks), more difficult and lower contrast stimuli were added. Once animals produced good psychometric functions and achieved a level of performance above 70% on several consecutive days (usually within 1-2 weeks), the response window was gradually shortened from infinite to 10

seconds and then to 1.5 - 5 seconds, depending on the animal. At the same time, the reward size was gradually lowered to motivate animals to perform more trials.

Animals that were trained on the 2AUC variant of the task were introduced to zero contrast trials once the response window had been shortened to the desired final length (animals learned to keep still during this condition within 1 week).

Animals trained on the contrast comparison task were then introduced to easy comparisons first where a high contrast was paired with a low contrast. Once the animals had learned to centre the high contrast stimulus, more difficult comparisons were introduced where the difference in contrast between the two sides became gradually smaller, until also equal contrast trials were introduced, during which animals had to make a random choice.

In parallel, the baseline period was gradually lengthened and the quiescent period was introduced, starting with a short period (0.3-0.5 seconds), gradually building up to 1-2 seconds.

Once animals achieved steady performance with the final task parameters, they were introduced to the imaging rig. When the animals were accustomed to the new rig and performed well in the new environment, each animal was imaged during behaviour for 3-5 sessions.

Training in the auditory task began after animals had been imaged during the visual task (none of the animals trained in the contrast comparison task and none of the bilaterally imaged animals were trained in any other task). Training took place in training rigs that had been fitted with acoustic foam

on all sides except the bottom in order to reduce acoustic reflections and resonances that could have distracted from the auditory stimuli. Animals were first introduced to high amplitude stimuli, and once they learned the association between stimulus pitch and wheel movement and performed above 60% consistently, lower amplitude stimuli were added. Learning rates in this task varied widely, from 1-6 weeks.

Animals performing the auditory distractor task were not formally 'trained' in this task, the irrelevant auditory stimuli were simply added in some blocks that alternated with the visual task. The animals successfully disregarded the auditory stimuli, as the performance in the auditory distractor blocks was comparable to their performance in the visual blocks (shown in Results Section 4.2).

The majority of the training was conducted by myself. However, I received help with the training of some animals by two research assistants, Miles Wells and Laura Funnell, as well as another postdoctoral researcher, Philip Coen.

2.4 Neural recordings

2.4.1 Widefield imaging

In order to capture the signal from auditory cortex, the camera objective was tilted sideways to an angle of $-25°$ to $-30°$, so that it was approximately parallel to the headplate of the animals. The angles were measured with a Digital Inclinometer. The tilting was done for the unilaterally imaged animals only; for all other animals, the camera objective remained at a horizontal position.

The majority of experiments were conducted with dual wavelength imaging, alternating between blue illumination to excite the GCaMP signal, and a second wavelength that served to capture the hemodynamic signal. However, some early experiments were performed using only a single wavelength to collect the GCaMP signal only.

In all cases, GCaMP6 fluorescence was excited with a blue LED (470nm; LEX2-B, Brain Vision or Cairn OptoLED, P1110/002/000).

In addition, the monowavelength imaging experiments were non-continuous: the imaging was stopped at the end of each trial or repeat to allow for saving of the data, and restarted 1.8 seconds into the baseline period of the next trial/repeat.

All dual wavelength imaging experiments were performed as continuous recordings.

Mono wavelength imaging

The excitation light was diverted to the brain via a dichroic mirror (FF506-Di03, Semrock) and passed through a bandpass filter (FF01-482/35-25, Semrock).

The GCaMP6 signals were reflected by a dichroic mirror (FF593-Di03, Semrock), passed through an emission filter (FF01-543/50-25, Semrock) and collected by a scientific complementary metal oxide semiconductor camera. Imaging was performed at an acquisition rate of 50Hz, 19 ms exposures, with 4x4 binning, using a PCO Edge 5.5 CMOS camera and a macroscope (Scimedia THT-FLSP) with a 0.63x objective lens (Leica 10450027).

Dual wavelength imaging at the primary set-up

This set-up consists of the monowavelength imaging set-up, but with a green ring-illuminator containing 5-6 miniLEDs (528nm; Thorlabs LED528EHP), driven with a LEDD1B driver, that was fixed around a 1.0x condenser lens (Leica 10450028). Imaging was performed at acquisition rates between 35-50Hz per colour, 10-19ms exposures, with 2x2 or 4x4 binning.

Dual wavelength imaging at Nick Steinmetz's set-up

In this set-up, the excitation light passed through an excitation filter (Semrock FF01-466/40-25), a dichroic (425nm; Chroma T425lpxr), and 3mm-core optical fiber (Cairn P135/015/003), then reflected off another dichroic (495nm; Semrock FF495-Di03-50x70) to the brain. To capture the hemodynamic signal, the light was passed through a purple excitation filter (405nm, Chroma ET405-20x) on every other frame. Light from the brain passed

through a second dichroic and emission filter (Edmunds 525/50-55 (86-963)) to the camera.

The resulting resolution was $20^2\mu$m per pixel for both imaging set-ups.

2.4.2 Passive mapping of visual and auditory cortex

Visual stimuli were presented on two LCD monitors that cover 90° of the visual field contralateral to the imaged hemisphere. Visual stimuli used to generate retinotopic maps of visual cortex were moving bars sweeping either horizontally or vertically through the visual field at 2Hz (Kalatsky and Stryker, 2003).

All auditory stimuli were presented through MF1 open field speakers (TDT). Auditory stimuli used to identify auditory cortex consisted of pure tone pips presented at 2, 3 or 5.5 Hz during 5 seconds, randomly changing between the following frequencies: 4, 6, 8, 12, 16, 24, 32 kHz. In some cases, auditory sweeps from 2 to 64 kHz were used.

Baseline fluorescence levels were acquired for 2-4 seconds before stimulus presentation and/or using a blank condition.

The stimulus presentation tools that I used were developed by current and former members of the group; Matteo Carandini, Andrea Benucci, Andrea Pisauro, Daisuke Shimaoka, Mika Diamanti (see also Benucci et al. 2007; Pisauro et al. 2013; Carandini et al. 2015; Shimaoka et al. 2018).

2.4.3 Imaging during behaviour

Animals EJ006, EJ007 and EJ009 were imaged during behaviour using the non-continuous, mono wavelength imaging set-up.

Animals EJ010, EJ011, EJ012, EJ013, EJ015 and FR053 were imaged at the primary dual-wavelength imaging set-up. Andy Peters, a postdoctoral researcher in the group, helped with the data collection from EJ011. Otherwise, the data from these mice was collected by myself.

Animals Chain, Cori, Hench, Muller, Radnitz, Reichstein and Theiler were imaged at the second dual wavelength imaging set-up by Nick Steinmetz.

2.4.4 Concurrent monitoring of pupil size

All imaging experiments were conducted with concurrent monitoring of one of the eyes; in the case of unilaterally imaged animals this was the eye contralateral to the imaged hemisphere.

The eye was illuminated with an infrared LED (SLS-0208A, Mightex; driven with LEDD1B, Thorlabs), and recorded at a framerate of 16.5Hz using a 446 camera with an infrared filter and a zoom lens (Thorlabs MVL7000). The videos were recorded with MATLAB's Image Acquisition Toolbox (MathWorks).

Monitoring of whisking

In a subset of experiments (22/58 in the visual tasks), the frame containing the eye was expanded to include the whisker pad for coincident monitoring of whisker motion.

2.5 Data processing and analysis

All data were analysed using custom-written Matlab code. Unless otherwise stated, this code was written by myself.

2.5.1 Behaviour

Trial classification

In the 2AFC tasks, there were three possible trial outcomes:

- The animals made a correct choice by moving the stimulus into the centre of the visual field in the visual and auditory distractor tasks, or the central tonal frequency in the auditory task.
- The animals made an incorrect choice by moving the stimulus into the periphery in the visual and auditory distractor tasks, or away from the central tone pitch in the auditory task.
- The animals failed to provide a choice before the end of the response window, in which case a Neglect response was recorded.

Unless otherwise stated, 'choice trials' refers to correct and incorrect choices, as these two trial types were grouped together in the majority of analysis.

Note also that even if the animals moved the stimulus but insufficiently to cross the central or peripheral thresholds, this would also count as a Neglect response, as the animals usually provided a very stereotyped and fast response during choice trials.

In the 2AUC tasks, there was a fourth possible trial outcome:

- Correct no-go: when the animal successfully remained still throughout the response window during zero contrast trials.

Note that if the animals moved the wheel such that either threshold was crossed, an incorrect choice trial was recorded.

Inclusion criteria

In order to be able to look at variations in the level of engagement during a given behavioural session, I set a threshold for minimum numbers of trials per condition. All datasets that contained fewer than 10 choice or 10 neglect trials were excluded. Similarly, where correct and incorrect choices are compared, datasets that contained fewer than 10 of each trial type were excluded.

The value of 10 was chosen by using datasets with large numbers of trials per condition, and gradually decreasing the number of random trials per condition, until the results became skewed by outliers and differed from the result using all trials. 10 trials reliably produced results that were consistent with larger numbers of trials, and therefore this value was chosen as a threshold.

Psychometric curve fitting

In section 3.2 (*Mice can learn both visual and auditory tasks*) as well as Figures 4.1, 4.5, 4.38 and 4.39 of section 4 (*Main Results*), the decisions made by the mice were fitted with probabilistic models. These fits were generated using code written by Peter Zatka-Haas, another PhD student in the lab.

In the 2AFC tasks with infinite response windows, the responses were fit with logistic regression, using the following equations:

$$p = \frac{1}{(1 + e^{-z})} \tag{2.1}$$

where

$$z(t) = b + S_L C_L + S_R C_R \tag{2.2}$$

In each trial t, the decision variable z depends on a bias term b, sensory sensitivity terms S_L and S_R (one each for the left and right visual fields in the visual task, and the high and low tonal frequencies in the auditory task), and the left and right contrast values C_L and C_R in the visual task, which in the auditory task correspond to the high or low tonal frequencies. This gives the probability p of choosing right for a given contrast in the visual task, and the probability of choosing low tonal frequency in the auditory task.

In the 2AFC tasks which had finite response windows and in the 2AUC tasks, where in addition to choosing left or right, the animals could provide a no-go response, the responses were fit with the following equations:

$$z_L = b_L + S_L f(c_L) \tag{2.3a}$$

$$z_R = b_R + S_R f(c_R) \tag{2.3b}$$

where $f(c_L)$ and $f(c_R)$ are derived from:

$$f(c) = \frac{c^n}{c_{50}^n + c^n} \tag{2.4}$$

Using equation 2.1, this then gives the probabilities p_L of choosing left over choosing no-go, and p_R of choosing right over choosing no-go, and the probability p_0 of choosing no-go is then 1 - (p_L + p_R).

Baseline definition

In the non-continuous imaging datasets, the beginning of the baseline was considered to be the first frame 200ms post imaging onset in each trial. (The first 200ms following imaging onset were excluded in order to exclude possible laser onset artefacts.)

In the continuous imaging datasets, the beginning of the baseline was considered to be the first frame after the end of the previous trial's feedback period: 1s post reward receipt, 2s post negative feedback receipt.

The end of the baseline period was considered to be the last frame before stimulus or cue onset.

Trials with baselines shorter than 1 second were excluded from analysis.

Wheel movement quantification

In order to provide precise coupling between the wheel movement and the stimulus, the angle of the wheel was recorded using a framerate of 210Hz.

As a first step, wheel values were interpolated to match the timepoints of the neural recording.

Then, a matrix was constructed that contained the wheel trajectories of the baseline period of each trial. Each baseline period was zeroed to the wheel

value of the last frame, such that for each baseline, the wheel trajectory ended at zero.

Quiescent period

In order to define the quiescent period, an algorithm was employed that searched for the last non-zero value before the baseline end. Small movements (deviations from zero up to a value of 4 (in arbitrary units)) were considered to be involuntary twitches and were set to zero. Any larger deviations were considered voluntary movements.

In order to quantify wheel movement wm per trial z, the following calculation was used:

$$wm(z) = \sum_{i=1}^{T} |\frac{dw}{dt}| \tag{2.5}$$

where $w(t)$ is the wheel trajectory over time during the baseline of each trial.

Trials with quiescent periods shorter than 700ms were excluded from analysis.

No movement trials

In the analysis comparing choice and neglect trials with no movement (Figure 4.19), no movement trials were defined as follows:

First, trials with a value of $wm(z) > 35$ were exluded. A non-zero threshold was used as it is difficult for animals to remain perfectly still for several seconds, and manual inspection of the datasets showed that this value allowed for occasional small wiggles, which usually consisted of deviations up to 5 (in arbitrary units). Since animals were required to keep still for up to 2 seconds, a threshold of 35 allowed for several of such small wiggles.

Whilst a threshold of 35 allowed for several small wiggles, it also allowed for one or two larger deviations, which would have corresponded to bigger movements. In order to exclude such bigger movements and make sure that only small wiggles were occurring during the selected trials, if the trials contained deviations larger than 10 (arbitrary unit) from the final wheel position, the threshold was decreased until this second requirement (no single deviations larger than 10) was also met.

Finally, to ensure there remained no bias towards more movement in one condition than the other (such as choice or neglect), for as long as there was a significant difference in the amount of wheel movement between choice and neglect trials (Wilcoxon rank sum test $p < 0.05$), the threshold was further decreased until no difference remained. This was done to ensure that any differences between conditions were not driven by differences in movement - even if it was small movements such as wiggles.

Only trials that fulfilled all these conditions were used in the analysis assessing power differences between choice and neglect trials with no wheel movement.

2.5.2 Neural recordings

Dimensionality reduction

Except for the data shown in Figures 3.1, 3.2 and 3.3 in Section *Imaging visual and auditory cortex simultaneously with widefield imaging* of Chapter 3, all imaging data were compressed and denoised by computing the singular value decomposition (SVD) of the 3D image stack. This method was developed by two postdoctoral researchers in the lab, Marius Pachitariu and Nick Steinmetz.

First, the 3D stack was reshaped into a 2D matrix S of dimensions p x t, where p is the number of pixels and t is the number of time points. Then, we performed SVD of S:

$$S = A\Lambda B^T \tag{2.6}$$

The physiological spatiotemporal dynamics of the data were fully captured with the top 500 singular values, accordingly all the presented analyzes were performed using the top 500 singular values. Therefore, each pixel was expressed as a linear combination of the first 500 temporal components of B^T, which we called V; weighted by the corresponding spatial matrix U, derived from $A\Lambda$.

This computation was performed separately for the images containing the neural and the hemodynamic signal (from the blue and the green/purple excitation cycles, respectively).

Hemodynamic correction

In all datasets acquired by the dual wavelength imaging method, a hemodynamic correction was applied to the GCaMP signal in all datasets. This method was developed by Kenneth Harris.

Both GCaMP and hemodynamic signals were first linearly de-trended and high-pass filtered above 0.01Hz, and then bandpass filtered in the frequency range corresponding to the heart beat, 9-13Hz, where hemodynamic artefacts are strongest. The filtered signals were then used to compute a linear regression coefficient for each pixel, which served as a scaling factor that provided a measure of how much of the GCaMP signal was contaminated by hemodynamics. The GCaMP signal was corrected by subtracting a multiple (given by the regression coefficient) of the hemodynamic signal from the GCaMP signal. Pixel-wise multiplication and subtraction were performed in the SVD space to allow faster computation.

Pre-processing of mono wavelength imaging datasets

When the hemodynamic correction could not be applied, the GCaMP signal was linearly detrended.

Usage of F instead of dff

With the exception of the imaging data in Chapter 3: *Proof of Principle Experiments*, where data are represented as dff (defined as $(F-F_{baseline})/F_{baseline}$ where *baseline* was the period prior to stimulus presentation), all presented analysis were performed using F (defined as $F - F_{mean}$ where *mean* was the mean image across the imaging session). The SVD method was developed

shoftly after the results presented in Chapter 3 had been obtained. To take advantage of the ease of performing calculations in SVD space, this method was adopted for all later analyses, as any linear operation can be performed on the temporal component V, and the result can then be multiplied into the spatial component U to reconstruct the result in fluorescence values. To confirm that this approach was valid for the analyses presented in this thesis, the analysis from Figure 4.13 from the Main Results Chapter was replicated using dff, which produced the same result (Appendix B).

Mapping of visual and auditory cortex in Chapter 3

Outlines of visual and auditory cortices were identified in each mouse by sensory stimulation using sweeping bars (Kalatsky and Stryker, 2003) for visual cortex, and repeated pure tone pips of different frequencies for auditory cortex (see section 2.4.2). The resulting visual and auditory responses in Chapter 3 were analysed using tools developed by other members of the group (Benucci et al., 2007; Pisauro et al., 2013; Carandini et al., 2015; Shimaoka et al., 2018).

For visual cortex, retinotopic maps were generated by applying a Fourier analysis to the neural responses and extracting the component at the frequency of the sweeping bars. The phase of the component is given by when the response reached its maximum value relative to the beginning of the stimulus cycle. This maximum value varied according to when the bar moved through the receptive field, and since the receptive fields in visual cortex are retinotopically organised, this phase analysis allows the creation of the retinotopic maps. A retinotopic map was considered 'good enough' when a

horizontal phase gradient was observed that was indicative of primary visual cortex (V1) (in most cases, phase reversals were also clearly visible, indicating higher visual areas), and the visual stimuli elicited amplitude responses that were restricted to the cortical region that was stereotaxically expected to be visual cortex. All animals whose data are presented in this thesis passed this criterion except EJ012, which was excluded from analysis pertaining to visual cortex. In order to generate the outlines of visual cortex in section 3.1 (*Imaging visual and auditory cortex simultaneously with wide-field imaging*), the amplitude of the component was used and thresholded to yield responses restricted to visual cortex.

For auditory cortex, amplitude maps were generated by averaging the responses across the different tonal frequencies of stimulation. The resulting average amplitude map was then used and thresholded, same as for visual cortex, to yield responses restricted to auditory cortex. An auditory cortex map was considered 'good enough' when auditory stimuli provoked the largest amplitude responses in the cortical region that was stereotaxically expected to be auditory cortex, and when high (above 12kHz) and low (below 8kHz) tonal frequency stimuli elicited responses in spatially separate cortical regions. (In many cases, a given tonal stimulus also elicited responses in several cortical regions, indicating primary and secondary auditory responses.) All animals whose data are presented in this thesis passed this criterion.

ROI selection in Chapter 4

The visual cortex (VIS) region of interest (ROI) was chosen as the centre of the stimulus response to contralateral stimuli within the visual task. The

auditory cortex ROI (AUD) was based on the auditory cortex maps obtained by passive stimulation. The responses to different frequencies were averaged and the ROI was selected from the area with the highest mean response and which was responsive to the frequencies used within the auditory task.

The somatosensory cortex ROI (SS) was chosen from the area that was stereotaxically estimated to be the barrel cortex and which was qualitatively observed to be active during whisking and movement. The retrosplenial cortex ROI (RSP) was estimated stereotaxically and chosen from posterior RSP as this was the visible part of RSP in the unilateral imaging experiments. The secondary motor cortex ROI (MO) was estimated stereotaxically.

In the unilaterally imaged animals, ROIs were placed in visual, auditory, somatosensory and retrosplenial cortex, except in the following animals:

- FR053: Only one ROI in visual cortex was considered because of the smaller 2-photon imaging window.

- EJ012: ROIs were placed only in auditory, somatosensory and retrosplenial cortex. Visual cortex was excluded because of growth under the imaging window above visual cortex which rendered the fluorescence signal too noisy.

In the bilaterally imaged animals, ROIs were placed in visual, somatosensory, retrosplenial and secondary motor cortex in all animals. Each ROI was selected as a single pixel, which in practice however covers more than the single pixel due to the spatial smoothing resulting from the SVD representation (see Section 2.5.2: *Dimensionality reduction*, and Appendix A).

Spectral analysis

Spectral analysis was performed using the chronux toolbox (http://chronux.org; Mitra & Bokil 2008).

Due to technical constraints (the slow dynamics of GCaMP, and the maximal imaging frame rates of 30-50Hz that imposed a Nyquist limit of between 15-25Hz), the spectral analysis focused on low frequency oscillations.

Where experiments had been conducted in animals from different genotypes, their results were pooled together and analysed together. This was done because the spectral analysis yielded consistent results according to behavioural condition in all genotypes examined, including between GCaMP6f and GCaMP6s animals (detailed further in Section 4.1.1).

Power difference map computation

As explained under Section 2.5.2 (*Dimensionality reduction*), for a given pixel n, the fluorescence over time was represented by

$$f_n(t) = U_n \cdot V = \sum_{i=1}^{500} U_{ni} V_{it} \tag{2.7}$$

where U_n is the row within U corresponding to pixel n. Therefore, the Fourier transform of $f_n(t)$ was calculated as

$$\hat{f}_n(\omega) = \sum_{i=1}^{500} U_{ni} \hat{V}(\omega) \tag{2.8}$$

where $\hat{}$ denotes the Fourier transform and ω denotes frequency.

To compute the power in the frequency band of interest 3-6Hz, I calculated:

$$\sum_{\omega=3Hz}^{6Hz} \hat{f}_n(\omega)\hat{f}_n{}^*(\omega) \tag{2.9}$$

The power spectrum for all pixels was then computed using matrix multiplication. This procedure allowed for a more efficient computation, at least an order of magnitude faster than without the SVD compression.

Finally, this was reshaped into a 2-dimensional 'Power map' $P(x, y)$ where x and y are spatial dimensions.

This method was devised by a former postdoctoral fellow in the group, Michael Okun.

I computed these power maps during the ITI or quiescent period for each trial separately and then computed the average power for choice and neglect conditions:

$$P_{choice}(x, y) = \frac{1}{z_{choice}} \sum_{i=1}^{z_{choice}} P(x, y) \tag{2.10a}$$

$$P_{neglect}(x, y) = \frac{1}{z_{neglect}} \sum_{i=1}^{z_{neglect}} P(x, y) \tag{2.10b}$$

The power difference maps were then computed as follows:

$$P_{Diff}(x, y) = 10 \cdot log_{10}(\frac{P_{choice}}{P_{neglect}}) \tag{2.11}$$

The multiplication by 10 is applied to turn the power ratios into units in decibels.

The same principle applied for computing power difference maps between movement and no movement trials, correct and incorrect trials, and so on.

In the power difference maps shown in the figures, pixels with average power (over time) below the 20th percentile were set to black. This procedure effectively masks pixels outside the brain.

Computation of powerspectra in Figure 4.4

The fluorescence time course $f_n(t)$ was reconstructed for the pixel n representing the visual cortex ROI. Then, the baseline period was extracted for each trial and the powerspectrum computed using a multi-taper Fourier transform. The 'Power Ratio' was computed for each experiment by computing the average powerspectra for choice and neglect trials:

$$\hat{f}_{choice}(\omega) = \frac{1}{z_{choice}} \sum_{i=1}^{z_{choice}} \hat{f}_n \tag{2.12a}$$

$$\hat{f}_{neglect}(\omega) = \frac{1}{z_{neglect}} \sum_{i=1}^{z_{neglect}} \hat{f}_n \tag{2.12b}$$

and then taking the ratio between the two:

$$\hat{f}_{ratio}(\omega) = \frac{\hat{f}_{choice}(\omega)}{\hat{f}_{neglect}(\omega)} \tag{2.13}$$

Finally, the mean and SEM across all experiments were computed.

Stimulus response analysis

In order to exclude possible effects of movement, I only considered the data from animals that had been trained to remain still after stimulus onset in the analysis of stimulus responses. EJ012 was excluded from this analysis as it had developed growth under the imaging window above visual cortex, which rendered the signal from visual cortex too noisy. EJ011 was excluded from the analysis because of poor performance in the visual task during imaging days. Therefore, only the data from EJ010, EJ013, EJ015 and FR053 was considered in this analysis.

Amplitude

The amplitude of the stimulus response was estimated as the fluorescence at the visual cortex ROI averaged over 0.1-0.3 seconds post stimulus onset in the GCaMP6f animals, and 0.2-0.4 seconds post stimulus onset in the GCaMP6s animals (the different time window was used because of the slower dynamics of GCaMP6s). Unless otherwise stated, the stimulus response was baseline subtracted and the frame at time zero of stimulus onset was used as the baseline.

Spatial spread

To assess whether there was a difference in the extend of cortical activation around the centre of the stimulus response, I created a square ROI around the central pixel that extended 25 pixels in each direction (medial, lateral, frontal and posterior). I computed the average stimulus response to the smallest contralateral contrast in each dataset, and used this as a threshold to ask how many pixels within the extended ROI had a value higher than

this threshold. The resulting number of pixels was used as a measure of the spatial spread of the stimulus response. In the majority of datasets, 10% was the smallest contrast condition. In the datasets in which 25% was the smallest contrast condition, the threshold was normalised by dividing by 2, as the average response amplitude to a 25% contrast was approximately twice the average response amplitude of a 10% contrast; otherwise, the threshold in these datasets would have been higher than in the ones containing 10% contrast trials.

2.5.3 Pupil analysis

The eye recordings were analysed using custom written software developed by a postdoctoral researcher, Michael Krumin.

In short, for each video frame, the image is cropped to a manually selected ROI containing the pupil. The image is smoothed with a 2D Gaussian filter of manually selected width and thresholded using a manually selected intensity threshold that differentiates between pixels inside and outside the pupil. A 2D ellipse is fitted to the contour corresponding to the selected intensity value by minimizing the mean squared error of the following equation:

$$Ax_i^2 + Bx_iy_i + Cy_i^2 + Dx_i + Ey_i = 1 \tag{2.14}$$

where x_iy_i are the coordinates of the contour. The pupil area was computed from this fit ellipse, and this measure was used as the pupil size.

Frames for which no contour could be detected or for which the fit ellipse was outside the range of possible values were excluded. This usually occurred due to blinks or grooming. In order to detect such frames, the frame was cropped to the lower half of the eye, and the correlation coefficient between the cropped frame and the corresponding average frame was calculated, as well as the mean intensity of the cropped frame. These two measures were then plotted against each other, and a classifier was manually adjusted to find combinations of values that were indicative of blinks or grooms (see Figure 2.3). All frames that fell within the ranges in the classifier, as well as the 10 previous and following frames, were set to NaN values and thereby excluded.

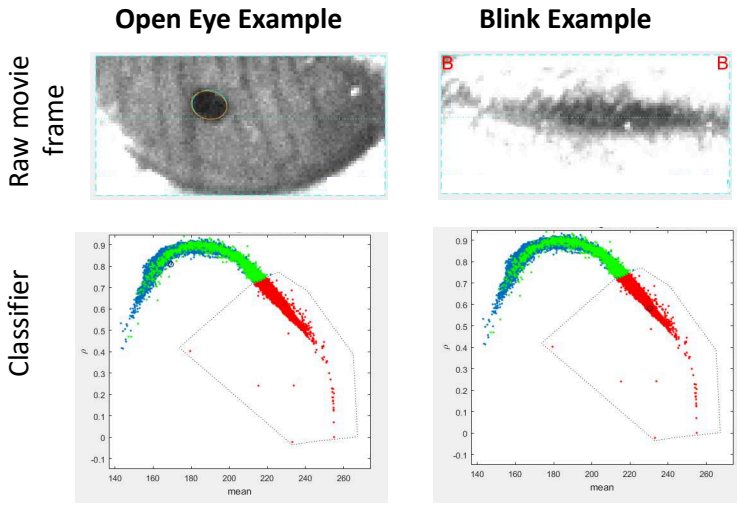

Figure 2.3: Illustration of the classifier used to identify blinks.
Top: The orange and cyan circle around the pupil in the open eye example indicates the pupil fit found by the algorithm. The red 'B's in the top corners in the blink example indicate that the algorithm identified this as a blink frame. The cyan fine dotted line going across the centre of image corresponds to the upper border of the cropped frame.
Bottom: The mean intensity of each frame (mean) plotted against the correlation coefficient ρ. Each dot corresponds to one frame. The dotted outline indicates the classifier that has been manually adjusted to include frames that are blinks: all the dots inside the classifier are classed as blinks and are coloured red; the remaining dots (outside the classifier) are green or blue and indicate non-blinks. The black circles highlight the dots that correspond to the frames at the top.

After this process, a further pre-processing step was applied during which the pupil trace was filtered using a second order digital Butterworth filter between 0.0001 and 1Hz. Finally, the filtered pupil trace was linearly interpolated to correspond to the time points of the neural recordings.

A few datasets were entirely excluded entirely from analysis due to poor quality. (Note that the corresponding neural recordings were still included.)

Whisker motion analysis

The whisker motion analysis was performed using a software developed by a former PhD student in the lab, Carsen Stringer.

In the eye movies that also contained the whisker pad, an ROI was drawn around the whiskers near the snout of the animal. The whisker motion was computed as the absolute value of the difference of two frames within the ROI and summed over pixels greater than a threshold that was manually adjusted for each experiment.

2.5.4 Statistics

Unless otherwise specified, all statistical tests were carried out with a one-sample t-test to test the null hypothesis that the power differences or reaction time correlations across experiments in each ROI come from populations with mean zero. This test was chosen because a single experiment was often underpowered to detect a significant difference between conditions (the behavioural conditions could not be balanced since they were a result of the natural fluctuations in behaviour of the animals, which were highly variable across days and animals).

In addition, one-way ANOVAs were employed to test the null hypothesis that the power differences did not differ between the different cortical regions of interest. Multiple comparisons were adjusted using Tukey's honest significant difference criterion.

Where correlations are reported, these were calculated using Pearson's correlation coefficient. The confidence interval was calculated for each dataset (and therefore each correlation), but since the correlation coefficients were pooled together to ask whether there was a consistent correlation across experiments, the confidence intervals reported consist of the averaged confidence intervals across datasets.

In the pupil analysis (Sections 4.1.4 and 4.2.2), data were analysed with one-way analysis of covariance models (ANCOVA) fitting separate but parallel lines to the data per behavioural condition. To assess whether behavioural condition improved the prediction of cortical state from pupil size, we tested the null hypothesis that behavioural condition had no effect and that the

intercepts of the resulting fitted lines would therefore not differ. To quantify the size of the effect of the condition, we computed the 'intercept difference' between the conditions. Multiple comparisons were adjusted using Tukey's honest significant difference criterion.

Chapter 3

Proof of Principle Experiments

In this chapter, I will present results from selected early experiments which served as a foundation for the main experiments and results presented in Chapter 4.

This chapter contains:

- The results that demonstrate that simultaneous widefield imaging of visual and auditory cortex is possible.
- The behavioural experiments and the conclusions I drew from them that determined the parameters of the visual and auditory tasks I used in my main experiments.

3.1 Imaging visual and auditory cortex simultaneously with widefield imaging

To assess brain state in visual and auditory cortex, I needed to image both areas at the same time. Visual cortex was routinely imaged in the lab, and although some of auditory cortex had also been previously imaged with widefield imaging (Carandini et al., 2015), this was largely restricted to the secondary auditory cortical areas that lie dorsally. Primary auditory cortex is very lateral on the mouse brain and therefore not entirely visible from a top view. Accordingly, I needed to establish new surgical and imaging methods that would provide access to the more lateral parts of the auditory cortex, including primary auditory cortex. I received help in learning how to expose auditory cortex during surgery and how to perform imaging in auditory cortex from Andrew King's Lab at the University of Oxford and Tara Keck's Lab at UCL. The surgical and imaging procedures that I established are described in Sections 2.2 and 2.4 of the *Methods* Chapter.

3.1.1 Retinotopic mapping of visual cortex

The imaging angle during my experiments was steeper than usual to capture the signal from auditory cortex. Therefore, it was important to evaluate whether this may have a detrimental effect on the signal obtained from visual cortex. An easy method for evaluating this was to perform retinotopic mapping (see *Methods*, Section 2.4.2).

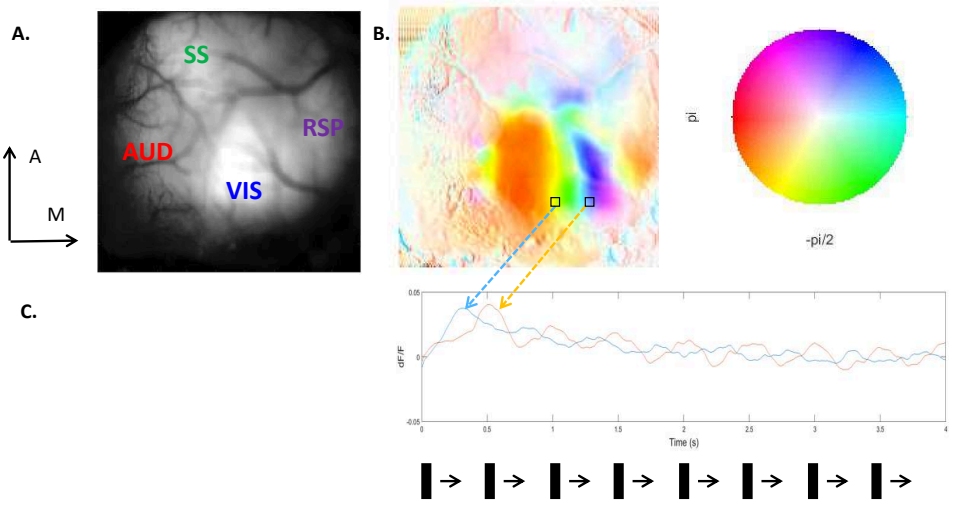

(i) Retinotopy Example 1

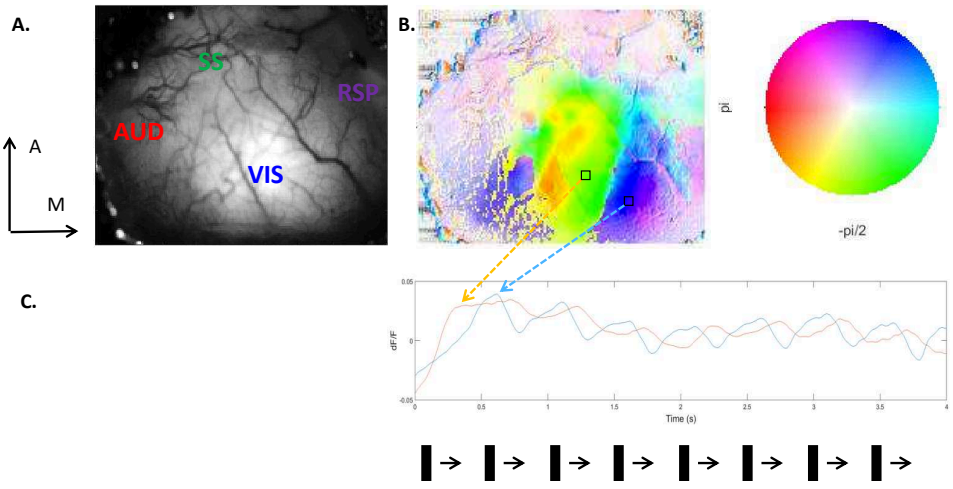

(ii) Retinotopy Example 2

Figure 3.1: Retinotopic responses in visual cortex to a sweeping bar at 2Hz.
A. Overview of the cortical areas within the imaging window. SS = somatosensory cortex, RSP = retrosplenial cortex, VIS = visual cortex, AUD = auditory cortex.
B. Phase map of the response to the sweeping bar stimulus (depicted at the bottom of C), where colour denotes phase and colour intensity denotes amplitude of the response.
C. Space averaged fluorescence traces from the ROIs (black squares) denoted in B. The traces show 2Hz oscillations that are out of phase with each other. The peaks correspond to the (delayed response) to the time-points during which the bar crossed the respective visual receptive fields.

The two examples in Figure 3.1 show that despite the steeper imaging angle, reliable retinotopic responses could be captured from visual cortex.

3.1.2 Auditory cortex mapping

The next step was to confirm that I could get a good signal from auditory cortex and that I also captured primary auditory cortex in my imaging window. To do this, I played auditory stimuli (either tone sweeps from to 2 to 64kHz, as shown in the example in Figure 3.2, or tone pips ranging from 4 to 32kHz, repeating at 2 or 3Hz) during the same imaging session during which I had played visual stimuli.

The presence of several peaks within auditory cortex in response to a given frequency (Figure 3.2) indicates that I successfully captured responses from primary and secondary auditory cortices.

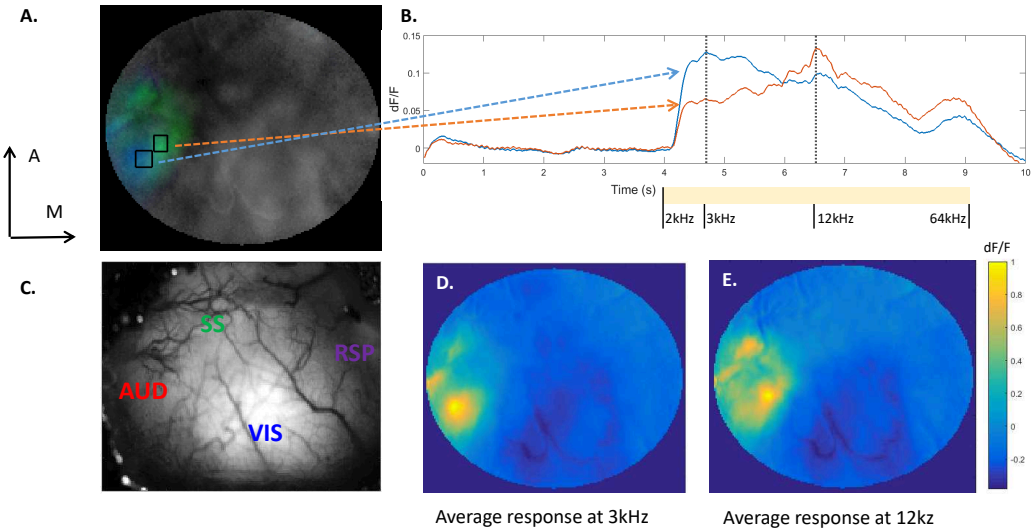

Figure 3.2: Auditory cortex response to an auditory stimulus sweeping from 2 to 64 kHz.
A.
B. Time traces obtained from the ROIs (black squares) in A. Yellow bar indicates stimulus duration.
C. Overview of cortical areas in the imaging window (same as in Figure 3.1(ii)).
D. & E. Average responses at 3kHz and 12kHz, respectively, corresponding to the frames at the time points of maximal response in ROI 1 (blue) and ROI 2 (orange).

Putting visual and auditory cortex maps together

The final step was to produce maps of visual and auditory cortex in each animal. To achieve this, I used the mean amplitude maps obtained from each sensory stimulation (see *Methods*, Section 2.5.2), set a threshold at 60% of the maximum amplitude for each sensory modality, and included all pixels that had amplitudes above this threshold.

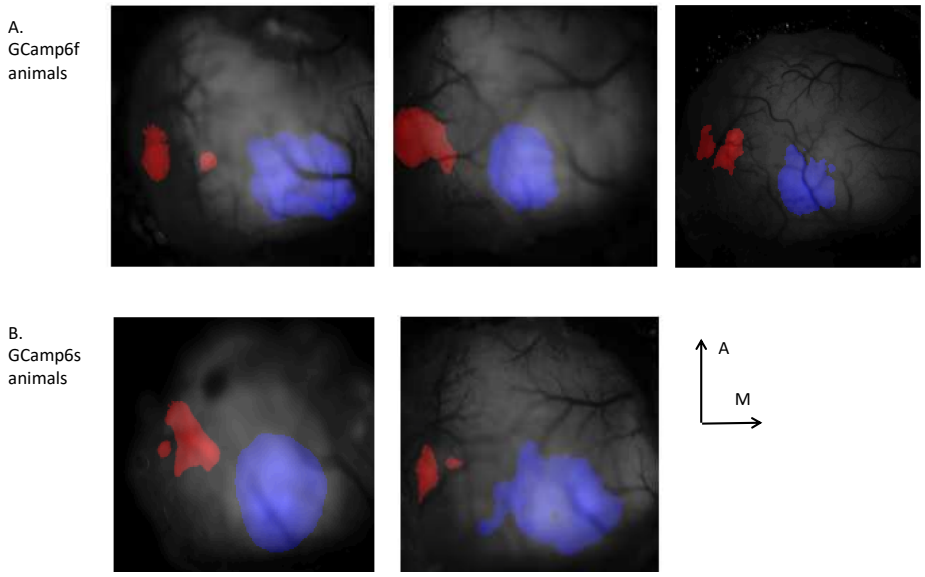

Figure 3.3: Maps of visual and auditory cortex obtained during a single imaging session in 5 different animals.
Areas shaded in blue denote visual cortex, areas shaded in red denote auditory cortex. The shaded areas were obtained by calculating the mean amplitude map for each sensory stimulus.

3.1.3 Summary & Conclusions

I showed that it is possible to obtain satisfactory maps of both visual and auditory cortical function during the same session by imaging at an angle of -30°. This demonstrated that it was possible to obtain a good signal from both sensory cortices simultaneously.

3.2 Mice can learn both visual and auditory tasks

3.2.1 Training mice on visual and auditory 2AFC tasks

I began the behavioural training by training three pilot animals (EJ001, EJ002 and EJ003; female C57Bl/6 mice, aged 8 weeks at behavioural training onset) in the visual 2 alternative forced choice (2AFC) task that is commonly used in the lab. All animals successfully learned this task and achieved 70% performance within 15 training days and produced good psychometric curves (Figure 3.4).

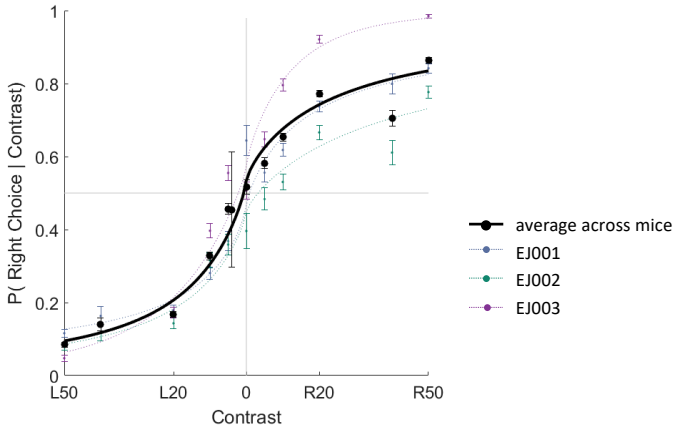

Figure 3.4: Pilots Performance in the Visual 2AFC.
L50 and L20 denote left contrast values, 50% and 20%, respectively, and R20 and H50 corresponding denote right contrast values. Data was pooled from 23, 20 and 13 sessions from EJ001, EJ002 and EJ003, respectively, after the animals reached a threshold of 60% performance. Errorbars represent standard error of the mean. Psychometric curves were fitted with the model described in Section 2.5.1 (equations 2.1, 2.2).

I then introduced the animals to the first version of the auditory task, in which the stimuli had tonal frequencies of 8 and 32 kHz, and the animals

had to bring the stimuli to a middle tonal frequency of 16kHz.

I started the auditory training by giving a block of auditory stimuli after a block of visual stimuli, but in this case, the animals didn't seem motivated to perform a new task after the familiar one. I therefore proceeded to train the animals on the auditory task only until they showed learning in this task. Upon this change, all pilot animals successfully learned the auditory task and achieved above 70% within 10 training days (Figure 3.5).

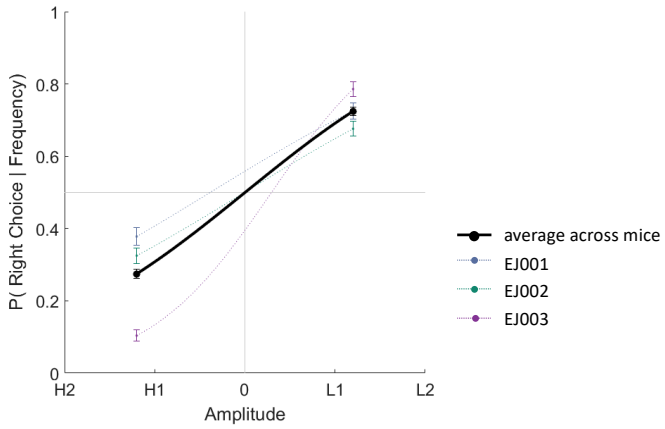

Figure 3.5: Pilots Performance in the Auditory 2AFC.
H2 and H1 refer to high tonal frequency, while L1 and L2 refer to low tonal frequency. Only one amplitude level was used at this early stage of training. Data was pooled from 5 sessions from each animal after they reached a threshold of 60% performance. Errorbars represent standard error of the mean.

At this point, I began training the animals with consecutive blocks of visual and auditory stimuli, and I introduced more difficult stimuli into both tasks to obtain psychometric curves. The visual task was made more difficult by introducing lower contrasts, and the auditory task was made more difficult by introducing background white noise over which the auditory stimuli had to be detected, and by lowering the amplitude of target stimuli. All animals obtained 60% performance or higher on the more difficult versions of both

tasks.

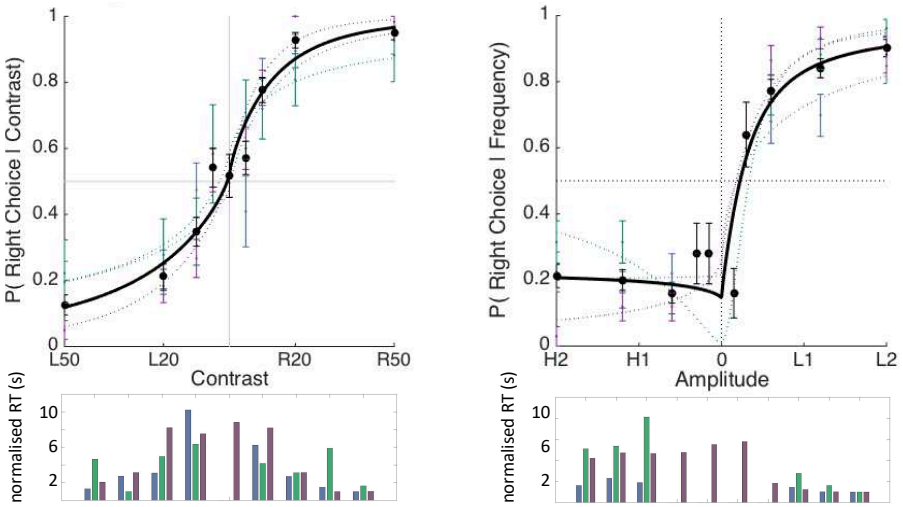

(i) Visual 2AFC (ii) Auditory 2AFC

Figure 3.6: Pilots Performance when performing both tasks on the same day. Top: Psychometric curves. Bottom: normalised reaction times (RT) $\frac{RT}{min(RT)}$.

However, the auditory task appeared to be more difficult, as the animals consistently performed better in the visual task (Figure 3.6i). In addition, their responses and reaction times to the high frequency stimuli made me suspect that they were performing the auditory task using a detection rather than a discrimination strategy: they responded much faster to low frequency stimuli, and only showed an amplitude dependent modulation in response to low frequency stimuli (Figure 3.6ii).

I therefore tested how animals would respond to zero amplitude trials. If they had learned to discriminate between the high and low frequency stimuli, then zero amplitude trials should evoke a random choice, akin to zero contrast trials in the visual task. Instead, the animals consistently made 'high frequency' choices in response to zero amplitude trials (Table 3.1).

	EJ001	EJ002	EJ003
1^{st} **attempt**	82% Right Choice	60% Right Choice	77% Right Choice
Including bait trials	66% Right Choice	58% Right Choice	67% Right Choice

Table 3.1: Pilot animals give the same response to zero amplitude trials as to high frequency trials.
Note that a trial is repeated when the animal makes an incorrect choice; these trials are referred to as bait trials.
Total trial numbers were between 150-200 trials per mouse.

Since these results suggested that the animals may not have been able to hear the high frequency stimuli, I reduced the frequency range to 11.3kHz - 22.6kHz, whilst keeping the same target frequency of 16kHz.

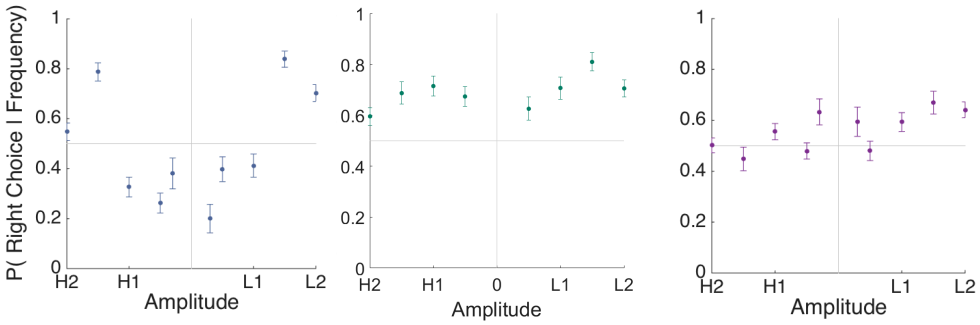

(i) EJ001 (ii) EJ002 (iii) EJ003

Figure 3.7: Pilots Auditory Task Performance on second frequency range.
Average over 7 days.

I continued training the pilot animals on this task for 6 weeks, however they did not show any learning with the new frequency range and their responses remained heavily biased or at chance level (Figure 3.7). Since they may have simply been confused by the change, I aborted their training and started to train new animals.

Training mice on the auditory task first

Two animals (EJ004 and EJ005; male GCaMP3 transgenic mice) which had previously been used to pilot audio-visual widefield imaging were recruited to serve as behavioural pilot animals. Specifically, I wanted to know whether starting behavioural training with the auditory task might be helpful for learning this task.

I started training them on the auditory 2AFC task with the modified frequency range (11.3 to 22.6 kHz). These animals however did not show any motivation to learn the task during the first week of training (at this early learning stage, animals usually turn the wheel randomly to obtain some reward, these mice however performed barely any trials), so I aborted their training (Data not shown).

I tried training another animal (EJ010) on the auditory task first (with a frequency range of 6-10kHz), but this mouse also did not show any learning after 2 weeks of training. However, when I introduced this animal to the visual task, it successfully learned this within a week (Data not shown).

Conclusions drawn from these pilot experiments

Altogether, these results showed that although the mice did not pick up the desired strategy in the auditory 2AFC task, mice were capable of learning 2 tasks, using visual and auditory stimuli, and that they could perform both visual and auditory tasks consecutively on the same day.

In addition, these experiments suggested that the visual task is easier, and that learning to respond to auditory stimuli was easier for animals that already knew the visual task. This may be because they were already familiar with the concept of having to move the steering wheel to obtain a reward. In order to make the learning of the tasks easier, the behavioural training of all subsequent animals was started on the visual task.

3.2.2 Training mice on 2AUC versions of the tasks

Since the first pilot animals had performed the auditory task as a detection rather than discrimination task, I modified the task to incorporate a feature that had been successfully implemented by another postdoctoral researcher in the group (Nick Steinmetz) in the visual task: setting a finite response window and including zero contrast trials in which animals had to report the absence of a stimulus by remaining still (not moving the wheel in either direction) during the response window, which was called a no-go response. This version of the task is referred to as the 2 alternative unforced choice (2AUC) task. In the visual task, this paradigm forces the animal to attend both visual fields. In the visual 2AFC task, it would also be possible to perform the task with a detection rather than discrimination strategy by paying attention to one visual field only: if there was no stimulus in one field, the stimulus had to be in the other field. Whereas in a 2AUC task, the absence of a stimulus in one visual field could indicate either a stimulus in the other visual field, or no stimulus altogether. I therefore decided to change both visual and auditory tasks to 2AUC versions, with the auditory 2AUC task having zero amplitude trials added that would require no-go responses.

My next animals were GCaMP6 triple transgenic animals, which were also imaged during behaviour in order to obtain the first data sets of my main experiments (described in more detail in Chapter 4). These animals successfully learned the visual 2AFC task, and when they performed equally well with a finite response window (Figure 3.8), I introduced the zero contrast trials. All animals achieved good performance in the visual 2AUC task

(Figure 3.9). (The data in Figure 3.9 comes from days during which the animals were imaged during behaviour. The neural recording results will be discussed in Chapter 4.)

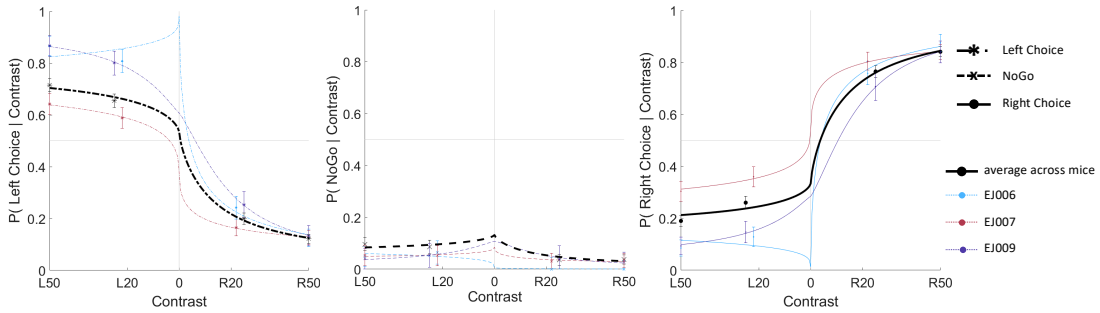

Figure 3.8: Visual 2AFC Performance with a finite response window.
Note the low occurrence of no-go responses (middle panel), which shows that the animals successfully make a choice within the response window. The responses in this task were fit with a probabilistic model, described in Section 2.5.1 (equations 2.1, 2.3, 2.4).

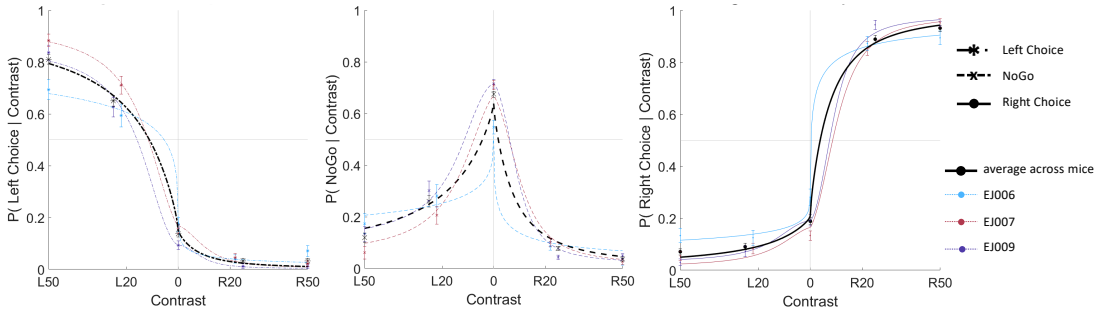

Figure 3.9: Visual 2AUC Performance.
Note the high probability of no-go responses at zero contrast (middle panel), which is the correct response in this condition. The responses were fit with the same model as in Figure 3.8.

After obtaining neural recordings from the animals on the visual 2AUC task, I proceeded to train them on the auditory task. I began by training the animals on the 2AFC version of the auditory task, with a modified tonal frequency range: 8-15kHz. This range was chosen in order to avoid animals

becoming incapable of hearing the higher frequency stimuli as they aged since behavioural training could extend over several months. In addition sound calibration experiments in the training rigs showed that the amplitudes of the different frequencies within this range were mostly stable and unaffected by potential resonances (Appendix A).

All animals successfully learned the auditory 2AFC task with a finite response window in the new frequency range (Figure 3.10), although one animal (EJ009) appeared to respond only to the lower frequency stimulus. I then proceeded to introducing the zero amplitude trials that required no-go responses.

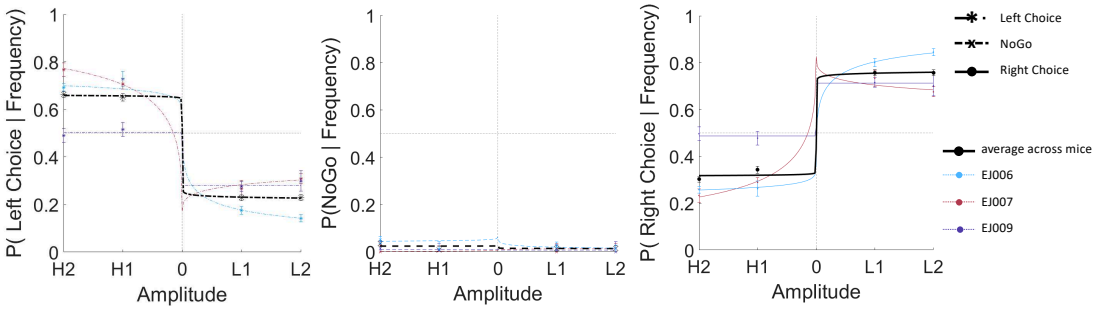

Figure 3.10: Auditory 2AFC Performance with a finite response window and a frequency range of 8-15kHz.
The responses were fit with the same model as in Figure 3.8.

Disappointingly, the introduction of zero amplitude trials in the auditory task seemed to confuse them. They did not generalise the concept of a no-go to the auditory task and did not achieve a performance level above 55%. Figure 3.11 shows their performance in the auditory 2AUC task after 4 weeks of training. Note that it seemed that EJ006 and EJ007 adopted opposite strategies: EJ006 appeared to perform the task by paying attention to the low frequency stimuli only and correctly providing right choices in

this condition, whilst performing at chance level between no-go and left choices for the high frequency and zero amplitude stimuli. EJ007 in contrast appeared to pay attention to the high frequency stimuli, as it correctly provided left choices with high probability in this condition, but its responses to the low frequency and zero amplitude stimuli were random.

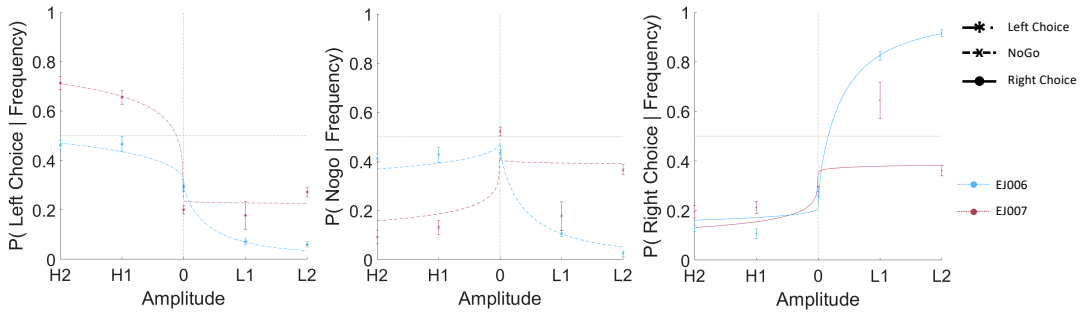

Figure 3.11: Auditory 2AUC Performance.
Only animals EJ006 and EJ007 were trained on the 2AUC version of the task, as EJ009 was performing poorly on the 2AFC version (see Figure 3.10). The responses were fit with the same model as in Figure 3.9.

Conclusions drawn from the 2AUC experiments

Mice readily learned a 2AUC version of the task with visual stimuli, but not with auditory stimuli. They did not generalise the concept of a no-go response from the visual to the auditory task, possibly because they associated the no-go response with the visual task, or maybe because the auditory task was harder than the visual task.

I cannot exclude that they may have learned the auditory 2AUC task after prolonged training. However, since this would have taken disproportionately longer than with the visual 2AUC task, which the animals learned within 2 weeks whilst after 4 weeks of training in the auditory 2AUC they were still

performing poorly, I decided to not pursue the 2AUC versions in my future experiments, and return to the 2AFC format.

3.2.3 Summary & Conclusions

Altogether, these experiments showed that mice could learn both visual and auditory tasks, and that they could perform them on the same day. Specifically, whilst mice learned both visual and auditory 2AFC tasks readily, they only did well on a visual but not auditory 2AUC task. I therefore decided to proceed with the 2AFC versions in future experiments, even if this meant that the mice might employ a detection rather than discrimination strategy.

Since a detection strategy still engages the animals with the stimulus in a given sensory modality - vision or hearing - I concluded that this was still sufficient in terms of behaviour for the scientific question I want to ask: Does engaging with a sensory stimulus desynchronise the sensory cortex of the modality that is being attended to? With this strategy, I could still make animals perform blocks of visual and auditory behaviour back to back, and investigate what may change in terms of brain states.

Chapter 4

Main Results:

Cortical state fluctuations during sensory decision-making

In this chapter, I will be addressing the main question of my thesis:

- Does engaging with a specific sensory modality lead to a localised brain state in the cortex of the sensory modality being used?

In order to do this, I will first go through the results from the visual tasks (Section 4.1), and then the results from the auditory 2AFC and an auditory distractor task that I devised (Section 4.2).

My initial plan had been to image animals as they were performing these tasks in consecutive blocks, which would allow me to assess what happens when animals switch attention from one sensory modality to another. However, this was not possible in the end (explained in detail in Section 5.1 of the Discussion Chapter), which meant that I had to change my strategy for investigating the main question of my thesis. As the subsequent sections will show, I found differences in cortical states within a given task; specifically I found that cortical states correlated with fluctuations in the level of

engagement during task performance. This allowed me to address the main question of my thesis from the following angle:

- Are the performance related cortical state changes local or global?
- Do these changes depend on the sensory modality that was required in a given task?
- In other words, is optimal performance related to localised state changes in the cortex of the sensory modality being used?

4.1 Brain state fluctuations during visual decision making

The level of engagement varies during task performance

Following the results from my behavioural pilot experiments (see Chapter 3), I returned to using the 2AFC format in the visual task with a finite response window (see also Methods Section 2.3). As I wanted to investigate performance, I classified trials into three groups according to outcome: correct trials; incorrect trials (turning the wheel in the wrong direction); and neglect trials, in which no response was made before the trial timed out.

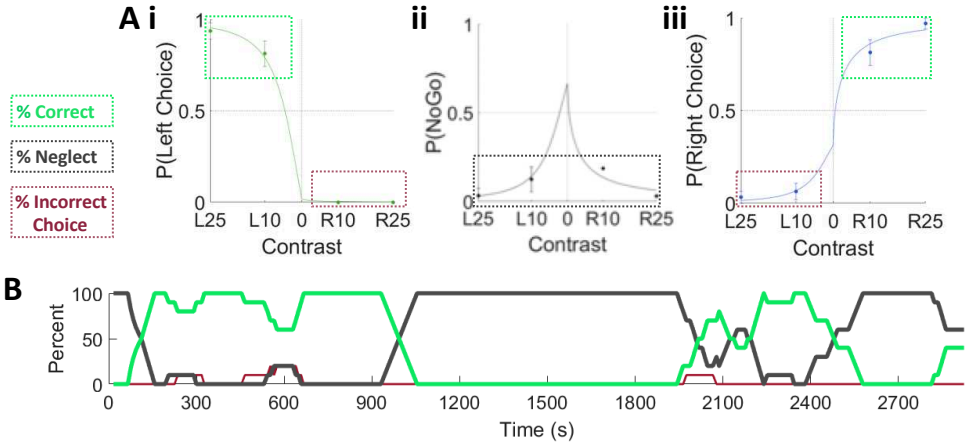

Figure 4.1: Example behavioural session from a visual 2AFC task.
A. Psychometric Curves. B. Performance over time in the course of one experimental session.

Figure 4.1 illustrates that despite an otherwise good performance during the task (A), the level of engagement fluctuated and intermittent incorrect and neglect trials occurred throughout the session. Although the example in

Figure 4.1B shows an extreme example of disengagement in which the animal provided neglect responses for several consecutive trials before engaging with the task again, the majority of datasets contained neglect trials (Figure 4.2A) which often occurred in sequence, thus making for periods of neglect of varying lengths across the datasets (Figure 4.2B).

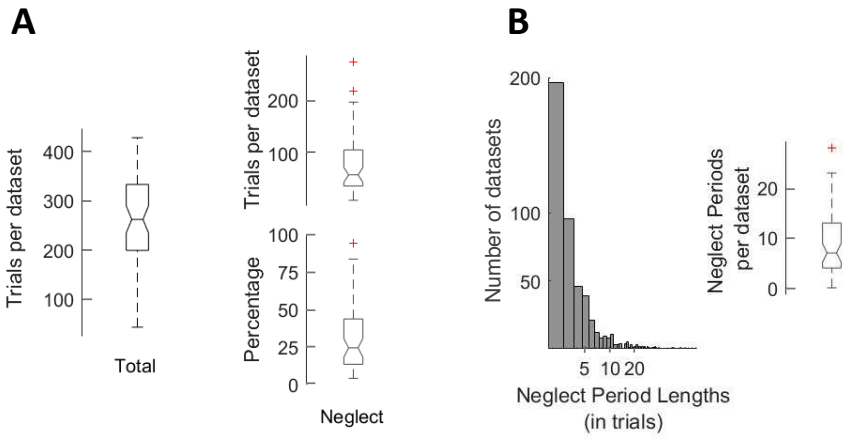

Figure 4.2: Neglect trial occurrences across sessions.
A. Overall neglect trial occurrences. Left: box-whisker plot illustrating distribution of total number of trials across all datasets. Right top: Number of neglect trials per session across datasets. Right bottom: Neglect trials as a percentage per session across all datasets.
B. Neglect period occurrences and lengths. Left: distribution of neglect period lengths across all datasets, right: number of neglect periods per session across all datasets

4.1.1 Cortical state in V1 correlates with engagement

Given the relationship between arousal and brain states, I hypothesized that the periods of disengagement would correspond to a more synchronized cortical state, characterised by increased low frequency power. I began the analysis of this question by investigating cortical states in visual cortex, and I focused on the region of primary visual cortex (V1) retinotopically aligned to the task stimuli (see Figure 4.3 Ai).

I found a robust relationship of trial type to the power spectrum of the calcium signal during the pre-stimulus baseline period of each trial (Figure 4.3 B-C). Low frequency power was greater in neglect than choice trials, with the largest difference in the 3-6Hz frequency band which is why I used this frequency band in all further analysis. This relationship was present consistently across all datasets (Figure 4.4).

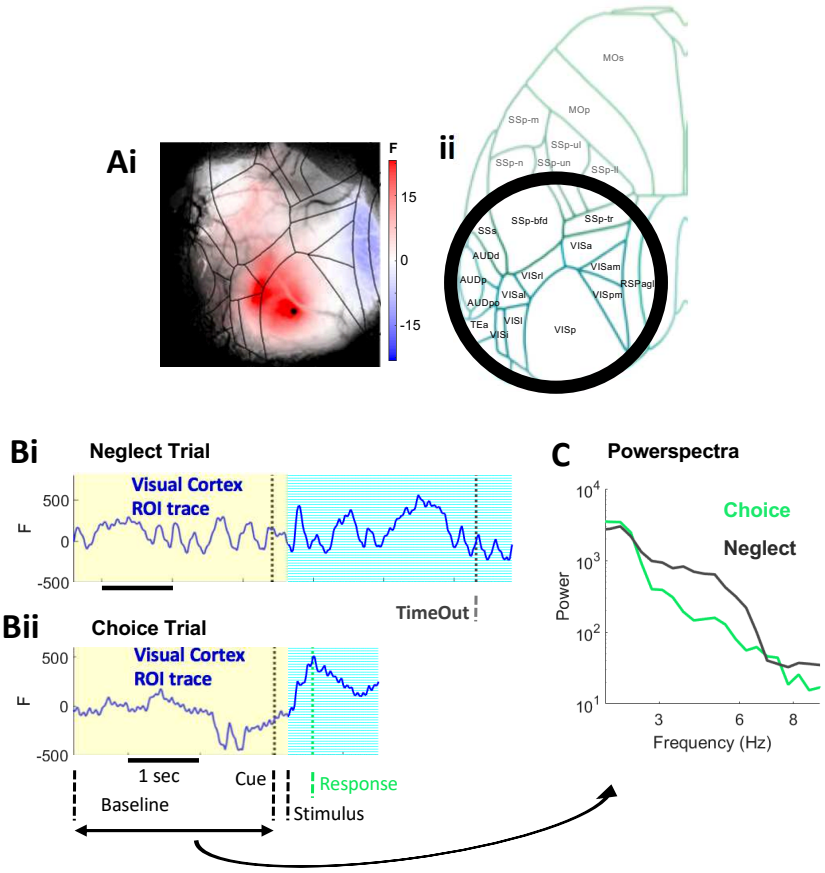

Figure 4.3: Low frequency power correlates with behavioural state.
A. (i) Stimulus triggered average response with the Allen atlas cortical borders superimposed. Black dot indicates the pixel from which the traces in B are drawn. (ii) Cartoon of the Allen common-coordinate framework atlas highlighting the outlines of the cortical regions within the imaging window in (i).
B. Single trial examples from representative choice (ii) trial and neglect (i) trials. Yellow background indicates baseline period, during which there was no stimulus present. Blue background indicates presence of a contralateral visual stimulus. Green dotted line in the choice trial indicates choice time (when the stimulus crossed the threshold in the centre). Dark grey dotted line in the neglect trial indicates timeout (the animal failed to provide a choice and a neglect trial is registered).
C. Powerspectra computed from the baseline (yellow highlights in B) periods of the example trials.

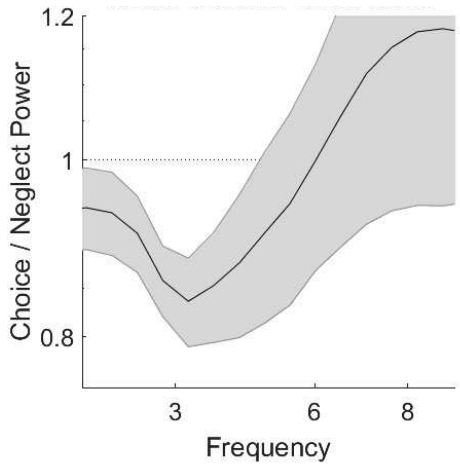

Figure 4.4: Summary Choice/Neglect Power Ratio.
Black line equals mean, shaded area SEM. n = 58 experiments from 15 animals.

The correlation between cortical state and task engagement is not genotype dependent

All my mice, including the ones whose data are shown in Figures 3.8 - 3.11 and 4.1 - 4.4, were triple-transgenic GCaMP6 animals, which our laboratory discovered to be prone to interictal (epileptiform) activity (Steinmetz et al., 2017). At the time of the discovery, I had already collected the bulk of my data, and I had also already analysed my visual data and found the results described above. Even though the results fit with the well established relationship between cortical state and arousal, the discovery of the interictal activity in some of my datasets nevertheless raised the question whether the results were due to artefacts of the potentially pathological state of these animals.

Luckily, another postdoctoral researcher in the group (Nick Steinmetz, who was the one to discover the epileptiform activity) had been training animals of different genotypes that also expressed GCaMP6s or GCaMP6f in cortical

excitatory neurons on a similar visual decision making task as I had been using, and also imaged them during behaviour using widefield imaging (see *Methods* Chapter for details). I therefore included his data in my analyses and asked whether I could replicate my results from his datasets.

Figure 4.5 depicts the performance of a tetO-GCaMP6s mouse in a 2AUC version of the visual task, which also presented periods of neglect, which allowed me to ask whether I would see the same relationship between cortical state and choice and neglect trials.

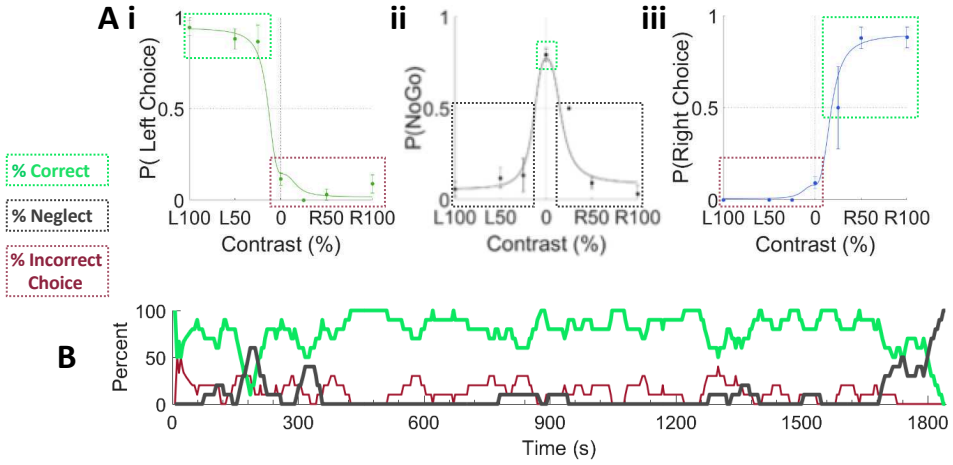

Figure 4.5: Performance in a visual 2AUC task of an animal of a different genotype.
A. Psychometric Curves. B. Performance over time in the course of one experimental session.

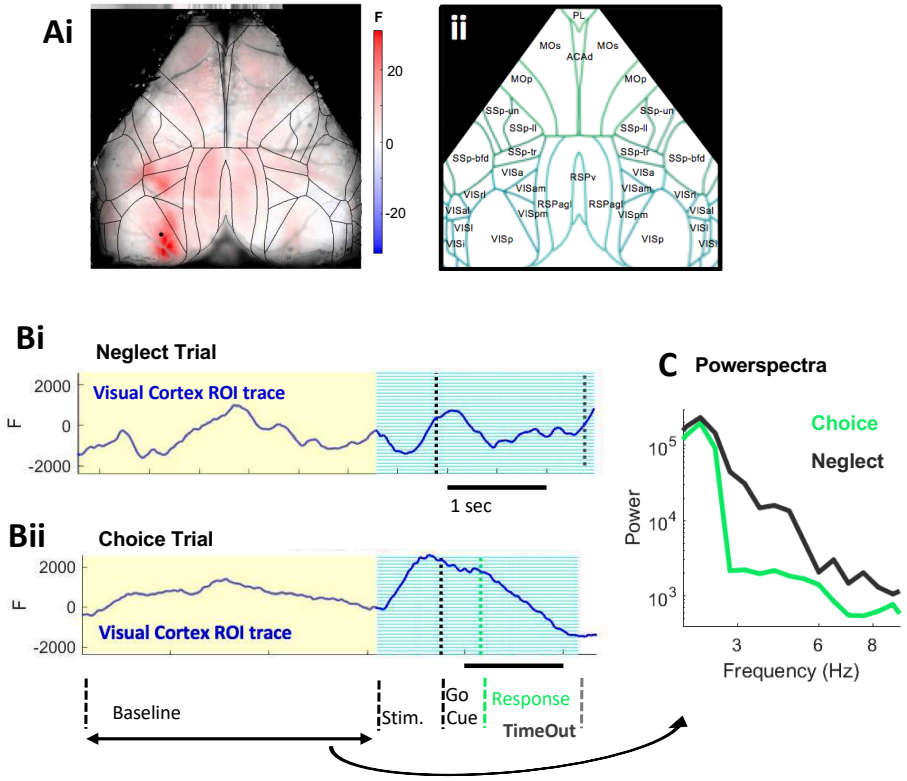

Figure 4.6: Low frequency power correlation with behavioural state in a tetO-GCaMP6s mouse.
A. (i) Stimulus triggered average response with the Allen atlas cortical borders superimposed. (ii) Cartoon of the Allen common-coordinate framework atlas showing the outlines of the cortical regions within the imaging window in (i).
B. Single trial examples from representative choice (ii) trial and neglect (i) trials. Yellow background indicates baseline period, during which there was no stimulus present. Blue background indicates presence of a contralateral visual stimulus. The stimulus appears first and is fixed in position until the go cue appears (indicated by black dashed line), after which the animal can move the stimulus to provide a choice. Green dotted line in the choice trial indicates choice time (when the stimulus crossed the threshold in the centre). Dark grey dotted line in the neglect trial indicates timeout (the animal failed to provide a choice and a neglect trial is registered).
C. Powerspectra computed from the baseline (yellow highlights in B) periods of the example trials.

Importantly, there was indeed a difference in low frequency power between choice and neglect trials (Figure 4.6), and there were no significant differences between 3-6Hz power between genotypes (Figure 4.7, ANOVA $p>0.05$). I therefore took this as validation of the results I had observed in my data. (An extensive discussion on the possible effects of interictal activity is provided in the Limitations Section of the *Discussion* Chapter.)

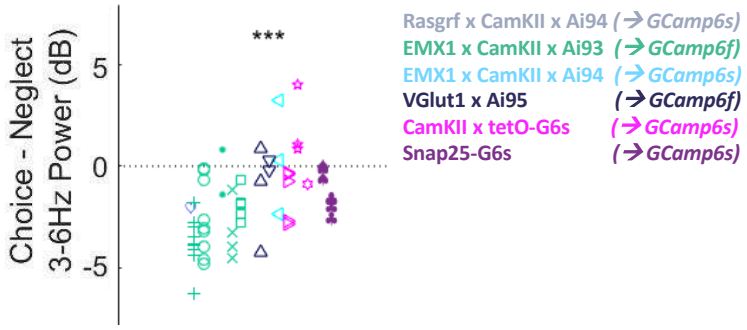

Figure 4.7: Summary 3-6Hz Choice - Neglect power difference in Visual Cortex. Different genotypes are indicated by different colours; green and dark blue colours correspond to GCaMP6f expressing animals, all others expressed GCaMP6s. Different symbols indicate different animals.

Overall, these results suggested that there was a significant decrease in low frequency power during choice trials (Figure 4.7), indicating increased desynchronisation in the visual cortex when the animals were engaged in a visual task.

Stimulus responses in V1 do not correlate with behaviour

I next investigated whether I would observe any state dependent differences in stimulus responses in primary visual cortex (V1) in my data.

Given the difference in pre-stimulus state that I had observed between choice and neglect trials, I started by asking whether there was a difference in the amplitude of the stimulus responses between choice and neglect trials.

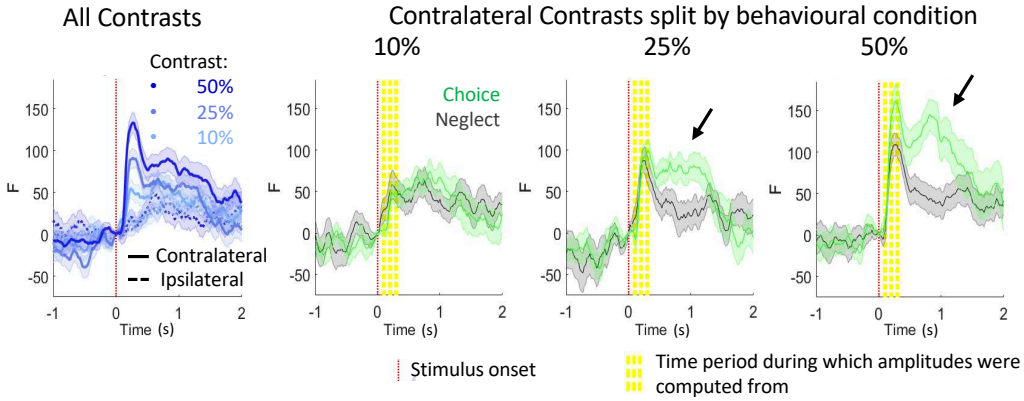

Figure 4.8: Stimulus response example.
Left: Average stimulus responses to all contrasts presented. Solid lines indicate contralateral stimuli, dashed lines ipsilateral stimuli. Different shades of blue indicate different contrast values of the stimulus. Red dotted line indicates stimulus onset.
Middle and right panels: contralateral stimulus responses for choice (green) and neglect (black), ordered by ascending contrast. Yellow background indicates the time period that was used to compute the response amplitude. Arrows indicate a secondary response that was discounted in the analysis as this time period coincided with when the animals were making their behavioural responses.

As expected, there were reliable contrast dependent responses, with increasing contrasts evoking larger amplitude responses (Figures 4.8 and 4.9; $p<0.01$, 2-way ANOVA main effect of contrast). Although there was in some cases a larger stimulus response in choice than in neglect trials (Figure 4.8, 50% contrast), this effect was not consistent across datasets (Figure 4.9;

p>0.05, 2-way ANOVA main effect of behavioural condition). Note that the difference between choice and neglect trials beyond 0.3 seconds (Figure 4.8, highlighted with black arrows) was most likely caused by movement, either due to the animal providing a response and/or of the resulting displacement of the visual stimulus, and was therefore not considered.

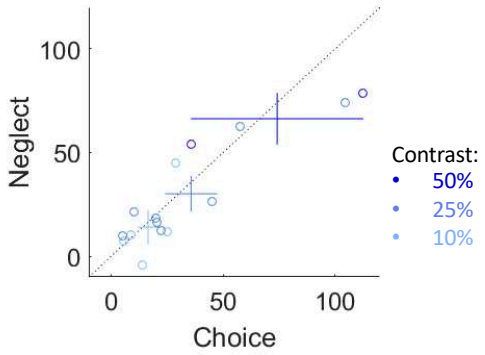

Figure 4.9: Choice versus neglect stimulus response amplitudes in V1.
Circles represent individual datasets, bars represent mean and SEM.

I next asked whether the amplitude of the stimulus response correlated with any behavioural factors that I had measured (Figure 4.10). There was only a marginally significant correlation between stimulus response amplitude and reaction time for the 15% and 50% contrasts (p<0.05, pearson's correlation); the larger the amplitude the shorter the reaction time.

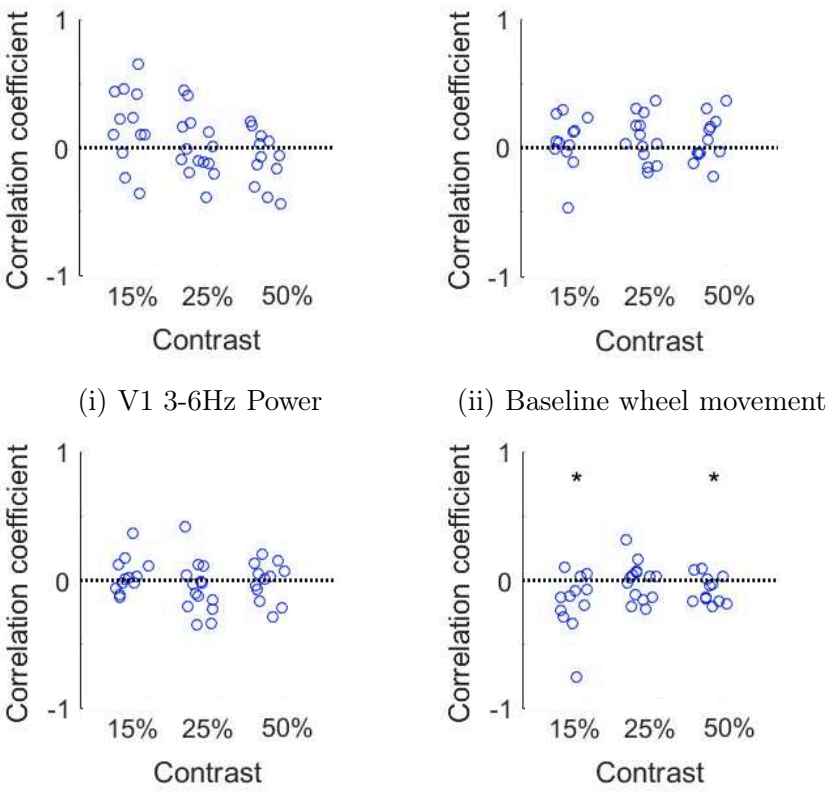

(i) V1 3-6Hz Power

(ii) Baseline wheel movement

(iii) Time since last movement

(iv) Reaction Time.

Figure 4.10: V1 stimulus response correlations.
Circles represent individual datasets. Mean correlations with average confidence intervals:
(i) 15% 0.18 (-0.29 0.46), 25% 0.01 (-0.33 0.29), 50% -0.09 (-0.43 0.26);
(ii) 15% 0.05 (-0.32 0.44), 25% 0.08 (-0.2 0.42), 50% 0.06 (-0.32 0.4);
(iii) 15% 0.04 (-0.45 0.33), 25% -0.06 (-0.37 0.26), 50% -0.01 (-0.39 0.32);
(iv) 15% -0.17 (-0.51 0.23), 25% -0.01 (-0.38 0.24), 50% -0.07 (-0.46 0.21).

Finally, I considered whether there was a difference in the extend of cortical activation around the centre of the response (Figure 4.11). There were no significant differences between the different contrasts nor between choice and neglect (Figure 4.12, $p>0.05$ 2-way ANOVA main effects contrast, behavioural condition).

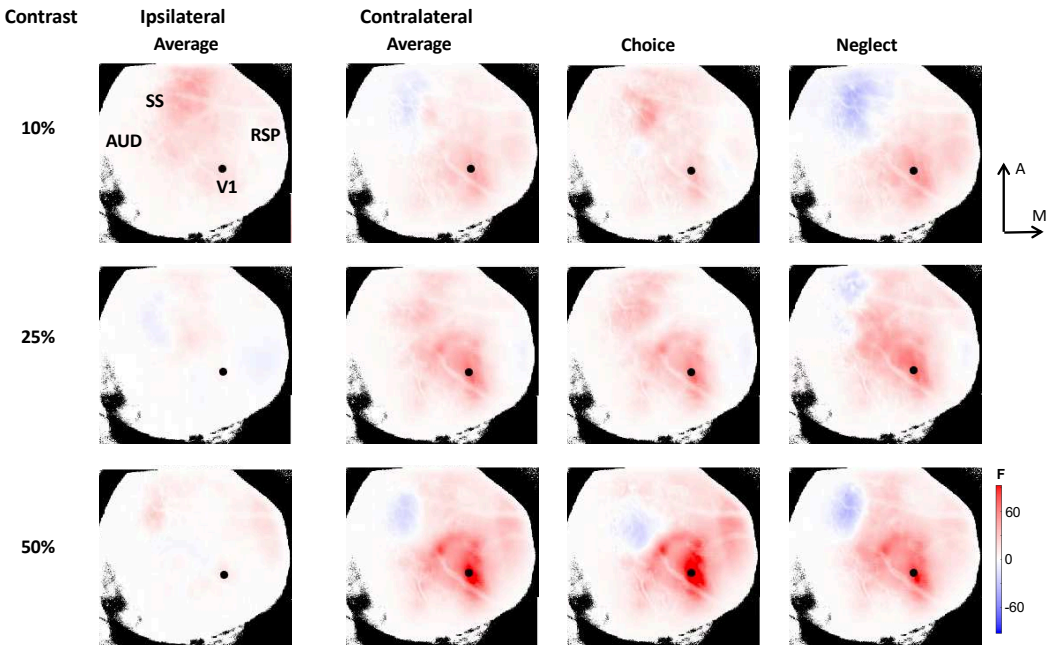

Figure 4.11: Spatial stimulus response example at the time point of the yellow highlight in Figure 4.8. Black dot indicates pixel from which the traces are shown in Figure 4.8. SS (somatosensory), AUD (auditory) and RSP (retrosplenial) cortex are indicated for reference only.

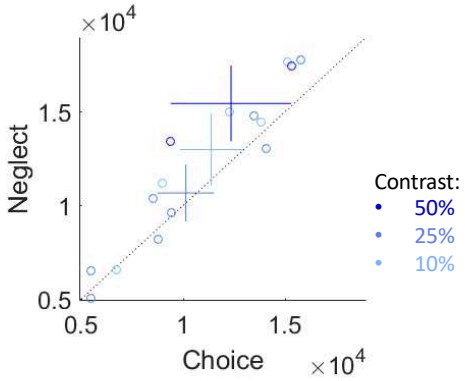

Figure 4.12: Spatial extend of choice versus neglect stimulus responses in V1. Circles represent individual datasets, bars represent mean and SEM.

In sum, although I observed the typical variability in stimulus responses in V1, I did not find a consistent relationship between this variability and a behavioural measure. It is possible that stimulus responses do not correlate with behaviour in this task, or a larger dataset may be required to detect an effect.

4.1.2 Cortical state fluctuations are mostly global

The aim of my experiments was to determine whether cortical state fluctuations are global, or whether local differences can occur. Therefore, I next asked whether the increase in desynchronisation during choice trials was specific to visual cortex, or whether this was a global feature of task engagement.

To assess cortical state across as many regions of interest (ROIs) as possible, I combined the experiments performed by myself and Nick Steinmetz. In my experiments, the left cortical hemisphere was imaged unilaterally which provided data from all sensory cortices (visual, auditory and somatosensory) as well as retrosplenial cortex. In Nick's experiments, the entire dorsal surface was imaged, which provided data from visual, somatosensory, retrosplenial and motor cortex.

I found a global decrease in 3-6Hz power which was significant in visual, somatosensory, secondary motor and retrosplenial cortex but not auditory cortex (one-sample t-tests per ROI, Figure 4.13). Contrary to expectation, I found the largest effect occurred not in visual cortex but in somatosensory cortex, which was significantly more desynchronised than visual, auditory and retrosplenial cortex but not motor cortex ($p<0.001$; SS vs AUD, RSP $p<0.01$, SS vs VIS $p<0.05$, SS vs MO $p>0.05$, one-way ANOVA). In addition, visual cortex was also significantly more desynchronised than auditory cortex ($p<0.05$, on-way ANOVA).

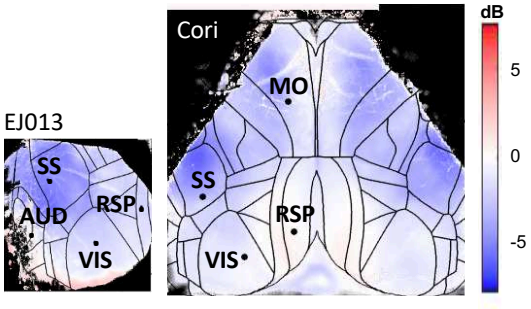

(i) Example Power Difference Maps in uni- and bilaterally imaged animals.

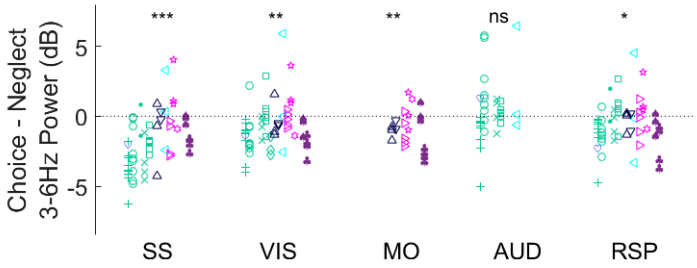

(ii) Summary across all experiments in selected ROIs.

Figure 4.13: 3-6Hz power differences between choice and neglect trials.
SS: somatosensory cortex, VIS: visual cortex, MO: motor cortex, AUD: auditory cortex, RSP: retrosplenial cortex.
Different colours indicate genotypes, different symbols different mice (same convention as in Figure 4.7).
Mean power differences per ROI with SEM: SS -1.74 +/-0.28dB, VIS -0.72 +/-0.23dB, MO -0.85 +/- 0.30, AUD 0.45 +/-0.40dB, RSP -0.53 +/-0.22dB
*** $p<0.001$; ** $p<0.01$; * $p<0.05$; ns: non significant; one-sample t-tests.

There was no difference in low frequency power prior to correct and incorrect choice trials (Figure 4.14) and I subsequently kept them grouped together under Choice trials. This suggested the difference in cortical state was more correlated with arousal and engagement than performance.

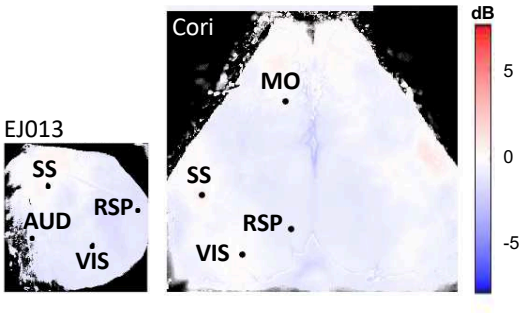

(i) Example Power Difference Maps in uni- and bilaterally imaged animals.

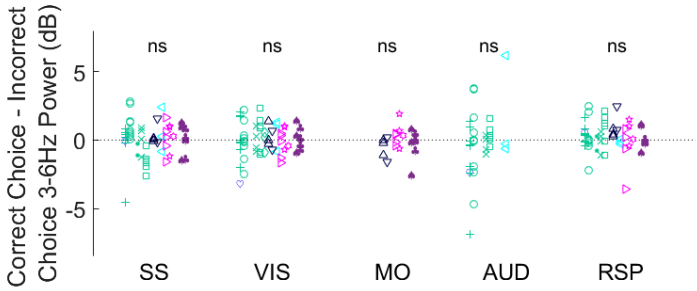

(ii) Summary across all experiments in selected ROIs.

Figure 4.14: 3-6Hz power differences between correct choice and incorrect choice trials.
Mean power differences per ROI with SEM: SS 0.06 +/-0.18dB, VIS 0.10 +/-0.16dB, MO -0.05 +/- 0.2dB, AUD -0.17 +/-0.43dB, RSP 0.26 +/-0.14dB.

In addition, cortical state also correlated with reaction time. Choice trials for which the pre-stimulus baseline showed less low frequency power had faster reaction times (Figure 4.15). The strength of this correlation differed between areas and the strongest correlations were seen in somatosensory cortex ($p<0.001$; SS vs RSP $p<0.001$, SS vs VIS, AUD $p<0.01$, SS vs MO $p>0.05$; one-way ANOVA).

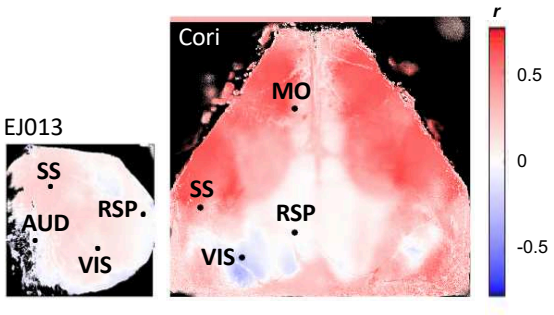

(i) Example Power-Reaction Time Correlation Maps in uni- and bilaterally imaged animals.

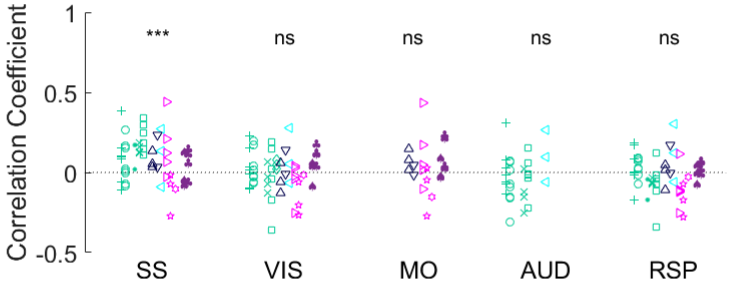

(ii) Summary across all experiments in selected ROIs.

Figure 4.15: Correlation between 3-6Hz power and reaction time.
Mean correlation per ROI with average confidence intervals: SS 0.092 (0.018-0.022), VIS 0.005 (0.018-0.019), MO 0.048 (0.028-0.039), AUD -0.027 (0.025-0.029), RSP -0.014 (0.018-0.019).

Altogether, these results suggested that although cortical state did not predict success, it predicted how quickly an animal responded to a stimulus, which further supported the idea that cortical desynchronisation related to task engagement and not performance.

4.1.3 Movement does not explain the differences in cortical states

Running is associated with more desynchronised states (Vinck et al., 2015). In the decision making tasks that I described, the mice could not run but their forepaws were free to move the steering wheel with which they provided responses, and this type of movement could still have had an effect on cortical state. The existence of a correlation between state and reaction time but not state and accuracy particularly suggested that cortical state might be related to an increased inclination to make movements. I therefore next asked to what degree movement was driving the differences in cortical state between choice and neglect trials.

During engaged periods (when the animal was making choice responses), animals were more likely to make wheel movements during the pre-stimulus baseline period than during periods of disengagement (when the animal was giving neglect responses) (Figure 4.16).

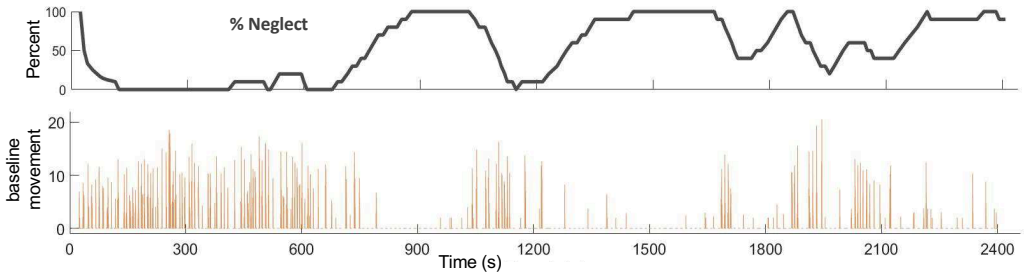

Figure 4.16: Animals move more during the baseline during engaged periods. Top: Percent neglect trials over time. Bottom: Wheel movement per baseline over time.

However, all animals were trained to initiate trials by holding the steering

wheel still: stimuli would only appear after a quiescent period (QP) of at least 1 second with no wheel movement. This meant that any baseline wheel movement that occurred was restricted to the beginning of the baseline period and that each baseline ended with a period of no movement (Figure 4.17).

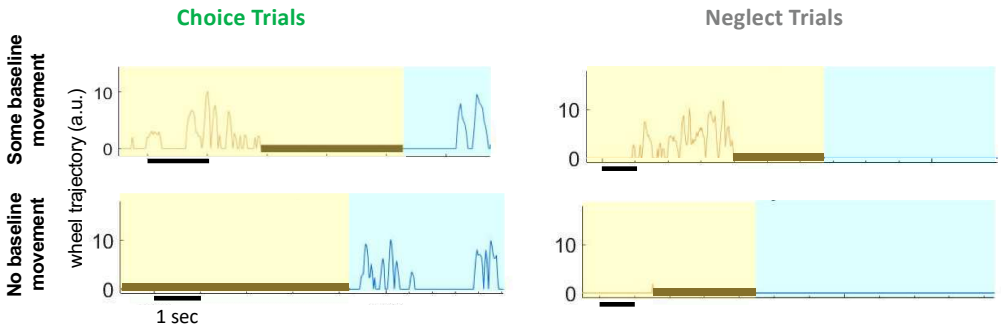

Figure 4.17: Example trials showing wheel movement during baseline.
Choice (left column) and Neglect (right column) trial examples with some (top row) and no (bottom row) baseline movement.
Yellow background: baseline period, blue background: stimulus on. Thick brown bar indicates the quiescent period.

The increased desynchronization prior to choice trials persisted when focusing the analysis on the quiescent periods (one-sample t-tests per ROI, Figure 4.18). Interestingly, auditory cortex also became significantly more desynchronised prior to choice trials during the quiescent period, and there was no longer a significant difference between visual and auditory cortex. Nevertheless, the biggest difference occurred again in somatosensory cortex, where the difference was significantly bigger than in all other ROIs but motor cortex ($p < 0.001$, one-way ANOVA).

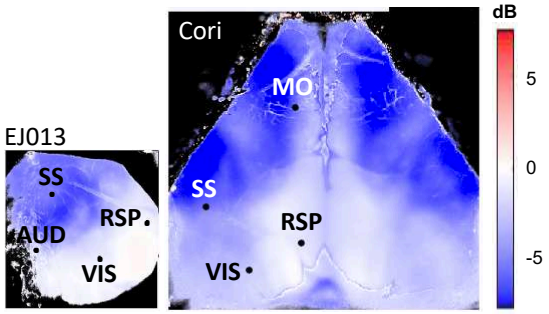

(i) Example Power Difference Maps in uni- and bilaterally imaged animals.

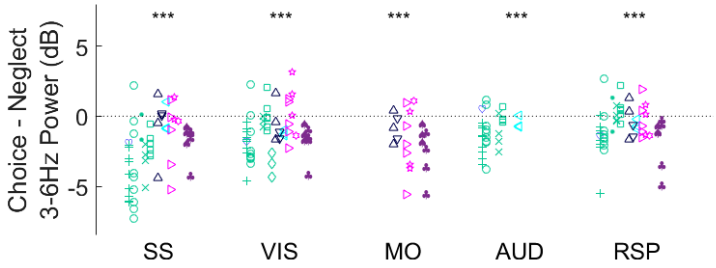

(ii) Summary across all experiments in selected ROIs.

Figure 4.18: 3-6Hz power differences between choice and neglect trials during the quiescent period.
Mean power differences per ROI with SEM: SS -2.20 +/-0.32dB, VIS -1.12 +/-0.22dB, MO -1.70 +/-0.42dB, AUD -1.04 +/-0.22dB, RSP -0.74 +/-0.20dB.

Since movements preceding the quiescent period might have continued to affect brain state during the quiescent period, I also repeated this analysis on trials during which the animal remained still throughout the entire ITI (including the period before the QP). This yielded the same results: prior to choice trials, there was less low frequency power than prior to neglect trials (one-sample t-tests per ROI, Figure 4.19).

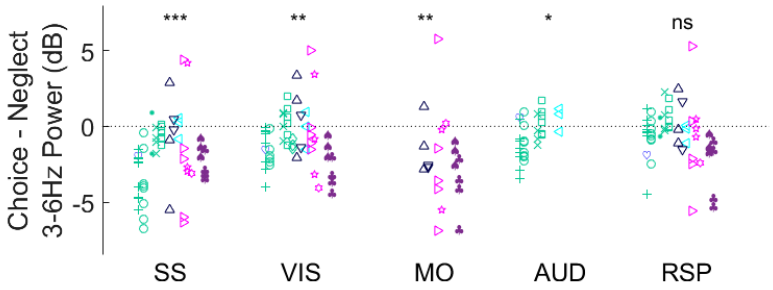

Figure 4.19: Summary 3-6Hz power differences between choice and neglect trials in trials with no baseline movement.
Mean power differences per ROI with SEM: SS -1.93 +/-0.33dB, VIS -0.81 +/-0.25dB, MO -2.58 +/-0.71dB, AUD -0.63 +/- 0.23dB, RSP -0.50 +/-0.25dB.

In addition, the correlation with subsequent reaction time persisted during the quiescent period (Figure 4.20; $p<0.001$, SS vs RSP $p<0.001$, SS vs VIS $p<0.01$, SS vs AUD, MO $p>0.05$, one-way ANOVA) and there was also no significant difference between correct and incorrect trials (Figure 4.21).

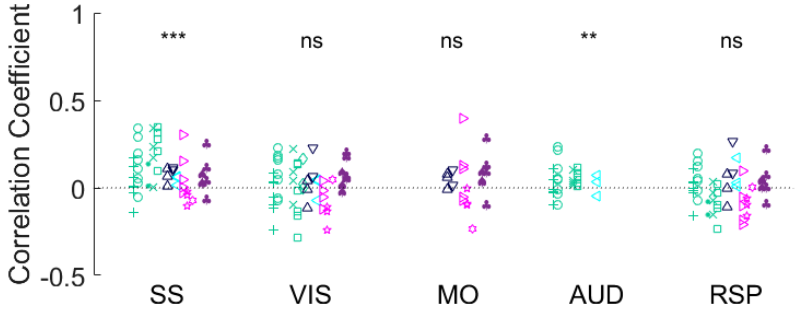

Figure 4.20: Summary correlations between 3-6Hz power and reaction time during the quiescent period.
Mean correlation per ROI with average confidence intervals: SS 0.1 (-0.08 0.27), VIS 0.02 (-0.17 0.2), MO 0.05 (-0.13 0.21), AUD 0.04 (-0.14 0.22), RSP -0.01 (-0.13 0.21).

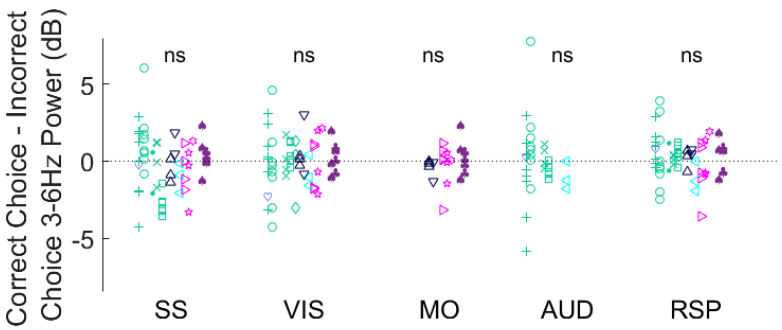

Figure 4.21: Summary 3-6Hz power differences between correct and incorrect choice trials during the quiescent period.
Mean power differences per ROI with SEM: SS 0 +/-0.32dB, VIS 0.26 +/-0.29dB, MO -0.08 +/-0.25dB, AUD -0.02 +/-0.4dB, RSP 0.22 +/-0.18dB

Altogether, these results suggested that desynchronisation was not driven by (overt) movement.

Desynchronisation does not reflect an increased tendency to move

Although the results from the previous section (4.1.3) suggested the desynchronisation prior to choice trials was not driven by ongoing movement, these results did not exclude the possibility that desynchronisation may reflect an ongoing state in which animals had an increased tendency to move. In order to distinguish between this possibility, and the alternate possibility that the desynchronisation might relate to a cognitive state of engagement, I looked at the data from the tasks in which a correct response did not always require a wheel movement: the 2AUC tasks that included zero-contrast trials when the mice had to withhold movement and keep the steering wheel still to receive a reward. This provided a trial type during which the response and movement pattern was the same as during neglect trials but where the cognitive state would have been different.

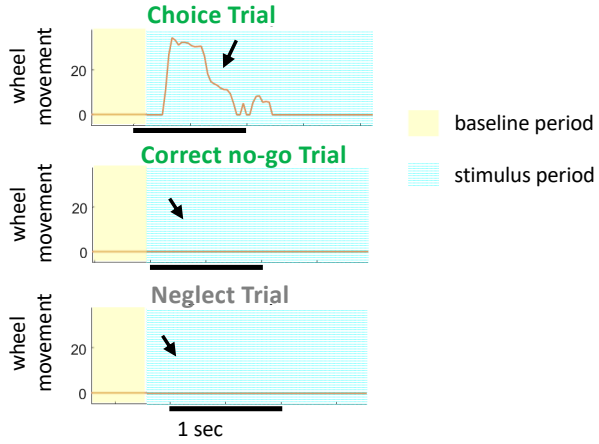

Figure 4.22: Example wheel traces during the stimulus period.

In the 2AUC task, trials were classified into 4 types (Figure 4.22): correct and incorrect choices (where a stimulus was present and the wheel was moved); correct no-go (where no stimulus was present and the wheel was not moved); and neglect (where a stimulus was present but the wheel was not moved). Providing a response during a no-go trial was considered an incorrect choice.

Consistent with desynchronization reflecting increased cognitive engagement rather than an inclination toward movement, correct no-go trials showed a similar pattern of desynchronization as choice trials (Figures 4.23 and 4.24).

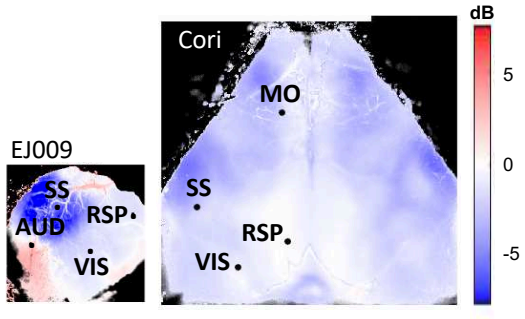

(i) Example Power Difference Maps in uni- and bilaterally imaged animals.

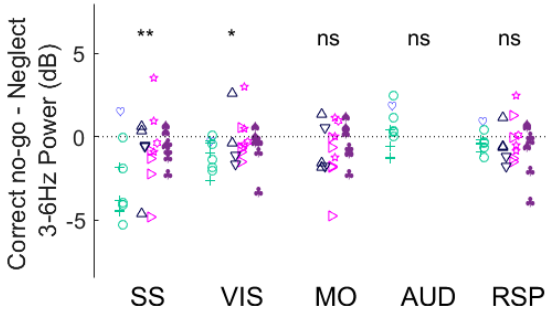

(ii) Summary across all experiments in selected ROIs.

Figure 4.23: 3-6Hz power differences between correct no-go and neglect trials. Mean power differences per ROI with SEM: SS -1.4 +/-0.39dB, VIS -0.49 +/-0.23dB, MO -0.65 +/-0.33dB, AUD 0.35 +/-0.42dB, RSP -0.41 +/-0.21dB.

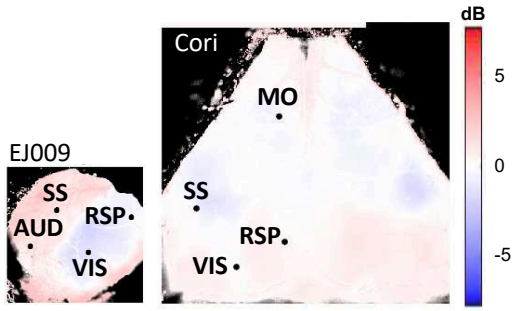

(i) Example Power Difference Maps in uni- and bilaterally imaged animals.

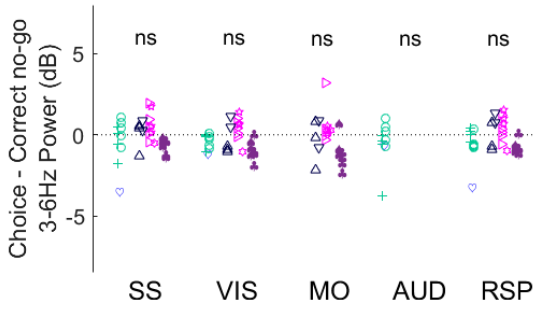

(ii) Summary across all experiments in selected ROIs.

Figure 4.24: 3-6Hz power differences between choice and correct no-go trials. Mean power differences per ROI with SEM: SS -0.07+/-0.19dB, VIS -0.24 +/-0.15dB, MO -0.2 +/-0.28dB, AUD -0.47 +/-0.42dB, RSP -0.19 +/-0.17dB.

The difference in cortical state is not driven by whisking

Given that the biggest difference occurred in somatosensory cortex, one possibility was that this was driven by increased whisking when the animal was engaged. I therefore quantified the amount of whisking in choice and neglect trials and found that there was no difference (Figure 4.25, $p<0.05$ t-test).

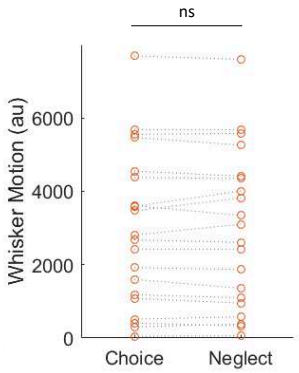

Figure 4.25: Average whisker motion in choice and neglect trials.
Each circle represents a dataset, the dotted line connects the corresponding choice and neglect averages from each dataset.

In conclusion, I have shown that the difference in cortical state prior to choice and correct no-go trials could not be explained by ongoing movements nor an increased tendency to move. Instead, I suggest that the difference in cortical state reflected a difference in cognitive state. Nevertheless, it is of course possible and indeed likely that there is a difference in muscle tone between the synchronised and desynchronised state, and that the desynchronised state during correct no-go trials reflect successful suppression of movement (discussed in more depth in Chapter 5).

4.1.4 Variations in cortical states are not fully explained by variations in pupil

Pupil diameter is known to better correlate with brain state than movement, and also correlates with mental effort in humans (de Gee et al., 2014; Kahneman and Beatty, 1966; McGinley et al., 2015). I therefore asked how pupil diameter related to engagement and brain state, and whether a common effect of pupil size could explain the correlation between them.

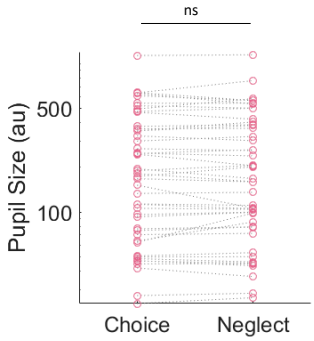

Figure 4.26: Average pupil sizes in choice and neglect trials.
Each circle represents a dataset, the dotted line connects the corresponding choice and neglect averages from each dataset.

There was no difference in baseline pupil size between choice and neglect trials (Figure 4.26; $p>0.05$, t-test), however, pupil size correlated negatively with low frequency power: the smaller the pupil, the greater the low frequency power (Figure 4.27). Nevertheless, pupil size did not fully explain the state-engagement correlation: even restricted to trials with similar pupil sizes, there was significantly less low frequency power in choice than neglect trials (Figure 4.27, ANCOVA).

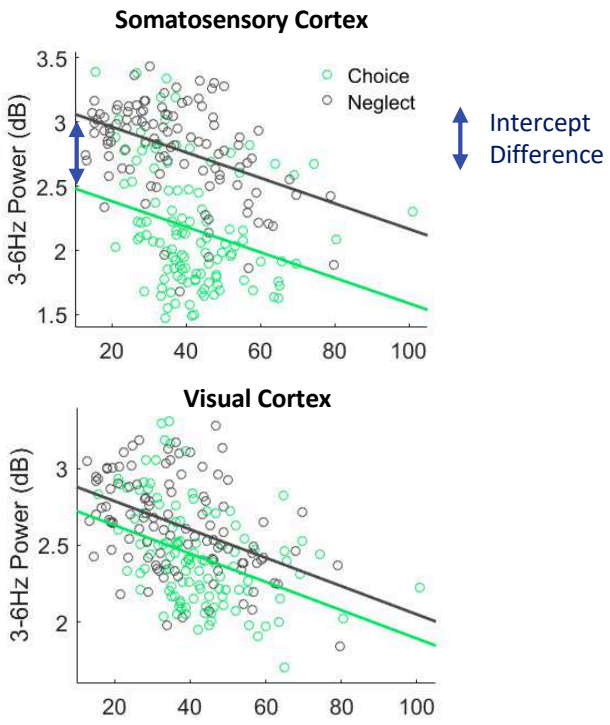

Figure 4.27: 3-6Hz Power as a function of pupil size in choice and neglect trials. Example of a typical dataset, each circle represents a trial.

A consistent effect of behavioral condition on the relationship between pupil size and low frequency power was present in all ROIs except for auditory cortex (Figure 4.28, one-sample t-tests per ROI). The biggest effect of behaviour was again seen in somatosensory cortex, which was significantly different from visual, auditory and retrosplenial cortex ($p<0.001$, ANOVA).

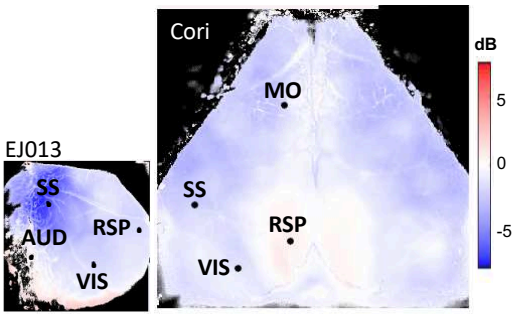

(i) Example 'Intercept Difference' Maps in uni- and bilaterally imaged animals.

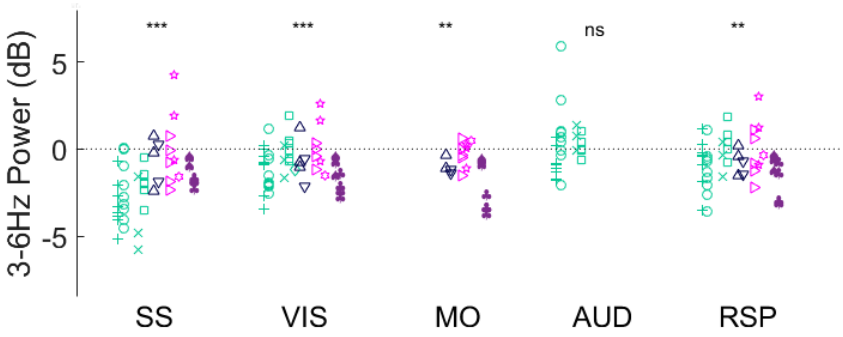

(ii) Summary across all experiments in selected ROIs.

Figure 4.28: Intercept differences between choice and neglect power as a function of pupil size.
Mean intercept differences per ROI with SEM: SS -1.76 +/-0.28dB, VIS -0.77 +/-0.18dB, MO -1.01 +/-0.28dB, AUD 0.21 +/-0.32dB, RSP -0.64 +/-0.2dB.

When looking at the relationship between pupil size and low frequency power during the quiescent period, the same result persisted: pupil size did not fully explain the state-engagement correlation, and there remained a significant effect of behavioural condition. This was now present in all ROIs including auditory cortex (Figure 4.29, one-sample t-tests per ROI), which followed the previous result that auditory cortex also desynchronised during the quiescent period (Section 4.1.3, Figure 4.18). The effect in somatosensory cortex was still significantly bigger than all other ROIs except secondary motor cortex ($p<0.001$, ANOVA).

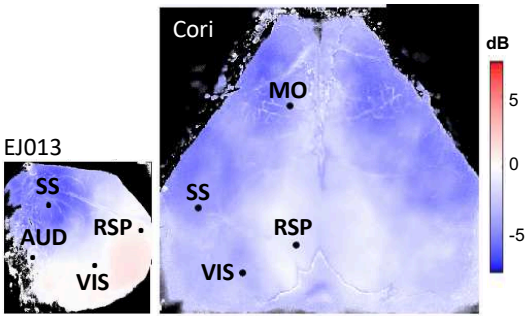

(i) Example 'Intercept Difference' Maps in uni- and bilaterally imaged animals.

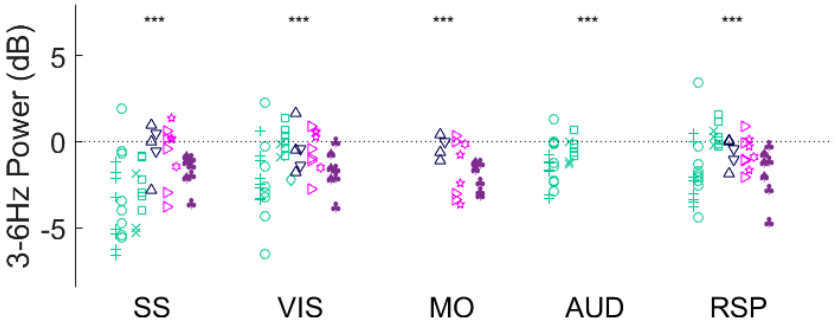

(ii) Summary across all experiments in selected ROIs.

Figure 4.29: Intercept differences between choice and neglect power as a function of pupil size during the quiescent period.
Mean intercept differences per ROI with SEM: SS -2.34 +/-0.36dB, VIS -1.2 +/-0.25dB, MO -1.3 +/-0.3dB, AUD -1.05 +/-0.22dB, RSP -1.03 +/-0.24dB.

In the 2AUC task, there was a significant difference in low frequency power between correct no-go and neglect trials (Figure 4.30) but not between choice and correct no-go trials during trials with similar pupil size (Figure 4.31).

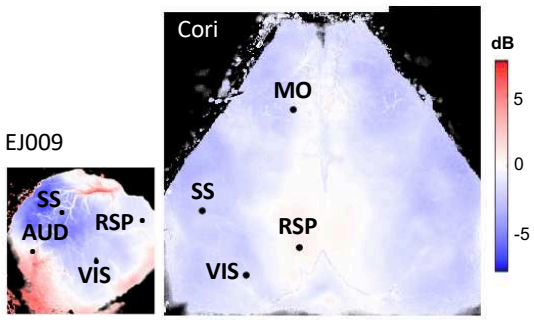

(i) Example 'Intercept Difference' Maps in uni- and bilaterally imaged animals.

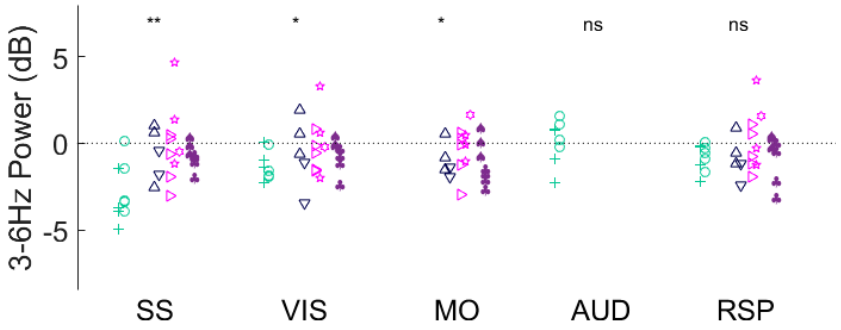

(ii) Summary across all experiments in selected ROIs.

Figure 4.30: Intercept differences between correct no-go and neglect power as a function of pupil size.
Mean intercept differences per ROI with SEM: SS -1.14 +/-0.37dB, VIS -0.6 +/-0.25dB, MO -0.7 +/-0.28dB, AUD 0.09 +/-0.41dB, RSP -0.5 +/-0.25dB.

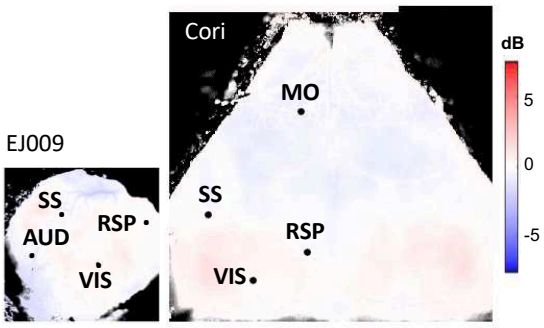

(i) Example 'Intercept Difference' Maps in uni- and bilaterally imaged animals.

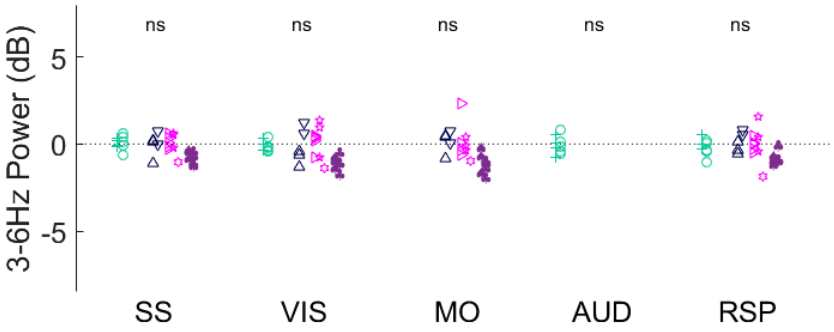

(ii) Summary across all experiments in selected ROIs.

Figure 4.31: Intercept differences between choice and correct no-go power as a function of pupil size.
Mean intercept differences per ROI with SEM: SS -0.1 +/-0.1dB, VIS -0.24 +/-0.14dB, MO -0.29 +/-0.2dB, AUD -0.06 +/-0.18, RSP -0.21 +/-0.13dB.

Altogether, these results suggest that a general measure of arousal, as indicated by pupil size, was not sufficient to explain the difference in cortical state between choice and neglect trials; if it were, the degree of synchronisation should have been entirely predicted by pupil size. Instead, whether the animal was engaged (choice and correct no-go trials) or disengaged (neglect trials) significantly improved the prediction of cortical state, further indicating that the observed engaged state corresponded to a cognitive state of engagement.

4.1.5 Reward has a lasting effect on cortical state

I have shown that cortical state was desynchronised across cortex during the baseline period prior to choice trials, and that this was the case regardless of whether the animal made a correct or incorrect choice (Section 4.1.2). I next asked whether this effect persisted after the trial had ended. In order to look at the trial end and thereby, any possible effects of trial outcome, I analysed the baseline period of the *subsequent* trial. Surprisingly, I discovered that cortical state differed following correct and incorrect trials, suggesting that cortical state could be influenced by reward.

To exclude possible effects of the action of reward consumption itself, I restricted the analysis to the quiescent period of the following trial when the animals were no longer moving the steering wheel. By then the animals had finished licking in 98% of trials (6148/6250, data not shown).

There was a significant difference between correct and incorrect choice trials in somatosensory, visual and secondary motor cortex during the quiescent period of the subsequent trials (Figure 4.32). Since both correct and incorrect trials involved moving the wheel to provide a choice, but only correct trials were rewarded, this suggested that reward was the factor driving the difference in cortical state.

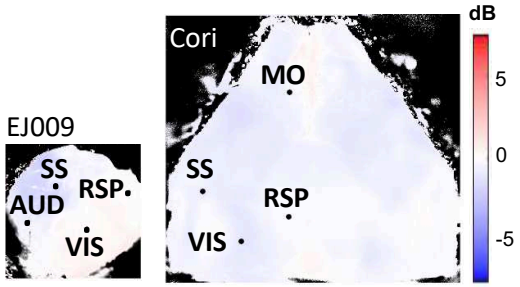

(i) Example Power Difference Maps in uni- and bilaterally imaged animals.

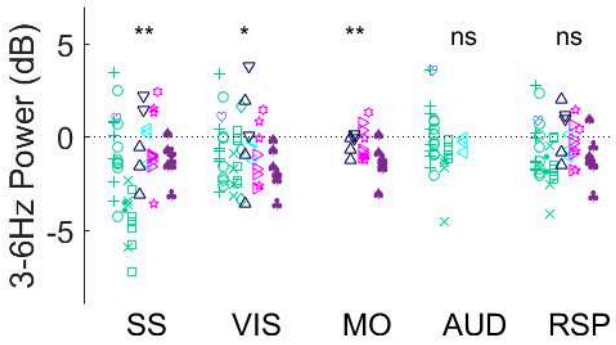

(ii) Summary across all experiments in selected ROIs.

Figure 4.32: Post response 3-6Hz power differences between correct choice and incorrect choice trials.
Mean power differences per ROI with SEM: SS -2.14 +/-0.44dB, VIS -0.96 +/-0.37dB, MO -1.67 +/-0.4dB, AUD -0.93 +/-0.37dB, RSP -0.89 +/-0.38dB.

I next compared correct no-go and neglect responses (Figure 4.33): these trial types were both characterised by no movement, but equally only one of them was rewarded. Again, there was significant desynchronisation after the rewarded trial, this time everywhere except for auditory cortex (Figure 4.33).

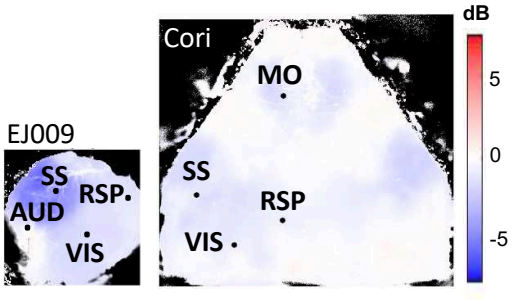

(i) Example Power Difference Maps in uni- and bilaterally imaged animals.

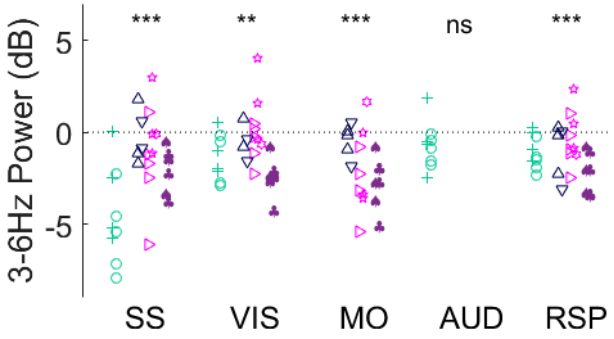

(ii) Summary across all experiments in selected ROIs.

Figure 4.33: Post response 3-6Hz power differences between correct no-go and neglect trials.
Mean power differences per ROI with SEM: SS -2.19 +/-0.49dB, VIS -0.96 +/-0.3dB, MO -1.83 +/-0.4dB, AUD -0.73 +/-0.44dB, RSP -1.1 +/-0.25dB.

Correct and incorrect choices as well as correct no-go trials were associated with an engaged state (Sections 4.1.2 and 4.1.3). Thus, in the correct and incorrect choice comparison, the difference was indeed most likely driven by the reward. However, in the correct no-go and neglect comparison, it is possible that the difference was at least partly due to the already existing difference in brain state between these trial types. In order to make a further comparison of trial types that were both engaged but where only one type was rewarded, I looked at the difference between correct no-go and incorrect choice trials (Figure 4.34). In this case, there was only a significant difference

in visual cortex, which was more desynchronised after the correct no-go trials.

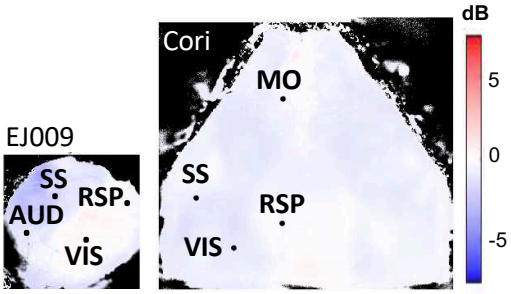

(i) Example Power Difference Maps in uni- and bilaterally imaged animals.

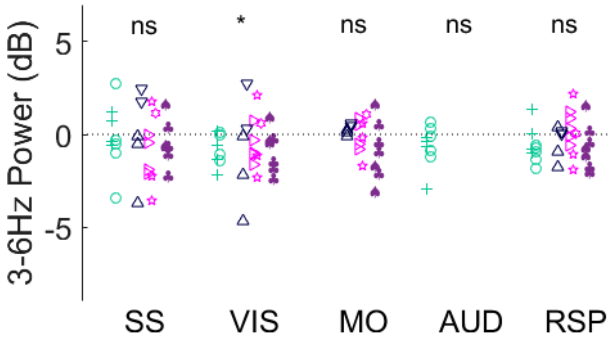

(ii) Summary across all experiments in selected ROIs.

Figure 4.34: Post response 3-6Hz power differences between correct no-go and incorrect choice trials.
Mean power differences per ROI with SEM: SS -0.39 +/-0.31dB, VIS -0.64 +/-0.27dB, MO -0.16 +/-0.26dB, AUD -0.59 +/-0.37dB, MO -0.16 +/-0.26dB.

Finally, I also compared correct choice and correct no-go trials: both trial types were characterised by an engaged state, both resulted in a reward, however they required different responses: movement in the correct choice trials, and withheld movement in the correct no-go trials (Figure 4.35). Interestingly, there was a significant difference in visual and secondary motor cortex, suggesting that the combination of movement and reward had a more powerful effect on cortical state in these ROIs than reward alone.

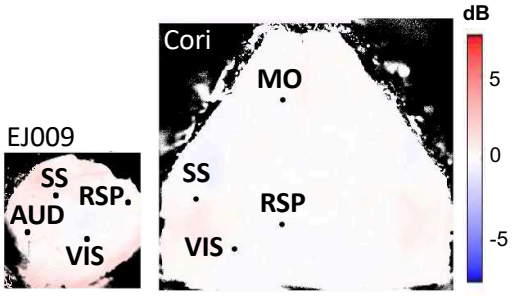

(i) Example Power Difference Maps in uni- and bilaterally imaged animals.

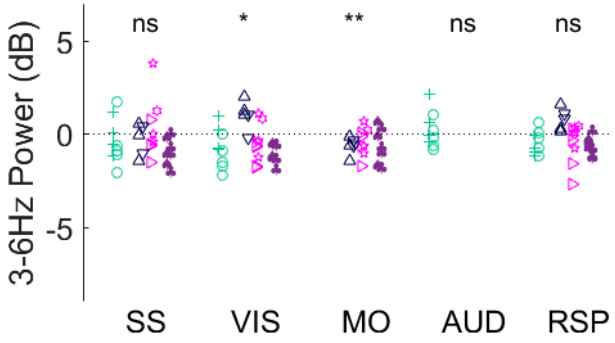

(ii) Summary across all experiments in selected ROIs.

Figure 4.35: Post response 3-6Hz power differences between correct choice and correct no-go trials.
Mean power differences per ROI with SEM: SS -0.24 +/-0.23dB, VIS -0.43 +/-0.2dB, MO -0.47 +/-0.17dB, AUD 0.21 +/-0.33dB, RSP -0.28 +/-0.16dB.

In summary, these results reveal a previously unrecognised effect of reward on cortical state. In contrast to the engagement related cortical state differences, the effect of reward was not global and may depend on what action lead to the rewarded outcome.

Effect of white noise in incorrect trials

In some of the animals, incorrect responses (incorrect choices or neglects) were accompanied by a white noise burst during the time-out. It is possible that time-out alone versus time-out with white noise burst had different effects on cortical state. To investigate this, I computed the "correct - neglect" and "correct - incorrect" post-response power differences (with the same procedure that was used to assess the reward effect), and asked whether there was a difference between animals that had or had not received a white noise burst. (All animals trained in the 2AUC version of the task were trained with a white noise burst, therefore I could not make any comparisons with correct no-go trials. Similarly, all bilaterally imaged animals were trained with a white noise burst, therefore I could not assess the effect in motor cortex.)

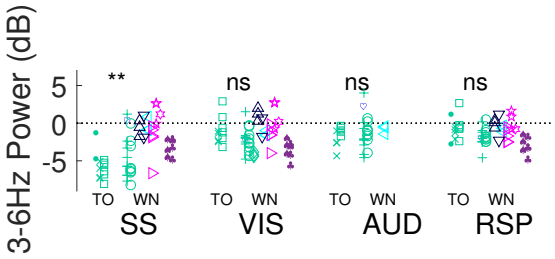

Figure 4.36: Summary post response 3-6Hz power differences between correct and neglect trials, comparing time-out only (TO) and white noise burst (WN) datasets. ** and ns indicate whether there was a significant difference between TO and WN.

When comparing the "correct - neglect" post response power, there was no effect of whether or not a noise burst was present except in somatosensory cortex, where the difference between correct and neglect low frequency power was significantly bigger in the time-out only than the noise burst condition (Figure 4.36).

However, when comparing the "correct - incorrect" post response power, the difference between correct and incorrect power was significantly bigger in the time-out only than the noise burst condition everywhere except in visual cortex (Figure 4.37).

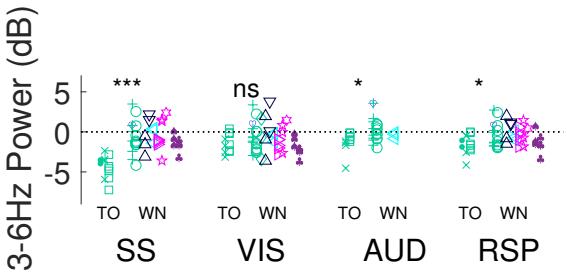

Figure 4.37: Summary post response 3-6Hz power differences between correct and incorrect trials, comparing time-out only (TO) and white noise burst (WN) datasets.
***, * and ns indicate whether there was a significant difference between TO and WN.

Altogether, these results suggest that the white noise burst may have had a desynchronising effect as well: since reward is desynchronising, if the white noise also had a desynchronising effect, this would lead to a smaller difference between rewarded and white noise comparisons than between rewarded and time-out only comparisons. The white noise burst is designed to be unpleasant and a mild punishment, which may therefore have an effect on arousal and thus also on cortical state.

4.1.6 Summary & Conclusions

In this section, I have shown that:

- Fluctuations in the level of engagement in a visual decision making task correlated with fluctuations in cortical state.

I started by showing that this is the case in visual cortex; the area of the cortex that is processing the stimuli that are task relevant. I then considered other cortical regions of interest, and to be able to assess state fluctuations in as many cortical areas as possible, I combined experiments performed by myself and a postdoctoral researcher in the group, which allowed me to evaluate state fluctuations in auditory, somatosensory, secondary motor and retrosplenial cortex. I thus found that:

- The cortical state fluctuations were mostly global,
- Although auditory cortex did not significantly desynchronise unless periods of wheel movement were excluded.
- Surprisingly, the biggest difference between engaged (choice) and disengaged (neglect) trials occurred in somatosensory cortex.

I then asked whether the differences in cortical state were driven by movement or reflected a more cognitive state of engagement by excluding periods of wheel movement during the baseline, and found that:

- Movement did not explain the differences in cortical states,
- Except in auditory cortex, which became desynchronised like the rest of the cortical ROIs during the quiescent periods of engaged trials.

I looked at the data from tasks that included a no-go response option, which required the animals to refrain from moving the wheel in zero contrast trials. By looking at the brain state in these trials, I could ask whether the desynchronisation in choice trials was related to an increased likelihood of making *any* movement, since there was no difference between correct and incorrect choice trials.

- Cortical state was more desynchronised during correct no-go and neglect trials and there was no difference between choice and correct no-go trials, suggesting that
- A desynchronised state was not a state of increased likelihood of moving.

I also asked whether whisking, which is another form of movement unrelated to making a response, was correlated with the differences in cortical state and found that:

- Whisking did not explain the differences in cortical state,
- Suggesting that the effect in somatosensory cortex was not caused by differences in whisking.

Next, I asked to what extend the cortical state changes could be explained by a measure of global arousal: pupil size. I found that:

- Although there was no difference in pupil size between choice and neglect trials,
- There was a negative correlation between pupil size and low frequency power: the more synchronised the brain state the smaller the pupil size.

- However, behavioural state (engaged or disengaged) had a significant additional effect on cortical state that could not be explained by pupil size alone: behavioural state significantly improved the prediction of low frequency power from pupil size.

Finally, I discovered a:

- Long-lasting effect of reward on cortical state,
- which was not global,
- and that may depend on the action leading to the reward.

Altogether, these results suggest that cortical desynchronisation is associated with a cognitive state of engagement that can be distinguished from purely arousal related factors such as movement and pupil size. The implications of the results as well as the observation that the largest effect occurred in an unexpected cortical region will be discussed in Chapter 5 (*Discussion*).

4.2 Brain state fluctuations during auditory 2AFC and auditory distractor tasks

In the following section, I will repeat the analyses that I presented in the visual task section (4.1) but apply them to the auditory 2AFC and auditory distractor tasks. I was the only one in the lab training animals on these task variations and since I used the laterilized widefield imaging preparation that allowed me to include auditory cortex in my imaging window, I could analyse cortical state changes in visual, auditory, somatosensory and retrosplenial, but not secondary motor cortex. Apart from the absence of secondary motor cortex, all the analyses procedures are the same.

Since in the visual task, auditory cortex desynchronisation depended on whether or not the animal was moving, I will pay special attention to the following question:

- Does movement suppress auditory cortex desynchronisation in the auditory 2AFC and the auditory distractor task as well?

In addition, since I found the biggest difference in cortical state between engaged and disengaged periods in somatosensory cortex, I will also ask:

- Is the biggest effect in the auditory 2AFC and auditory distractor tasks also in somatosensory cortex?

Performance in the auditory 2AFC and auditory distractor tasks

I trained 3 animals to perform a head-fixed auditory 2AFC task (see Methods Section 2.3). The mice indicated whether tone pips were of high (15kHz) or low (8kHz) tonal frequency by turning a steering wheel (identical to the visual tasks) which modulated the tonal frequency, and the aim of the task was to bring the tonal frequency to a central tone target (11kHz).

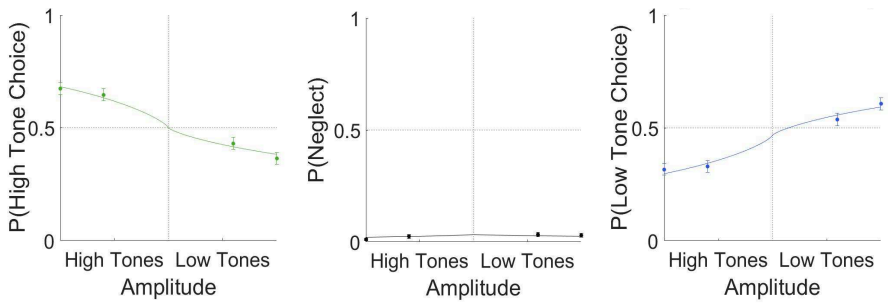

Figure 4.38: Psychometric curve from the auditory 2AFC task.
n = 8 experiments from 1 example animal. Errorbars represent SEM.

I also used 2 animals that had learned the visual task but failed to learn the auditory task (see Chapter 3, Section 3.2.2) as "controls" by exposing them to auditory stimuli that were irrelevant during the visual task (see Methods Section 2.3). I carefully compared the behaviour of the animals during the visual and auditory distractor tasks and found they ignored the auditory stimuli and produced psychometric curves that were entirely dependent on visual stimuli (Figure 4.39, plus other data that is not shown).

As in the visual task, the datasets from the auditory 2AFC and auditory distractor tasks contained neglect trials that often occurred in sequence, indicating periods of neglect during task performance (Figure 4.40).

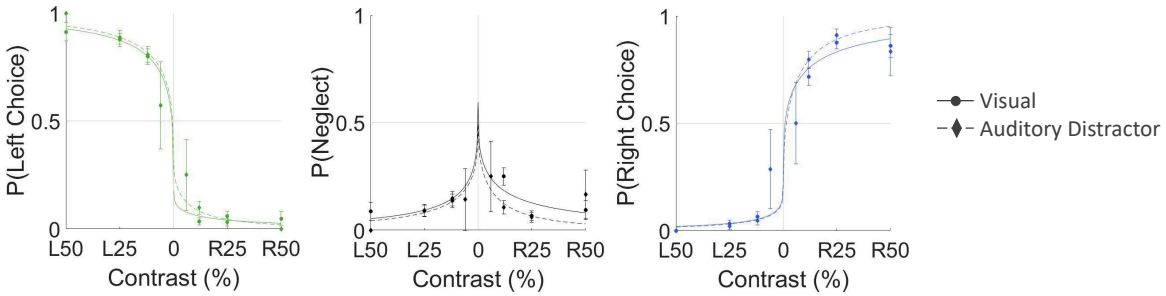

Figure 4.39: Psychometric curves from the visual 2AFC and auditory distractor tasks.
n = 10 and 9 experiments respectively from 2 animals. Errorbars represent SEM.

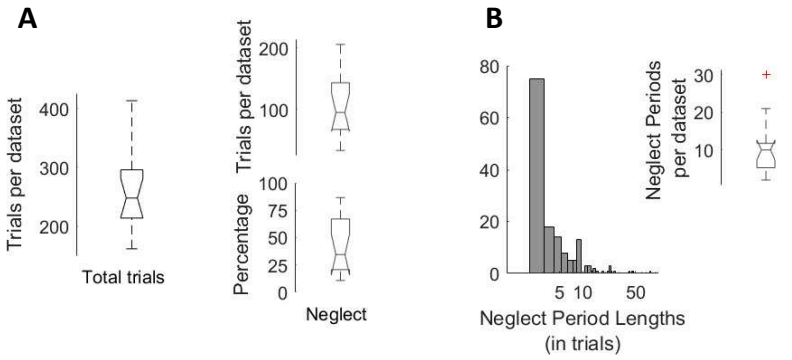

(i) Auditory 2AFC

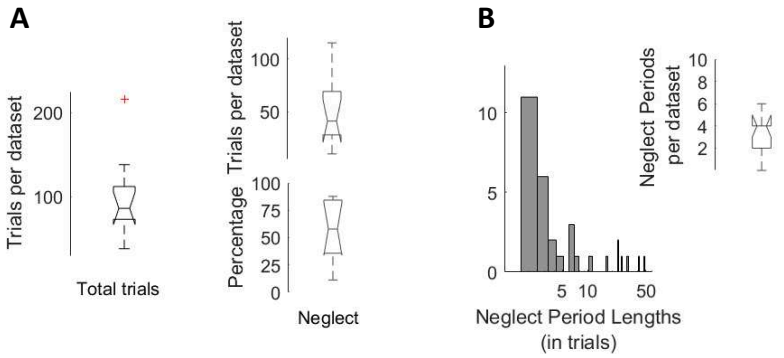

(ii) Auditory Distractor

Figure 4.40: Neglect trial occurrences in the auditory 2AFC (i) and auditory distractor (ii) tasks.
A. Overall neglect trial occurrences.
B. Neglect period occurrences and lengths.

4.2.1 Movement differently affects state in auditory cortex depending on whether auditory stimuli are relevant or not

In the visual task, I had found that unless I excluded periods when the animal was moving the wheel, visual cortex was more desynchronised than auditory cortex, which remained synchronised (Section 4.1.2, Figure 4.13). I therefore asked if I would see the same or a different pattern in the auditory task. If the same pattern occurs, this would suggest that movement suppresses auditory cortex desynchronisation. If instead auditory cortex desynchronised in the auditory 2AFC but not auditory distractor task, this would suggest that whether or not auditory stimuli are relevant determines whether movement suppresses auditory cortex desynchronisation or not.

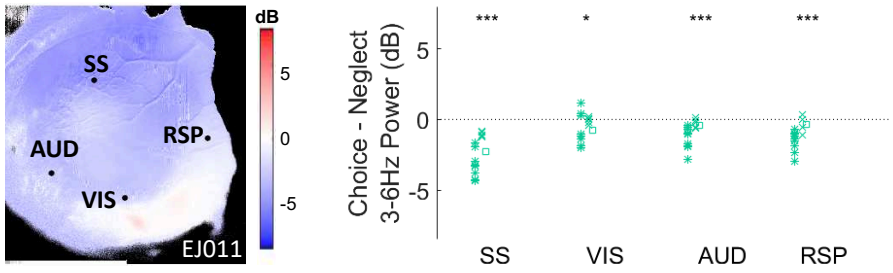

(i) Example Power Difference Map.

(ii) Summary across all experiments in selected ROIs.

Figure 4.41: 3-6Hz power differences between choice and neglect trials in the auditory 2AFC task.
Mean power differences per ROI with SEM: SS -2.33 +/-0.33, VIS -0.59 +/-0.26dB, AUD -0.92 +/-0.22dB, RSP -1.08 +/-0.23dB.

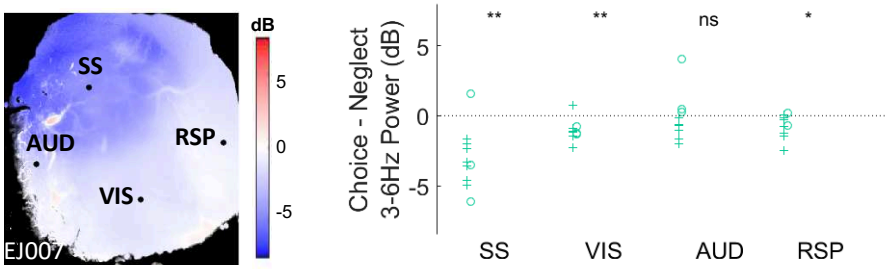

(i) Example Power Difference Map.

(ii) Summary across all experiments in selected ROIs.

Figure 4.42: 3-6Hz power differences between choice and neglect trials in the auditory distractor task.
Mean power differences per ROI with SEM: SS -3.05 +/-0.7dB, VIS -1.06 +/-0.25dB, AUD -0.24 +/-0.57dB, RSP -0.75 +/-0.27dB.

Interestingly, the results support the the latter option (Figures 4.41 and 4.42). Indeed, auditory cortex was significantly more desynchronised in the auditory task than in the visual task, but not the auditory distractor task ($p < 0.05$ and $p > 0.05$, respectively, t-test). There was no difference in visual cortex desynchronisation between the auditory and the visual task, nor were there any differences in any ROI desynchronisation between the visual and auditory distractor task. However, in both auditory 2AFC and auditory distractor tasks, somatosensory cortex showed the biggest effect (p=5.6e-5, SS vs AUD, RSP $p < 0.01$, SS vs VIS $p < 0.001$ in the auditory 2AFC task; p=8e-4, SS vs AUD $p< 0.001$, SS vs RSP $p < 0.01$, SS vs VIS $p < 0.05$ in the auditory distractor task; ANOVA).

Cortical state correlated with reaction time in the auditory 2AFC task but did not reach significance in the auditory distractor task (Figures 4.43 and 4.44).

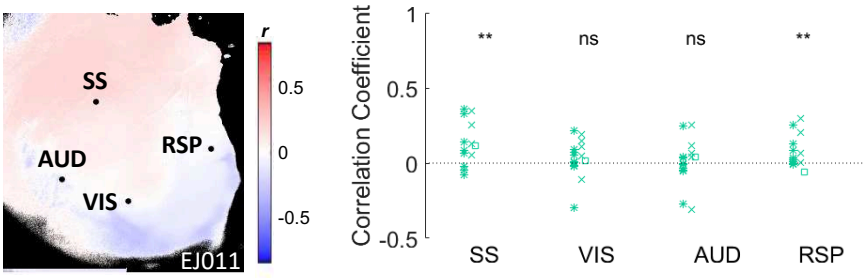

(i) Example Power-Reaction Time Correlation Map.

(ii) Summary across all experiments in selected ROIs.

Figure 4.43: Correlation between 3-6Hz power and reaction time in the auditory 2AFC task.
Mean correlations with average confidence intervals: SS 0.14 (-0.07 0.32), VIS 0.03 (-0.16 0.23), AUD 0.01 (-0.19 0.2), RSP 0.08 (-0.12 0.28).

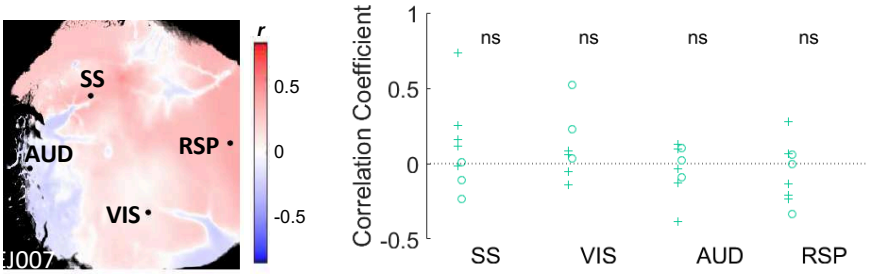

(i) Example Power-Reaction Time Correlation Map.

(ii) Summary across all experiments in selected ROIs.

Figure 4.44: Correlation between 3-6Hz power and reaction time in the auditory distractor task.
Mean correlations with average confidence intervals: SS 0.11 (-0.25 0.44), VIS 0.1 (-0.31 0.43), AUD -0.04 (-0.4 0.35), RSP -0.06 (-0.4 0.35).

Finally, also matching the result in the visual task, there were no differences in desynchronisation between correct and incorrect choice trials in either auditory 2AFC (Figure 4.45) or auditory distractor (Figure 4.46) tasks.

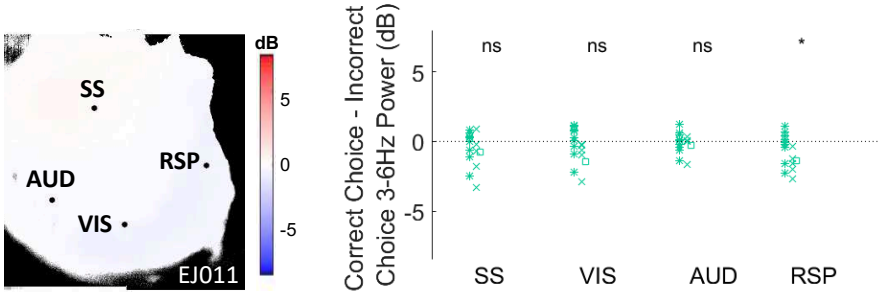

(i) Example Power Difference Map

(ii) Summary across all experiments in selected ROIs.

Figure 4.45: 3-6Hz power differences between correct and incorrect choice trials in the auditory 2AFC task.
Mean power differences per ROI with SEM: SS -0.52 +/-0.33dB, VIS -0.39 +/-0.31dB, AUD -0.08 +/-0.2dB, RSP -0.78 +/-0.31dB.

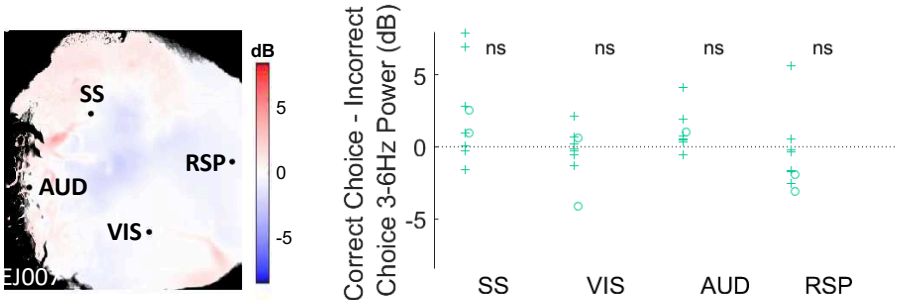

(i) Example Power Difference Map.

(ii) Summary across all experiments in selected ROIs.

Figure 4.46: 3-6Hz power differences between correct and incorrect choice trials in the auditory distractor task.
Mean power differences per ROI with SEM: SS 2.25 +/-1.14dB, VIS -0.31 +/-0.61dB, AUD 2.26 +/-1.35dB, RSP -0.59 +/-0.92dB.

To further investigate whether the difference in auditory cortex was indeed due to movement, instead of comparing choice and neglect trials, I compared trials with and without movement during the baseline. If movement indeed suppressed desynchronisation when auditory stimuli were not present or irrelevant, then the comparison of movement versus no movement trials should result in no difference in auditory cortex in low frequency power in the visual and auditory distractor tasks, but not in the auditory 2AFC task.

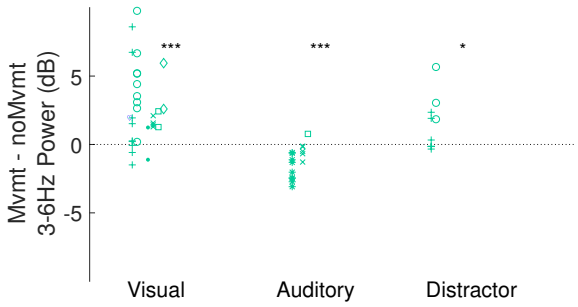

Figure 4.47: Auditory cortex 3-6Hz power differences between movement and no movement trials in the visual, auditory 2AFC and auditory distractor tasks. Mean power differences per task with SEM: Visual task 2.7 +/- 0.53dB, Auditory task -1.23 +/-0.3dB, Auditory distractor task 1.43 +/-0.64dB.

There were indeed significant differences in the effect of movement on low frequency power between the different tasks (Figure 4.47, $p<0.001$ one-way ANOVA): there was in fact significantly *more* low frequency power during movement in the visual and auditory distractor tasks ($p<0.001$ & $p<0.05$ in the visual and auditory distractor tasks respectively, one-sample t-tests; auditory 2AFC versus visual task $p<0.001$, auditory 2AFC versus auditory distractor task $p<0.01$, visual versus auditory distractor tast $p>0.05$, one-way ANOVA), whereas only in the auditory 2AFC task did the auditory cortex desynchronise when there was movement ($p<0.001$, one-sample t-test).

Altogether, these results suggest that whilst there was again a global desynchronisation during choice trials in both the auditory 2AFC and auditory distractor tasks, movement had a different effect on state in auditory cortex depending on whether auditory stimuli were relevant or not: movement suppressed auditory cortex desynchronisation only when auditory processing was not required. In addition, there was no difference again between correct and incorrect trials, providing further evidence that the desynchronisation is more related to task engagement than accuracy.

4.2.2 Engagement related cortical state changes are independent of sensory modality

I showed in the visual task that engagement related desynchronisation was a global effect: all cortical regions of interest, including auditory cortex, desynchronised when focusing the analysis on the quiescent period, and the strongest desynchronisation seen in somatosensory rather than visual cortex (Section 4.1.3, Figure 4.18). In addition I argued that by showing that the difference in cortical state between engaged (choice) and disengaged (neglect) trials was independent of movement, both prior (Figure 4.18) and future (Section 4.1.3, Figures 4.23 & 4.24) and a global arousal, as measured by pupil size, this suggested that cortical desynchronisation reflected a cognitive state of engagement. If this were true, then the results from the auditory 2AFC and auditory distractor task should both yield the same results.

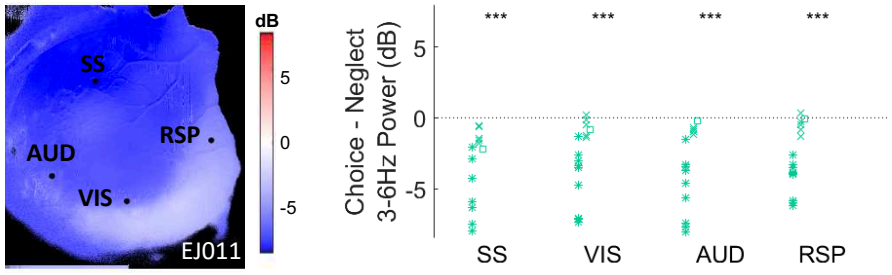

(i) Example Power Difference Map.

(ii) Summary across all experiments in selected ROIs.

Figure 4.48: 3-6Hz power differences between choice and neglect trials during the quiescent period in the auditory 2AFC task.
Mean power differences per ROI with SEM: SS -4.32 +/- 0.88dB, VIS -2.95 +/- 0.7dB, AUD +/- -3.33 +/- 0.75dB, RSP -2.79 +/-0.6dB.

Movement independent cortical states are global

Indeed, when focusing the analysis on the quiescent period, the results from both the auditory 2AFC and auditory distractor task paralleled the results from the visual task (Figures 4.56 & 4.57). All cortical ROIs significantly desynchronised, and in the auditory distractor task, somatosensory cortex again showed the strongest effect (p=0.008, SS vs VS, AUD, RSP $p < 0.05$, one-way ANOVA) but not in the auditory 2AFC task (p=0.43, one-way ANOVA). Similarly, there were no differences between correct and incorrect choices (Figure 4.50), and correlation between reaction time and synchronisation also remained (Figure 4.51).

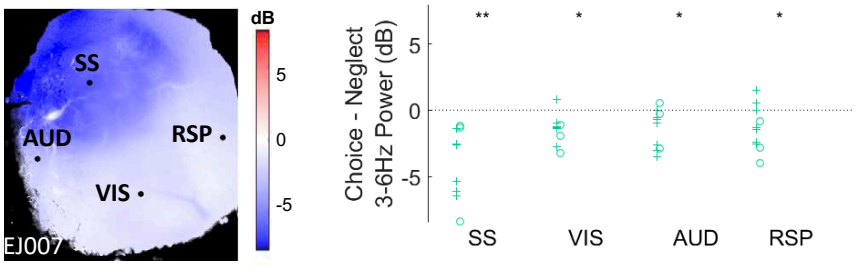

(i) Example Power Difference Map.

(ii) Summary across all experiments in selected ROIs.

Figure 4.49: 3-6Hz power differences between choice and neglect trials during the quiescent period in the auditory distractor task.
Mean power difference per ROI with SEM: SS -3.8 +/-0.86dB, VIS -1.24 +/-0.44dB, AUD -1.42 +/-0.49dB, RSP -1.34 +/-0.56dB.

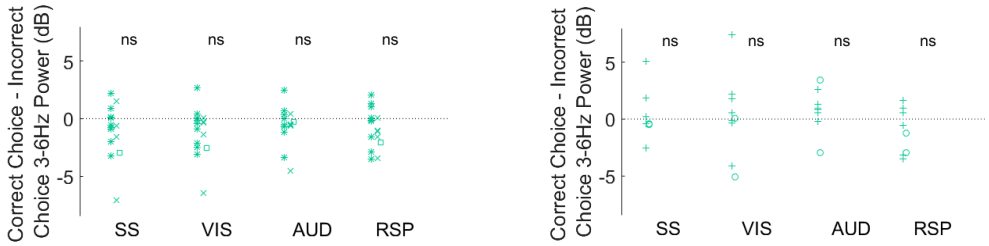

(i) Auditory 2AFC (ii) Auditory distractor

Figure 4.50: 3-6Hz power differences between correct and incorrect choice trials during the quiescent period.
Mean power differences per ROI with SEM: Auditory task SS -1.03 +/-0.6dB, VIS -1.14 +/-0.55dB, AUD -0.6 +/-0.44dB, RSP -0.87 +/-0.45dB; Auditory distractor task SS 1.55 +/-1.41dB, VIS 0.25 +/-1.29dB, AUD 0.86 +0.64dB, RSP 0.22 +/-1.49dB.

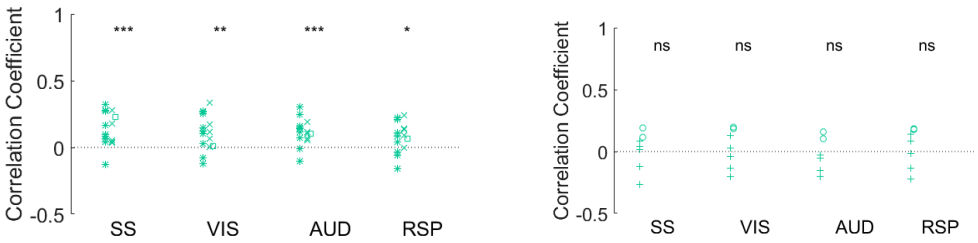

(i) Auditory 2AFC (ii) Auditory distractor

Figure 4.51: Correlation between 3-6Hz power and reaction time during the quiescent period.
Mean correlations per ROI with average confidence intervals: Auditory task SS 0.13 (-0.07 0.32), VIS 0.11 (-0.09 0.3), AUD 0.11 (-0.1 0.31), RSP 0.09 (-0.12 0.28); Auditory distractor task SS 0.01 (-0.33 0.36), VIS 0.02 (-0.39 0.26), AUD -0.12 (-0.32 0.38), RSP 0.03 (-0.33 0.37).

Behavioural state improves prediction of cortical state from pupil size

Matching the results in the visual task, there was no difference in pupil size between choice and neglect trials (Figure 4.52), although pupil size negatively correlated with low frequency power in both auditory 2AFC and auditory distractor tasks (Figure 4.53). In both tasks, behavioural condition

improved prediction of low frequency power from pupil size (Figures 4.53, 4.54 & 4.55).

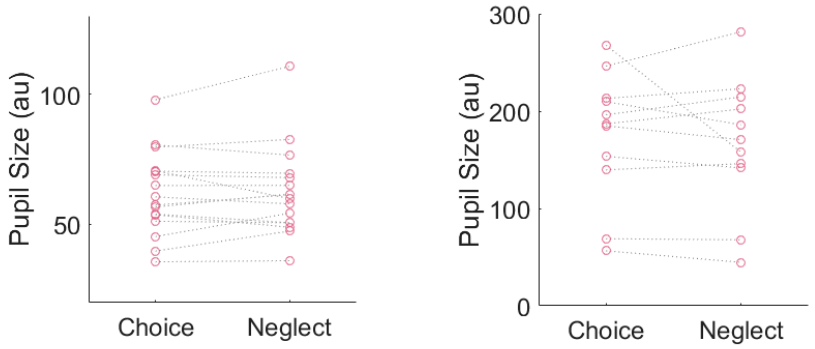

(i) Auditory 2AFC (ii) Auditory distractor

Figure 4.52: Average pupil sizes during choice and neglect trials in the auditory 2AFC (i) and auditory distractor (ii) task. Each circle represents a dataset, the dotted line connects the corresponding choice and neglect averages from each dataset.

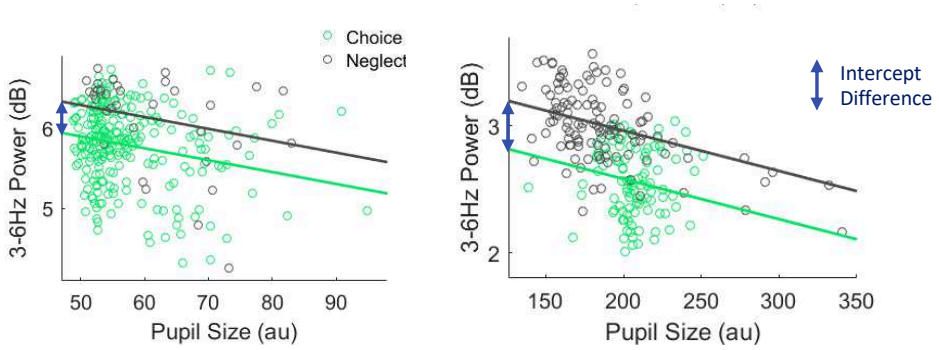

(i) Auditory 2AFC (ii) Auditory distractor

Figure 4.53: 3-6Hz Power as a function of pupil size in somatosensory cortex, where the effect of behavioural condition was largest. Each circle represents a trial from a typical example dataset, the circles are coloured according to behavioural condition.

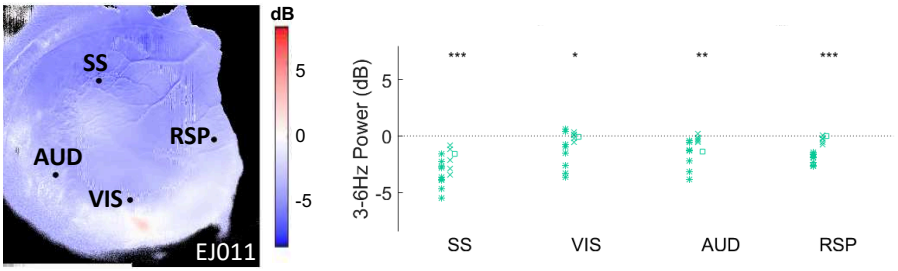

(i) Example 'Intercept Difference' Map.

(ii) Summary across all experiments in selected ROIs.

Figure 4.54: Intercept differences between choice and neglect power as a function of pupil size in the auditory 2AFC task.
Mean intercept differences per ROI with SEM: SS -2.87 +/-0.35dB, VIS -0.91 +/-0.36dB, AUD -1.2 +/-0.31dB, RSP -1.37 +/-0.27dB.

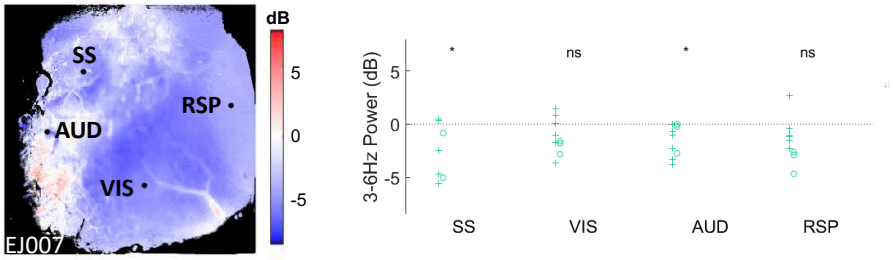

(i) Example 'Intercept Difference' Map.

(ii) Summary across all experiments in selected ROIs.

Figure 4.55: Intercept differences between choice and neglect power as a function of pupil size in the auditory distractor task.
Mean intercept differences per ROI with SEM: SS -3.11 +/-0.71dB, VIS -0.76 +/-0.32dB, AUD -0.69 +/-0.62dB, RSP -0.63 +/-0.31dB.

4.2.3 Reward may have a sensory modality specific effect on cortical state

In the visual task, I had discovered a long lasting effect of reward on cortical state: there was a significant increase in desynchronisation after correct trials, both correct choices and correct no-go's. In addition, this effect had not been global: visual cortex always desynchronised after a rewarded trial, and somatosensory and secondary motor cortex desynchronised after correct choices, so when there had been movement in combination with reward. (They did desynchronise after correct no-go's but only in comparison with neglect trials, in which case there was a bigger difference in state to begin with so it is unclear to what extend this was reward versus engagement related.) Only auditory cortex never became desynchronised after a reward. (See Figures 4.32, 4.33 and 4.34). This raised the intriguing possibility that reward may have an effect that depends on the sensory modality that is being used in the task. If this were true, then we would expect the following when comparing correct and incorrect choices:

- In the auditory 2AFC task, auditory but not visual cortex desynchronises after correct choices.
- In the auditory distractor task, visual but not auditory cortex desynchronises.

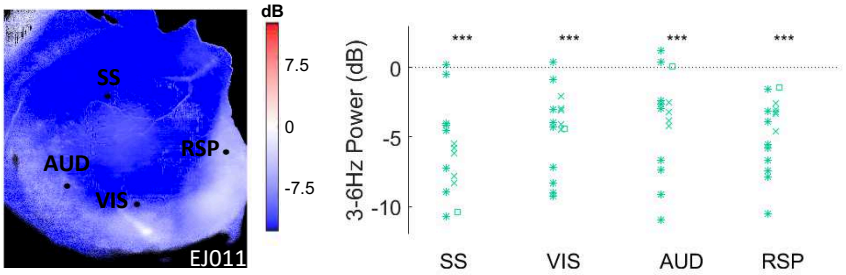

(i) Example Power Difference Map.

(ii) Summary across all experiments in selected ROIs.

Figure 4.56: Post response 3-6Hz power differences between correct choice and incorrect choice trials in the auditory 2AFC task.
Mean power differences per ROI with SEM: SS -6.43 +/-0.95dB, VIS -4.44 +/-0.77dB, AUD -3.89 +/-0.92dB, RSP -4.71 +/-0.69dB.

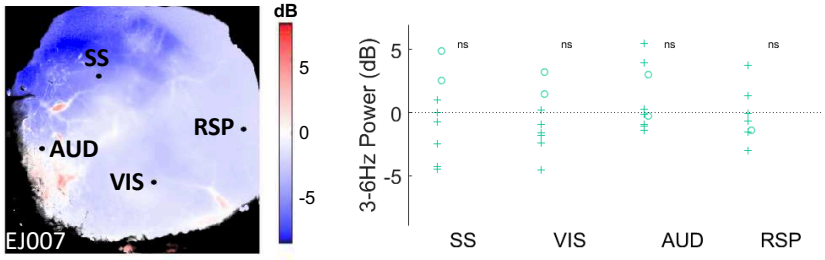

(i) Example Power Difference Map.

(ii) Summary across all experiments in selected ROIs.

Figure 4.57: Post response 3-6Hz power differences between correct choice and incorrect choice trials in the auditory distractor task.
Mean power differences per ROI with SEM: SS 0.38 +/-1.4dB, VIS 0.36 +/-1.47dB, AUD 1 +/-0.89dB, RSP 0.85 +/-1.38dB.

Interestingly, the results did not conform with either prediction. In the auditory 2AFC task, whilst auditory cortex now did show an effect of reward, so did visual cortex, as well as somatosensory and retrosplenial cortex. Here, the reward effect was robustly global: all ROIs were significantly more desynchronised after correct than incorrect choices (Figure 4.56). In contrast, in the auditory distractor task, reward had no effect at all - although when looking at the graph in Figure 4.57 (ii), it looks as though the two mice had opposite effects of reward, at least in visual and somatosensory cortex. Unfortunately, since the animals did not learn a 2AUC version in the auditory task (Section 3.2.2, *Training mice on 2AUC versions of the tasks*), I could not make any further enquiries into the effect of reward on cortical state.

4.2.4 Summary & Conclusions

In this section, I have shown that:

- Movement suppressed desynchronisation in auditory cortex when auditory stimuli were not present or irrelevant.
- When auditory stimuli were relevant, auditory cortex also desynchronised during movement.

Then, by excluding effects of movement and general arousal, I further confirmed that:

- Engagement related cortical state changes were global,
- Engagement related cortical state changes were independent of sensory modality,
- The biggest effect of behavioural state was in somatosensory cortex, irrespective of whether vision or audition was required by the task.

Finally, I demonstrated that:

- Reward also had an effect on cortical state in the auditory 2AFC task,
- but in this task it was global,
- and there was no effect of reward in the auditory distractor task.

Thus, further research will be needed to establish what effect reward has on cortical states.

Altogether, since the majority of results conform with the results from the visual task, they lend further support to the idea that cortical desynchronisation is associated with a cognitive state of engagement.

Chapter 5

Discussion

They key aims of my thesis were:

1. To ascertain whether desynchronisation is associated with performance,
2. To assess whether desynchronisation could occur locally, and specifically:
3. Determine whether a local desynchronisation would occur in the sensory cortex of the sensory modality being used.

I will first provide a technical discussion where I give a summary of the main findings of my research; discuss how well they fit with the aims outlined above; and consider how successful individual experiments were and what could be improved in the future. Then I will proceed to a discussion on how the results relate to the broader research; and end with final conclusions and suggestions for future work.

5.1 Technical discussion

Synopsis of main findings

To address the aims of my thesis, I trained mice in several different tasks: visual 2AFC and 2AUC tasks, an auditory 2AFC task, and an auditory distractor task. I recorded their cortical activity with widefield imaging, and I also included widefield data obtained by Nick Steinmetz from visual tasks in my analysis. I applied spectral analysis to determine whether cortical states were synchronised or desynchronised. My results revealed the following findings:

- Cortical state correlates with engagement rather than performance.
- This effect is mostly global and does not depend on what sensory modality is required in the task.
- The biggest effect does not occur in the cortex of the sensory modality that is being used, but rather in somato-motor cortex.
- Neither overt movement nor pupil fully explain the difference in cortical state during engagement, suggesting it is more of a cognitive state.

- Reward has an effect on cortical state.

5.1.1 Discussion of results with relation to the aims and hypothesis of the thesis

Aim 1:

Ascertain whether desynchronisation is associated with good task performance.

I successfully trained mice on several tasks that required them to use different sensory modalities: vision or hearing. The mice performed well in the tasks, albeit performance in the auditory task was not as high as in the visual tasks (discussed further under Section 5.1.2). By looking at the natural fluctuations in their performance, I was able to ask how cortical states related to performance, and by making comparisons across the tasks, identify what features, if any, were specific to performance rather than sensory processing.

I found that desynchronisation was indeed associated with task performance, however not necessarily with *good* performance: there was desynchronisation prior to choice trials as well as correct no-gos, but there was no difference in cortical state between correct and incorrect choices. This suggests that desynchronisation is more related to task *engagement* rather than performance, since there was no effect of cortical state on the accuracy of the choices.

My initial hypothesis that desynchronisation enables good performance by improving information processing therefore proved incorrect. Instead, the causality may go the other way around: good performance *drives* desynchronisation, as there was significantly more desynchronisation after correct trials. Further experiments that can explore this possibility will be discussed

in Section 5.3.2.

Aim 2:

Assess whether desynchronisation occurs locally.

To ascertain whether desynchronisation could occur locally within a given part of the cortex while other parts of the cortex may remain more synchronised, I needed a method that provided sufficient spatiotemporal resolution to compare cortical state across a wide area of cortex simultaneously. I successfully established that by analysing the low frequency content of the fluorescence traces obtained through widefield imaging of genetically encoded calcium indicators, I could distinguish between synchronised and desynchronised cortical states. I could thus create maps that showed how cortical states vary during task engagement with unprecedented spatial resolution. These revealed that cortical states were mostly global, with the exception of auditory cortex which remained synchronised when there was movement and no or irrelevant auditory stimuli. Nevertheless, by excluding periods of movement and assessing engagement related cortical states, I showed that desynchronisation did not occur locally within any of the regions of interest I considered: visual, auditory, somatosensory, secondary motor and retrosplenial cortex.

However, I discovered significant differences in the *degree of desynchronisation* between different cortical areas: I found that during task engagement, somatosensory cortex became significantly more desynchronised than visual, auditory and retrosplenial cortex. This effect occurred in all the tasks, which suggests that this was a general feature of task engagement in mice.

If the signal amplitude had a multiplicative effect, then it is possible

that increased fluorescence in the somatosensory cortex may be an artefact of this difference rather than a genuine difference in power. If the effect was multiplicative, then 1) the effect should be present in all frequency bands and 2) using dff rather than F should lead to differently scaled results. However, I found that the result using dff was almost completely identical to the one obtained using F (Appendix B), and that the power in somatosensory cortex was only larger than in the other ROIs in the 3-6Hz frequency band (Appendix B). Therefore, the differences between ROIs that I found are unlikely to be artefactual.

There was no overt need to use the whisker system in any of the tasks, however the whisker system is such an etiologically important part of a mouse's behaviour (Crapse and Sommer, 2008) that it is possible that they did so anyway. Although I observed no difference in overall whisker motion between choice and neglect trials, this did not provide the necessary resolution to distinguish if mice performed different types of whisker movements depending on whether they were engaged or disengaged. For example, the mice may have used their whisker system to feel the steering wheel with which they were providing responses, even though this would have been difficult, as they were raised sufficiently high above the steering wheel that their whiskers did not touch it during resting. Another possibility is that they were whisking their paws while they were providing a response. Alternatively, since the somatosensory system is so closely functionally linked to the motor system (Lee et al., 2008; Zagha et al., 2013; Sreenivasan et al., 2016), it is possible that the desynchronization in somatosensory cortex reflects a "being ready" to provide a response to the sensory stimuli in order to obtain a reward. The observation that desynchronisation correlated with

reaction time, and that there was no difference in desynchronisation between somatosensory and secondary motor cortex lends support to this interpretation.

Aim 3:

Determine whether a local desynchronisation occurs in the sensory cortex of the sensory modality being used.

By training mice on tasks that required two different sensory modalities, vision and hearing, and recording their cortical activity during task performance, I showed that desynchronisation is global and does not depend on the sensory modality being used. Visual and auditory cortex were both equally desynchronised in all tasks during task engagement. (The movement dependent effect on auditory cortex will be discussed in Sections 5.1.2 & 5.2.)

However, it is possible that the tasks that I used did not sufficiently "separate" the two sensory modalities. For example, in a task in which one sensory modality needs to be attended while the other is discounted there might be a bigger difference in cortical state between the sensory cortices. In fact, it had been my intention, after having collected data on the auditory and visual tasks separately, to train the mice to perform "audio-visual" 2AFC tasks in which I presented both auditory and visual stimuli together, but in each session the animals had to determine which sensory modality was relevant while the other served as a distractor. Unfortunately I did not succeed in running these experiments. The first animals that I had intended to image during visual and auditory behaviour failed to learn the auditory task, most likely because I had made it too difficult (see also Chapter 3

Section 3.2.2). In the second round of experiments, even though I had reverted to using the parameters in the auditory task with which prior mice had successfully learned the task, my mice took much longer to learn the tasks and did not achieve as good a performance as in the visual task. Then when I had finally begun collecting imaging data during the auditory task, our laboratory discovered that the transgenic line I (and many others) was using was prone to epilepsy and pathological neural activity (see also Section 5.1.2), and I therefore had to interrupt my experiments before I could try a more complicated task that combined both sensory modalities. Thus, my experiments only partially addressed this aim, but because I had already collected sufficient data from the other tasks, we decided to not pursue this further.

Nonetheless, the available results reveal that the hypothesis that desynchronisation occurs locally where the sensory information of the task is being processed also proved incorrect. Alternatively, the hypothesis that (sensory) information processing during sensory decision-making is localised may in itself be incorrect: it is possible that in such a complex task, information processing is distributed across cortex and therefore desynchronisation is global. Consequently, a more accurate hypothesis might be that there is increased desynchronisation in the sensory cortex of the sensory modality that is relevant compared to the sensory cortex of the modality that represents conflicting information that needs to be discounted.

Summary

My experiments and results successfully addressed the aims of my thesis by showing:

- Desynchronisation is more related to task engagement than task performance,
- Desynchronisation does not occur locally, although there can be local differences in the degree of desynchronisation.
- Desynchronisation is not restricted to the sensory cortex of the sensory modality being used.

5.1.2 Limitations

Pathological activity in some transgenic lines

It is not possible to observe a system without perturbing it.
As scientists, we tend to not give this truth much consideration, partly because there is no way around it, and mostly because we do our best to keep the perturbations to a minimum and hope that we are keeping the system we are studying in as natural a state as possible.

Genetically encoded calcium indicators are as ubiquitous as they are valuable in the study of neurophysiology because they allow a minimally invasive, high signal-to-noise measurement of neural activity (Chen et al., 2013; Madisen et al., 2015). However, they must alter the cellular physiology of neurons that express them because not only do they constitute synthetic molecules that are alien to the cellular environment, but particularly because they act as calcium buffers. Calcium is one of the most important intracellular messenger molecules (Chin and Means, 2000; Shen and Yakel, 2009), and while there is most likely a homeosthatic range within which neurons can adapt to the presence of exogenous molecules and buffers, it is equally possible that their presence will alter the function of not just individual cells but entire circuits in subtle ways that we don't even know how to assess.

In the fall of 2016, Nick Steinmetz, a postdoctoral researcher in the group, was performing electrophysiological recordings in the Emx1-Cre;Camk2-tTa; Ai93 mice after having identified regions of interest through widefield imaging, and realised that there were frequent aberrant events of very large amplitude, much larger than normal. Subsequent analysis showed that these events resembled interictal activity: a type of epileptiform activity that oc-

curs outside of overt seizures and is considered to be pathological (Rodin et al., 2009). Simultaneous imaging and electrophysiology experiments identified an equivalent signature in the widefield imaging data: brief and high amplitude deflections in the fluorescence.

At this point, the majority of my experimental animals were of the Emx1-Cre;Camk2-tTa;Ai93 genotype, and after having identified a signature I could look for, I proceeded to checking my recordings to see if they had been affected. Not all of my animals were affected, and in most cases the pathological activity developed and increased over time. In addition, in most of the animals that were afflicted, only some cortical regions were affected.

Our laboratory collaborated with several others to assess whether this was a general occurrence and what transgenic lines were affected. The Emx1-Cre;Camk2-tTa;Ai93 appeared to be the most severely affected line, however it was not the only one. We published our observations to alert the scientific community (Steinmetz et al., 2017), and thus the work presented in this thesis also contributed to a rather unexpected publication.

There are several possible reasons for the aberrant activity, including Cre toxicity (Schmidt-Supprian and Rajewsky, 2007), tTA toxicity (Han et al., 2012), and genetic background (Frankel et al., 2001). However, the feature in common between the lines that were affected was high levels of GCaMP expression and in large populations of neurons (Steinmetz et al., 2017). The Emx1-Cre;Camk2-tTa;Ai93 for example expresses GCaMP6f in all cortical excitatory neurons which leads to a very strong fluorescence signal, which in turn was exactly why I and others were using it for widefield imaging. This suggests that it was the high level of GCaMP expression that altered neural

physiology and lead to the pathological activity.

What does this mean for the results presented in this thesis?

Except in some rare cases where generalised seizures were observed, there were no obvious behavioural manifestations. In addition, many properties of neuronal responses seemed normal despite these events.

Not all of my recordings were affected, and in the animals in which interictal activity developed over time, I observed no difference in behaviour or the results concerning cortical states between the unaffected and affected datasets. Of course, it is possible that even when there was no overt pathological activity yet, that brain function was already altered. However, given that I could replicate my results in mice from unaffected lines, this makes it unlikely that the results presented in this thesis are an artefact of pathological brain activity. Furthermore, the result that cortical states correlate with arousal and engagement does not present an anomaly, but instead fits well with the already existing literature on this topic. Therefore, whilst I certainly concede that care should be taken whilst interpreting the results, I would argue that the results concerning cortical states I have presented are robust.

Auditory cortex measurements

Given the lateralised location of auditory cortex, this meant that auditory cortex was at the edge of my imaging window. Even though I imaged the animals with a steeper angle and obtained a reliable signal from auditory cortex, this signal was not as strong as in the other cortical areas. Similarly, overall power in auditory cortex was lower.

The result that movement suppressed desynchronisation in the auditory cortex could suggest that the measurement from auditory cortex was particularly prone to movement artefacts. However, this suppression did not occur in the auditory task. All the mice that were recorded in the auditory task were also recorded in the visual task, in the same imaging set-up, and although possible minor differences in set-up between the different days of recordings cannot be ruled out, it would be surprising if movement artefacts only occurred in the visual tasks. This makes it unlikely that differences in imaging windows or signal strength explain the differences in result in auditory cortex. Nevertheless, future studies should investigate this further, which could be achieved by using a procedure optimised for widefield imaging of auditory cortex (Issa et al., 2014), or by obtaining stimultaneous electrophysiological recordings from auditory and other cortical areas.

Signal origin

The signal from a single pixel consists of a composite of several different signals: firstly, it is a population signal, as a single pixel covers $20^2\mu$m of cortex, and therefore contains the signals from many neurons. Secondly, GCaMP is expressed throughout the neuron, which results in dendrites and axons also contributing to the signal. This means that there is also a possible non-local contamination in the signal from long-range projections. However, these are mostly negligible, as the signal must still be dominated by local indicators: else it would not be possible to obtain retinotopic and tonotopic maps. In addition, it has been shown suppressing action potentials locally abolishes most of the signal (Berger et al., 2007), further suggesting the signal is predominantly local. Lastly, as GCaMP is expressed across all

cortical layers in the transgenic mice that were used in my research, the signal is most likely a composite from different layers. Nevertheless, the superficial layer (layers 1 and 2/3) signals potentially dominate the signal, with deeper layers possibly influencing the signal via their upward projections. A recent study that compared widefield imaging with the summed signal from an entire 2-photon frame found that whilst the widefield signal correlates well with layer 2/3, the correlation is higher with layer 1 (Allen et al., 2017), whereas a study using simultaneous widefield imaging and electrophysiology found that the widefield signal associated with activity in the different layers was highly overlapping (Xiao et al., 2017). It thus remains unclear which layer most contributes to the widefield signal.

Altogether, I would argue that the widefield signal represents a mostly local signal in which some long-range influences may be present but are minor enough to be inconsequential. Nevertheless, future work is required to elucidate how much the different layers contribute to the signal. Although some work has suggested that synchronised and desynchronised states in a task-environment fluctuate coherently across cortical layers (Engel et al., 2016), this may not always be true. In such cases, the method employed in this thesis might not be suitable to distinguish layer-specific fluctuations in synchronisation and desynchronisation. Future work with soma-tagged and layer specific GCaMP expression will be useful to investigate layer specific effects on cortical states.

Performance in the different tasks

The performance of the imaged animals in the different tasks was not equal. The animals readily achieved an average performance of 70% in the visual

and auditory distractor (where visual stimuli were relevant) tasks, whereas in the auditory task the performance remained around 60%. This was partly due to the fact that two of the three animals performing the auditory task had not been learning the auditory task for long before I had to cut short my data collection because of the discovery of the pathological activity. (As we did not know how severe the situation was, we decided to temporarily halt all experiments using these lines until we had resolved the situation.) However, even the third animal that had learned the task did not perform as well in it as in the visual task (data not shown). This was surprising given that prior animals had learned the auditory task much faster and much better. Although previous mice that had learned the task had been of the same genotype, it is possible that these mice were particularly affected by a possible pathology resulting from the transgenic expression of GCaMP which made the auditory task difficult for them.

Given that my aim had been to relate cortical state differences to performance, this could have been a caveat, as in order to compare states during visual and auditory tasks, I would have needed those performances to be comparable. However, given that I did not find a difference between correct and incorrect trials in the visual task, and instead found that cortical states were more related to engagement and potentially preparation of coordinated behavioural responses, the differences in performance in the different tasks did not pose a problem after all. Indeed, the fact that I observed the same differences in cortical state during different behavioural conditions *despite* the differences in performance further support the idea that desynchronisation is not related to performing a task correctly, but a function of engagement, and that other mechanisms must be in place that determine

performance accuracy.

Pupil measurement

Given how closely pupil fluctuations have been found to correlate with cortical states and cognitive processes, it is somewhat surprising that I did not find a difference in pupil size between different behavioural states (choice and neglect), and only a correlation with low frequency power - despite low frequency power also being correlated with behaviour.

The temporal resolution in my experiments was high enough to pick up on smaller, transient pupil dilations, and some exploratory analysis suggested that more dilations occurred during engaged (choice) than disengaged (neglect) periods (data not shown). However this effect was not consistent across animals, which is why this analysis was abandoned. It is possible that in some datasets, microdilations could not be successfully detected because the spatial resolution was not high enough - the zoom and angle onto the eye varied between datasets because of small adjustments in camera position between users and experiments, which could have affected the quality of some recordings. The post-recording processing pipeline included manual steps which attempted to adjust for such differences (or make the decision to exclude datasets in which the pupil could not be reliably assessed), however it is possible that this process was not rigorous enough.

Other exploratory analysis used the pupil size at stimulus onset or the maximum pupil size during the baseline as the predictors in the ANCOVA analysis (Section Variations in cortical states are not fully explained by variations in pupil in Chapter 4), however this yielded the same result, which is why I chose to continue using the mean pupil size during the baseline as

the measure of pupil size.

Lastly, it is highly unlikely that saturation was a problem in the pupil assessments, as the animals were sitting in front of illuminated screens in all experiments: the pupil was never fully dilated in this condition, and a dynamic range of pupil sizes, from very constricted to dilated, could be measured in all datasets.

Stimulus responses

In order to keep the behavioural task design as unpredictable as possible, the contrast of a stimulus in any given trial was randomised. Given that the animals' behaviour; when they were alert or inalert, in other words when they provided choice or neglect responses, was also unpredictable, this often resulted in very unbalanced comparisons of choice and neglect conditions per contrast. If there was in fact a more subtle difference between choice and neglect stimulus responses, then it is possible that the datasets obtained in my experiments were not sufficiently large to pick them up.

The wisdom of hindsight

One is always wiser at the end of the journey. For future experiments that wish to build on this work, I recommend the following modifications for optimisation purposes:

1) It goes without saying that future experiments that intend to use wide-field imaging of GECIs to assess cortical states should choose transgenic lines that are not affected by epileptiform activity to avoid potential confounds in learning, behaviour, and physiology.

2) To equalise the performances between visual and auditory 2AFC tasks, I would recommend the following modifications:

   - The visual task could be made more difficult by dropping higher contrasts and using low contrasts only,
   - The auditory task could most likely be made easier by increasing the difference in tonal frequency between the two stimuli (to for example 5kHz and 20kHz).
   - I would however avoid increasing the frequency range further than the suggested 5 and 20 kHz to avoid difficulties of the mice hearing the stimuli. Most transgenic lines are congenic to C57BL/6J background, which exhibits faster age-related hearing decline for higher frequencies (Ison et al., 2007). As training animals on both tasks can take up to several months, a frequency range should be employed that mice will reliably be able to hear throughout the course of their training.

I suggest these modifications to the tasks not only to equalise the performances, but to provide tasks that can be combined to create the types of "audio-visual" tasks that I suggested under the discussion of Aim 3. This type of task, in which both stimuli are presented but only one modality is relevant, would most likely be challenging for the mice. One should therefore aim to have single modality tasks in which mice can reliably achieve a good performance. Otherwise, if they do not reliably respond to a given stimulus in a single modality task, it will be difficult to know in a cross-modal task whether the mistake was due to uncertainty of the relevant sensory modality, or because the animal did not know how to respond to the stimulus.

5.2 The big picture

For a long time, the prevalent view held that cortical states are a function of the sleep wake cycle (Steriade and Timofeev, 2003; Steriade, 2003), as the biggest and most obvious differences in state occurred during (non-REM) sleep and waking, with the cortical state during waking correspondingly being described as the active state. Even though Berger himself already noted that the EEG showed different signatures during different behavioural states during waking (Berger, 1929), the low frequency oscillations during waking were thought to be negligible compared to slow-wave sleep (SWS) and therefore received little attention until more recently (Rougeul-Buser et al., 1975).

Now it is broadly accepted that the waking state does not constitute a single homogenous state, but that different oscillatory patterns, including those of lower frequencies (<10Hz), are associated with different behavioural states (Zagha and McCormick, 2014). The following sections will discuss how the results reported here fit with our current understanding of cortical states during waking.

5.2.1 Engagement related cortical state changes

Several studies have shown that at least in rodents, quiet wakefulness, when the animals are awake but not engaged in any activity, is associated with low frequency oscillations in cortex, albeit with lesser amplitude than sleep or anesthetised states (Zagha and McCormick, 2014). Such oscillations have been observed in visual (Bennett et al., 2013; Vinck et al., 2015; Scholvinck et al., 2015), auditory (Zhou et al., 2014; McGinley et al., 2015), somatosen-

sory (Crochet and Petersen, 2006; Poulet and Petersen, 2008) as well as motor cortex (Zagha et al., 2013), suggesting they are a global feature of this behavioural state.

These slow oscillatory patterns disappear when the animal starts moving, for example when it starts running (Bennett et al., 2013; Vinck et al., 2015; Scholvinck et al., 2015; Zhou et al., 2014; McGinley et al., 2015) or whisking (Crochet and Petersen, 2006; Poulet and Petersen, 2008; Zagha et al., 2013). However, movement is not the only indication of arousal as there can be state changes in the absence of it, which can be non-invasively assessed via changes in pupil size (Reimer et al., 2014; Vinck et al., 2015). Indeed, it has recently been shown that pupil fluctuations closely correlate with neuromodulatory activity (of acetylcholine and noradrenaline) in cortex (Reimer et al., 2016).

By training animals to initiate trials by remaining quiescent, I was able to examine to what extend the changes in brain state were driven by movement and found that the results did not change by excluding movement. This agrees with previous research showing that whilst arousal and movement often co-occur and indeed influence sensory processing (Bennett et al., 2013; Niell and Stryker, 2010), their effects can be dissociated (Reimer et al., 2014; Vinck et al., 2015). In addition, by examining cortical state during correct no-go trials in which animals were required to keep still as a response, I was able to show that desynchronization was also not a state that signalled upcoming movement as correct no-go trials showed equal desynchronization as choice trials. Nevertheless, it is likely that the desynchronisation is associated with a state that is more primed to perform movements, which however are actively 'suppressed' to avoid making unnecessary movements.

As such, one would expect differences in muscle tone prior to correct no-go and neglect trials: in the latter, the muscle tone would most likely be much more relaxed than in the former. Similarly, the muscle tone prior to correct no-go trials would be much more tense and therefore similar, if not identical, to choice trials.

Interestingly, McGinley et al. (2015) found that movement was a signature of hyper-arousal, and that optimal performance occurred during a desynchronized state without movement. I did not find such a detrimental hyper-arousal effect of movement in the data, although this may be due to differences in task difficulty: McGinley et al. specifically designed the task to be as challenging as possible by using a paradigm that made the detection of relevant auditory stimuli over background noise very difficult. It is possible that the processing of such stimuli is much more sensitive to differences in cortical state. Indeed, a recent theoretical model by Zerlaut et al. (2018) has suggested that intermediate levels of arousal provide ideal conditions for decoding finely structured spatio-temporal stimuli, as were used in McGinley et al.'s study, whereas a high arousal state leads to amplification of a stimulus, which may be better for detection of a single stimulus, rather than a stimulus embedded in background noise.

Nonetheless, by having trained animals on alternative choice rather than go/no-go tasks, I was able to make a crucial distinction between perceptual errors and differences in task engagement. In a go/no-go task, a miss can be due to not perceiving the stimulus, or having disengaged with the task - thus, despite potentially having perceived the stimulus, the individual is not responding to it. Similarly, a go response may be due to the perceived

presence of a stimulus, or an accidental movement due to distraction or disengagement. In a 2AFC task, a miss most likely indicates disengagement as a perceptual error would lead to an incorrect choice.

If desynchronisation was the cortical state required for accurate performance, then there should be a difference between correct and incorrect choices, correct and incorrect no-gos. However, this is not what I found: in all of the tasks, cortical state was equally desynchronised in correct and incorrect choices. There was indeed a difference between correct and incorrect no-gos (the latter having been referred to as neglect throughout this thesis), and I showed that this was due to differences in engagement. This result emphasizes the importance of using tasks that are more complex than the frequently used go/no-go tasks if one wishes to understand the neural processes underlying sensory perception and motor selection.

Effects of movement on visual and auditory processing

Running has opposite effects in visual and auditory cortex: it enhances firing in spontaneous and stimulus evoked conditions in layers 2-4 in visual cortex (Niell and Stryker, 2010; Bennett et al., 2013; Polack et al., 2013; Erisken et al., 2014; Lee et al., 2014; Reimer et al., 2014; Vinck et al., 2015), whereas it suppresses spontaneous and evoked activity in layers 2/3 but not 4 of auditory cortex (Zhou et al., 2014; Schneider et al., 2014). It is therefore possible that these two cortical regions have different rules of engagement in different situations, which may explain why visual cortex desynchronised in all tasks whereas there was no desynchronisation in auditory cortex in the visual and auditory distractor tasks (during movement). It is interesting to note however that in Zhou et al. (2014), the mice were passively exposed

to auditory stimuli rather than engaging with them in a task, and in this state there was a decrease in low frequency power during both "active but not running" and "running" states compared to quiescent states (see their Figure 1d-f). This therefore contradicts the idea that auditory cortex desynchronises during movement only when the stimuli are relevant. In addition, Schneider (2018) has found that even prolonged training in an auditory discrimination task does not abolish the running induced decrease in auditory cortex responses. This implies that the effects I have seen in my tasks are not easily explained as training or learning effects either. Thus, either movement has very specific context and task dependent effects on auditory cortex, or alternatively running engages altogether different neural mechanisms than the steering wheel movements the mice made in my tasks. Indeed, Vanderwolf (2003) has suggested that different types of movement have distinct effects on cortical and hippocampal oscillations, and Stringer et al. (2018) found that dividing movement into several sub-dimensions substantially increased the explained variance of neural dynamics. Future work is required to disambiguate these disparate findings.

State dependent stimulus responses

Several studies have reported cortical state dependent stimulus responses in visual cortex, most of which have also reported decreased response variability and correlations during active and/or alert states (Niell and Stryker, 2010; Bennett et al., 2013; Polack et al., 2013; Erisken et al., 2014; Lee et al., 2014; Reimer et al., 2014; Vinck et al., 2015; Busse et al., 2017). Given these wide reports on cortical or behavioural state dependent stimulus responses, it was surprising that I did not find such an effect, although Beaman et al.

(2017) made the same observation. One possible explanation is that widefield imaging of calcium indicators does not provide sufficient resolution to pick up on the differences; the signal from a given pixel constitutes an averaged population signal, which is not necessarily even purely local: GCaMP is expressed throughout the entire neuron, which includes dendrites and axons, which contribute an unknown amount of fluorescence to the local population signal. It has been shown that the widefield calcium signal correlates better with activity in layer 1 than layers 2/3 (Allen et al., 2017). Given that most reports on state dependent stimulus responses were made in layer 2-4, the widefield signal may not be able to capture these if they are masked by activity in layer 1. Yet, previous studies using widefield imaging of voltage sensitive dyes have found that behavioural and brain state modulate response amplitudes as well as propagation patterns (Arieli et al., 1996; Petersen et al., 2003a,b; Ferezou et al., 2007). Future studies with better temporal and spatial resolution using 2-photon imaging or multi-electrode recordings can investigate this further.

5.2.2 Attention and cortical states

Spatial attention

The result that desynchronisation is neither localised nor associated with more accurate performance during sensory discrimination seems to disagree with previous work in primate visual cortex, which revealed a reduction in correlated neural population activity in parts of visual cortex corresponding to attended locations (Beaman et al., 2017; Cohen and Maunsell, 2009; Engel et al., 2016; Fries et al., 2001; Mitchell et al., 2009). One possible explanation

is that the discrepancy is due to species specific differences in local circuit mechanisms, facilitating the occurrence of a local desynchronised state in macaques over mice. Another possibility is that spatial attention requires a distinct strategy which invokes bigger differences in cortical state than attending one sensory modality versus another. The engagement related effects observed here may also be more related to arousal, which may activate more global state mechanisms, than attention, which may still produce more local effects. However, it is worth bearing in mind that the different studies also employed different methods for investigating and defining cortical synchronisation.

Engel et al. (2016) performed recordings using electrodes that were inserted perpendicular to V4 cortical layers in order to capture neurons from the same column with overlapping receptive fields. This allowed them to characterise how synchronously neurons within the same cortical column were firing during an attentional task in which a stimulus was placed in their receptive field in either covert or overt attention conditions: in covert attention conditions, the stimulus in the receptive field location was cued, and if a change occurred, the monkeys had to perform an anti-saccade to the stimulus on the opposite side. In the overt attention condition, the stimulus on the opposite side was cued and if a change occurred there, the monkeys had to perform a saccade into the receptive field.

They found that the neurons alternated between vigorous ('ON') and faint ('OFF') firing periods, which fluctuated synchronously across the cortical column. These ON and OFF dynamics could be observed during fixation, but also during the spatial attention task. By computing the power

spectrum from the LFP during ON and OFF periods, they found that ON periods had significantly less low frequency (<10Hz) power than OFF periods, therefore suggesting a more desynchronised state during ON periods and a more synchronised state during OFF periods. By further analysing how these ON and OFF dynamics related to performance in the spatial attention task, they found that the probability of detecting a change in the stimulus was significantly increased when the cortical column was in an ON period when the change occurred in the receptive field, but that there was no difference in detection probability between ON and OFF periods when the change occurred outside the receptive field. This lead the authors to suggest that attention selectively modulates cortical state in the receptive field of the attended stimulus.

There are several other interesting observations to note however. For example, there were some differences between covert and overt attention conditions: when comparing the lengths of ON and OFF periods, they found that ON periods were significantly longer during both covert and overt attention than control conditions, thus suggesting that both attentional conditions lead to increased desynchronisation. Furthermore, OFF periods were significantly longer during covert attention. This is particularly intriguing, since a stimulus change in the receptive field of the neurons would correspond to the covert attention condition. If a change is more likely to be detected during an ON period, then it is surprising that there are longer OFF periods in the covert rather than overt attention. If attention is supposed to optimise the detection probability, then there should be no difference in OFF periods, or indeed they should be shorter during covert attention. However this was not the case.

The reason I mention this distinction is that although the ON and OFF periods corresponded to the desynchronised and synchronised states, the fact that the state at or just (150ms) before change onset had an effect on detection probability suggests that a much finer temporal resolution is required to detect this effect. Prior to 150ms before change onset, there was no difference in detection probability between ON and OFF periods - and whilst it is possible to characterise ON and OFF periods by looking at the neuronal firing rates in such short time intervals, it would not be possible to determine their low frequency content (because of the Nyquist limit). Thus, I may have simply lacked the temporal resolution in my experiments to pick up on this local effect. I could of course ask whether there were any differences in firing rate between Choice and Neglect trials by comparing fluorescence values at the time of stimulus onset; interestingly however, a brief exploratory analysis indicated that this was not the case (results not shown). This may however also be due to a lack of temporal resolution because of the slower calcium dynamics of GCaMP.

Beaman et al. (2017) used yet another method to define synchronised and desynchronised states and found that local desynchronisation was associated with increased performance in a visual discrimination task. They performed recordings using electrodes in macaque V4 as well but classified cortical state by computing a population synchrony index (PSI), specified as the standard deviation divided by the mean (using 10ms bin sizes). Their monkeys performed a delayed match-to-sample task in which they had to indicate changes in orientation by holding a bar, and releasing the bar when there was no change. Note that this in essence means that monkeys had to report

the presence of a change by giving a 'no-go' response rather than a more typical 'go' type response. (In comparison, in Engel et al. the monkeys had to report a change by making an anti-saccade, and report the absence of a change by refraining from a saccade.) Using the median PSI across trials as a boundary, they classified trials with low PSI as desynchronised and with high PSI as synchronised, and found that percentage correct was significantly higher during desynchronised trials. They only looked at non-match trials in this analysis, which means that the monkeys more accurately detected changes during desynchronised trials, which agrees with Engel et al. Given their unusual response paradigm however, this also means that during synchronised states, they provided more incorrect 'go' responses than during desynchronised states. This is in direct contrast to the decreased likelihood of making choices during the synchronised state in my results (which Engel et al.'s results are compatible with in so far as the lack of saccade could be either a lack of detection or failure to provide a response). If the results by Beaman et al. indeed hold true, this may the first evidence that synchronisation indeed degrades sensory perception and leads to mistakes rather than neglect - unless holding onto the bar required so much effort that when the monkeys momentarily lost focus, they let go of the bar, rather than 'willingly' having made a 'no change' ie 'go' response. It is unfortunate that the Engel et al. study did not report ON-OFF dynamics in incorrect saccade trials (when there was a change in the receptive field but the monkeys reported it in a wrong spatial location); if desynchronisation indeed leads to mistakes rather than neglect, then there should also be more mistakes when there was an OFF period during the change in their task.

Comparisons with LFP power showed that high PSI trials were associated

with increased low frequency and decreased high frequency power, and low PSI trials showed the opposite pattern, suggesting the PSI measure provided an accurate indication of local cortical state. They further investigated how PSI related to pupil size and EEG power in three different cortical sites and found no correlations. However, close inspections of their supplementary figures suggests there seemed to be a trend in positive correlations between PSI and low frequency EEG power, which may have been too weak an effect to be picked up by statistical significance. The authors argued that the lack of correlations suggested a local desynchronisation that was independent of global cortical state, however given the trend in positive correlations between PSI and low frequency EEG power across the cortex, another possibility is that there was a global desynchronisation that was locally enhanced in V4. In addition, since the authors did not measure PSI in other cortical regions or provide comparisons of the PSI during correct trials in which the stimulus was inside versus outside the receptive field, it is difficult to assess how local the desynchronisation was.

Altogether, whilst the results in these two studies seemingly contradict the results presented here, it is likely that at least some of the differences can be explained by differences in methodology. Although the measures used in both cases correlated with low frequency power and thus agreed with the definition of synchronised and desynchronised used in this thesis, it is possible that by defining states from population firing rates, they were able to make more fine-grained distinctions in states than I could with the low frequency power measure.

Lastly, a spatial attention task has recently been developed in mice

(Wang and Krauzlis, 2018), which can be used in future studies to investigate whether the differences in result were due to differences in the task (spatial versus sensory modality attention), species (macaque versus mouse), or measure of cortical state (population firing versus low frequency power).

Cross-modal attention

As mentioned in Section 5.1.1 of the technical discussion, it is also possible that I did not observe localised differences in cortical state because my tasks did not demand specifically attending to one sensory modality whilst suppressing another. Even though I ran an auditory distractor task in which irrelevant auditory stimuli were played together with visual stimuli, the auditory stimuli did not represent conflicting information that needed to be explicitly ignored, and therefore the task most likely did not require suppression of the auditory stimuli in the way a multisensory task with incongruent trials would.

Multisensory contingencies like the ones I suggested, where mice are first trained on separate visual and auditory tasks until they achieve high performance and then moved onto a multisensory paradigm during which they have to attend one modality whilst disregarding the other, have successfully been employed before (Ahrens et al., 2015; Wimmer et al., 2015), although not to study effects on cortical states. It is widely reported that during multisensory paradigms, neural responses in sensory cortex are increased in attended compared to unattended conditions: when visual and auditory stimuli are presented together, responses in auditory cortex are bigger when the auditory stimuli are attended versus when visual stimuli are attended, and vice versa in visual cortex (Spong et al., 1965; Hackley et al., 1990; Kawashima

et al., 1995; Petkov et al., 2004; Johnson and Zatorre, 2006). Whether or not these differences in sensory responses are associated with differences in cortical state remains unexplored. Wimmer et al. (2015) showed that there was decreased inhibition, mediated by the TRN (thalamic reticular nucleus), in LGN when vision was attended and increased inhibition in LGN when audition was attended. This is likely to translate into increased and decreased thalamocortical drive to the visual cortex during attended and inattended conditions, respectively, and since thalamocortical drive is known to modulate cortical states, this could provide a possible mechanism for localised desynchronisation when attention is required, and localised synchronisation when suppression of stimuli is required. However, future experiments that monitor cortical states during an audio-visual attention-switching paradigm are required to test this hypothesis.

5.2.3 Possible role of reward

The term reward in neuroscience is almost synonymous with the term dopamine; so strong is the association of the latter with the former. The by now famous experiments by Schultz et al. (1997) showed that neurons in the midbrain respond to reward and stimuli predicting rewards, and subsequent work showed that the majority of these neurons are dopaminergic (Schultz, 2016). Dopamine is a neuromodulator and the midbrain dopaminergic neurons project to various targets across the brain (Bao et al., 2001). Although there are dopaminergic terminals in the cortex, these are restricted to frontal areas, and whilst there are dopaminergic projections to auditory cortex (Bao et al., 2001), there are none to visual cortex (Monti and Jantos, 2008). Thus, the effect I discovered that reward induced long lasting cortical desynchro-

nisation is unlikely to have been caused directly by dopamine release.

Nevertheless, several studies have shown that dopamine has an arousal-inducing effect (Ongini et al., 1985; Ongini and Longo, 1989), and there are dopaminergic projections to both cholinergic and noradrenergic centres, which in return project to sensory cortex and could thus modulate brain state (Day and Fibiger, 1993). Indeed, pharmacological studies have shown that dopamine can modulate the degree of acetylcholine induced desynchronisation (Vanderwolf, 2003), although these relied on systemic administration of dopamine agonists and antagonists and thus could not distinguish what pathway(s) may have caused the effects. Another possibility is that since there are dopaminergic projections to frontal cortex, the effect I observed may also have been caused by frontal top-down projections that were stimulated by dopamine (Monti and Jantos, 2008).

What could be a possible role of reward induced desynchronisation? One might consider that it constitutes a previously unrecognised form of reinforcement signal. For example, it has been suggested that reward modulates sensory responses and that this might be important during learning, as some studies have found changes in stimulus responses after learning (Poort et al., 2015; Shuler and Bear, 2006). What the mechanism of such modulation is however remains unknown. Since desynchronisation reduces correlated fluctuations in neuronal firing and is thereby thought to improve the signal-to-noise ratio of the neural code (Cohen and Maunsell, 2009; Mitchell et al., 2009), it is possible that this serves as a consolidation mechanism that allows the brain to associate a given stimulus with a particular action that resulted in a reward. This would also fit with the known role of dopamine in movement (Vanderwolf, 2003). However, this is entirely speculative, since I

imaged my animals when they had already learned the tasks. Future work is required to establish whether this effect is present from the start in response to rewards, or whether it emerges with learning.

5.3 Conclusion

I showed that cortical states can successfully be assessed from widefield imaging of genetically encoded calcium indicators. This opens up new possibilities for exploring how cortical states vary at a better spatial resolution than previously possible.

In addition, I showed that during sensory decision making, the biggest difference in cortical state occurred not in the cortical areas processing the relevant sensory stimuli, but in areas involved in the preparation of responses. This result emphasizes the importance of monitoring neural activity at a large spatial scale in order to understand how the brain performs a behavioural task, as this might reveal roles of brain areas previously unrecognised as contributing to a task.

In these final sections, I will provide suggestions for what my results might mean, as well as ideas for future work.

5.3.1 What does it all mean?

It is frequently assumed because attention and the desynchronised state lead to changes in firing rates, decreased response variability and decreased neuronal correlations, which in turn increase sensory response decodability, that this feature must be useful or even causally involved in guiding behaviour during active states. However if we accept the results I have presented in this thesis at face value, then this suggests that our thinking about attention and the meaning of cortical states has been misguided.

Firstly, given that I did not observe the biggest effect of brain state in

the cortex of the modality being attended, and I did not find any significant effect of brain or behavioural state on stimulus responses, this raises some interesting questions about the role of sensory processing during behaviour. These observations challenge the frequent assumption that optimal sensory processing is key to performing a task that requires processing of sensory stimuli. The sensory variability, which is often interpreted as resulting from noise, which in turn is thought to be detrimental to processing, may not be as much of an impediment to performing a task as previously thought. Instead, since the biggest effect occurred in somato-motor cortex, and state was correlated with reaction time rather than performance accuracy, this suggests that it might be more or at least equally as important to be ready to execute a motor plan to provide a response to the stimuli rather than processing the stimuli as accurately as possible. Thus, a desynchronised state may correspond to a state of motor preparation. Importantly, this does not invalidate the previous observations that a more desynchronized state decreases noise correlations, improves stimulus reliability and signal to noise ratios, which in turn improves the performance during a task. All of these observations might still point to an optimal information processing mode. However, such an optimal information processing mode might be energetically very costly, and it may therefore not be employed unless absolutely necessary - for example in a very challenging task. Instead, during less challenging conditions, the brain still solves the problem of sensory information processing via a more energetically favourable route that still provides a good enough means for performing the task at hand without exhausting resources unnecessarily.

Nonetheless, there are two additional interpretations as well. One is that

the activated, desynchronised state corresponds to a "conscious state" that is involved in monitoring and evaluating the behavioural state of the animal and the outcome of given actions and choices (Parvizi and Damasio, 2001). In this framework, cortical desynchronisation would still correspond to an attentive state, however it is dissociated from the "spot-light" type attention and does not causally contribute to the processing. Importantly, this does not suggest that the cortex is not needed, but simply that cortical state has no causal effect on performance.

A related interpretation posits that attention is an effect rather than a cause (Krauzlis et al., 2014). According to this proposal, attention is an effect of interpreting incoming sensory data in the context of internal states and other factors such as prior knowledge or expectation. This integration is thought to be centred in the basal ganglia involved in value-based decision making. According to the classical view of attention, there is competition between incoming sensory information, and attentional mechanisms select the relevant one for processing. In this alternative framework, there is competition between which state provides the best match to the incoming sensory information, internal state and prior knowledge. The dominant state then determines the decision and behavioural outcome.

The latter possibility strikes me as the most plausible for several reasons. First of all, it provides an explanation for all prior attention related results as well as the ones presented here, which according to the spot-light hypothesis are contradictory. If attention is an effect rather than a cause, then the attention related cortical state changes are simply correlational. In addition, it eliminates the need to find the source of the 'spot-light' that traditional attentional mechanisms imply. Secondly, by associating attention

with value-based decision making, it provides a link to the reward effect on cortical state I observed in my data. Lastly, it provides a circuit mechanism whose elements are evolutionarily conserved and can equally well explain attentional phenomena in species that do not possess cortices.

5.3.2 Future Directions

To test the hypothesis that desynchronisation corresponds to a state of motor preparation that is causally required, I suggest manipulating state to maintain the cortex in a synchronised state. The prediction from the hypothesis is that this would impair task performance. I suggest two different ways for achieving this.

The first possibility would be to use local application of cholinergic or noradrenergic antagonists. ACh and NA both drive cortical desynchronisation, and applying antagonists has been shown to reduce cortical desynchronisation (Vanderwolf, 2003). Thus, by applying doses that are strong enough to reduce desynchronisation but do not completely abolish cortical function to somatosensory cortex, one could assess if this manipulation increases reaction times.

The second possibility would entail optogenetic manipulation of cortical oscillations. Specifically, optogenetic pulses could be calibrated to entrain the somatosensory cortex in a synchronised state.

If maintaining somatosensory cortex in a more synchronised state increases reaction times, then this would suggest that desynchronisation is indeed causally involved in preparing fast motor responses, and if it doesn't, this suggests that the desynchronisation is correlational rather than causal.

Lastly, I propose experiments to explore the role of reward and dopamine in attention and cortical desynchronisation. If attention is a consequence of value-based decision making processes that are centred in the basal ganglia, then manipulating the reward pathways within the basal ganglia should shed further light on this.

A first step would be to optogenetically silence reward pathways during the reward period to investigate if the effect on cortical state is maintained. If it is not, then this would confirm that reward and dopamine are causally involved in driving the change in cortical state.

The next step would be to manipulate cortical state during the reward period using optogenetics to investigate the effects on behaviour. Similar to the experiment suggested in 2, optogenetic pulses could be used to entrain cortical regions of interest in a synchronised state. If reward induced desynchronisation serves as an instruction or reinforcement during learning, then abolishing it should impair learning, but not necessarily performance in a task that has already been learned. If reward induced desynchronisation serves as a signal about the motivational state of the animal, then abolishing it should increase neglect trials in a learned animal.

5.3.3 Closing Thoughts

Neuroscience as a discipline is in its infancy, and it is clear that many challenges remain. One of them may be how to reconcile psychological concepts such as attention with biological processes. Our thinking is defined by the languages we use, and whilst attention may seem like an intuitive concept, its translation into different languages attributes it different qualities, and different cultures have altogether different psychological theories (Vanderwolf,

2003; Diamond, 2012). Either the brain is malleable enough for the contextual shaping of neurobiological processes, or understanding how the brain produces complex behaviours may require an altogether novel approach that does not rely on traditional psychological concepts.

Time will tell; meanwhile it is an exciting moment to be a neuroscientist.

References

Ahrens, S., Jaramillo, S., Yu, K., Ghosh, S., Hwang, G.-R., Paik, R., Lai, C., He, M., Huang, Z. J., and Li, B. (2015). ErbB4 regulation of a thalamic reticular nucleus circuit for sensory selection. *Nat Neurosci*, 18(1):104–111.

Akerboom, J., Chen, T.-W., Wardill, T. J., Tian, L., Marvin, J. S., Mutlu, S., CalderAşn, N. C., Esposti, F., Borghuis, B. G., Sun, X. R., Gordus, A., Orger, M. B., Portugues, R., Engert, F., Macklin, J. J., Filosa, A., Aggarwal, A., Kerr, R. A., Takagi, R., Kracun, S., Shigetomi, E., Khakh, B. S., Baier, H., Lagnado, L., Wang, S. S.-H., Bargmann, C. I., Kimmel, B. E., Jayaraman, V., Svoboda, K., Kim, D. S., Schreiter, E. R., and Looger, L. L. (2012). Optimization of a GCaMP calcium indicator for neural activity imaging. *J Neurosci*, 32(40):13819–13840.

Allen, W. E., Kauvar, I. V., Chen, M. Z., Richman, E. B., Yang, S. J., Chan, K., Gradinaru, V., Deverman, B. E., Luo, L., and Deisseroth, K. (2017). Global representations of goal-directed behavior in distinct cell types of mouse neocortex. *Neuron*, 94(4):891–907.e6.

Arieli, A., Sterkin, A., Grinvald, A., and Aertsen, A. (1996). Dynamics of ongoing activity: explanation of the large variability in evoked cortical responses. *Science*, 273(5283):1868–1871.

Ayaz, Aslyand Saleem, A. B., Scholvinck, M. L., and Carandini, M. (2013). Locomotion controls spatial integration in mouse visual cortex. *Curr Biol*, 23(10):890–894.

Bao, S., Chan, V. T., and Merzenich, M. M. (2001). Cortical remodelling induced by activity of ventral tegmental dopamine neurons. *Nature*, 412(6842):79–83.

Beaman, C. B., Eagleman, S. L., and Dragoi, V. (2017). Sensory coding accuracy and perceptual performance are improved during the desynchronized cortical state. *Nat Commun*, 8(1):1308.

Bennett, C., Arroyo, S., and Hestrin, S. (2013). Subthreshold mechanisms underlying state-dependent modulation of visual responses. *Neuron*, 80(2):350–357.

Benucci, A., Frazor, R. A., and Carandini, M. (2007). Standing waves and traveling waves distinguish two circuits in visual cortex. *Neuron*, 55(1):103–117.

Berger, H. (1929). Ueber das eletroenkephalogramm des menschen. *Arch Psychiatr Nervenkr*, 87(1):527–570.

Berger, T., Borgdorff, A., Crochet, S., Neubauer, F. B., Lefort, S., Fauvet, B., Ferezou, I., Carleton, A., Luscher, H.-R., and Petersen, C. C. H. (2007). Combined voltage and calcium epifluorescence imaging in vitro and in vivo reveals subthreshold and suprathreshold dynamics of mouse barrel cortex. *J Neurophysiol*, 97(5):3751–3762.

Blake, H. (1937). Brain potentials during sleep. *Am J Physiol*, 119:692–703.

Bosman, C. A., Schoffelen, J.-M., Brunet, N., Oostenveld, R., Bastos, A. M., Womelsdorf, T., Rubehn, B., Stieglitz, T., De Weerd, P., and Fries, P. (2012). Attentional stimulus selection through selective synchronization between monkey visual areas. *Neuron*, 75(5):875–888.

Brainard, D. H. (1997). The psychophysics toolbox. *Spat Vis*, 10(4):433–436.

Burgess, C. P., Lak, A., Steinmetz, N. A., Zatka-Haas, P., Bai Reddy, C., Jacobs, E. A. K., Linden, J. F., Paton, J. J., Ranson, A., Schroder, S., Soares, S., Wells, M. J., Wool, L. E., Harris, K. D., and Carandini, M. (2017). High-yield methods for accurate two-alternative visual psychophysics in head-fixed mice. *Cell Rep*, 20(10):2513–2524.

Busse, L., Cardin, J. A., Chiappe, E. M., Halassa, M. M., McGinley, M. J., Yamashita, T., and Saleem, A. B. (2017). Sensation during active behaviors. *J Neurosci*.

Carandini, M., Shimaoka, D., Rossi, L. F., Sato, T. K., Benucci, A., and Knopfel, T. (2015). Imaging the awake visual cortex with a genetically encoded voltage indicator. *J Neurosci*, 35(1):53–63.

Carter, M. E., Yizhar, O., Chikahisa, S., Nguyen, H., Adamantidis, A., Nishino, S., Deisseroth, K., and de Lecea, L. (2010). Tuning arousal with optogenetic modulation of locus coeruleus neurons. *Nat Neurosci*, 13(12):1526–1533.

Chandler, D. J., Gao, W.-J., and Waterhouse, B. D. (2014). Heterogeneous organization of the locus coeruleus projections to prefrontal and motor cortices. *Proc Natl Acad Sci USA*, 111(18):6816–6821.

Chen, T.-W., Wardill, T. J., Sun, Y., Pulver, S. R., Renninger, S. L., Baohan, A., Schreiter, E. R., Kerr, R. A., Orger, M. B., Jayaraman, V., Looger, L. L., Svoboda, K., and Kim, D. S. (2013). Ultrasensitive fluorescent proteins for imaging neuronal activity. *Nature*, 499(7458):295–300.

Chin, D. and Means, A. R. (2000). Calmodulin: a prototypical calcium sensor. *Trends Cell Biol*, 10(8):322–328.

Cohen, M. R. and Maunsell, J. H. R. (2009). Attention improves performance primarily by reducing interneuronal correlations. *Nat Neurosci*, 12(12):1594–1600.

Crapse, T. B. and Sommer, M. A. (2008). Corollary discharge across the animal kingdom. *Nat Rev Neurosci*, 9(8):587–600.

Crochet, S. and Petersen, C. C. H. (2006). Correlating whisker behavior with membrane potential in barrel cortex of awake mice. *Nat Neurosci*, 9(5):608–610.

Crochet, S., Poulet, J. F. A., Kremer, Y., and Petersen, C. C. H. (2011). Synaptic mechanisms underlying sparse coding of active touch. *Neuron*, 69(6):1160–1175.

Davis, H., Davis, P. A., Loomis, A. L., Harvey, E. N., and Hobart, G. (1937). Changes in human brain potentials during the onset of sleep. *Science*, 86(2237):448–450.

Day, J. and Fibiger, H. C. (1993). Dopaminergic regulation of cortical acetylcholine release: effects of dopamine receptor agonists. *Neuroscience*, 54(3):643–648.

de Gee, J. W., Colizoli, O., Kloosterman, N. A., Knapen, T., Nieuwenhuis, S., and Donner, T. H. (2017). Dynamic modulation of decision biases by brainstem arousal systems. *elife*, 6.

de Gee, J. W., Knapen, T., and Donner, T. H. (2014). Decision-related pupil dilation reflects upcoming choice and individual bias. *Proc Natl Acad Sci USA*, 111(5):E618–25.

Diamond, J. (2012). *The World Until Yesterday: What Can We Learn from Traditional Societies?* Penguin Group, London, England.

Dipoppa, M., Ranson, A., Krumin, M., Pachitariu, M., Carandini, M., and Harris, K. D. (2018). Vision and locomotion shape the interactions between neuron types in mouse visual cortex. *Neuron*, 98(3):602–615.

Eggermann, E., Kremer, Y., Crochet, S., and Petersen, C. C. H. (2014). Cholinergic signals in mouse barrel cortex during active whisker sensing. *Cell Rep*, 9(5):1654–1660.

Engel, T. A., Steinmetz, N. A., Gieselmann, M. A., Thiele, A., Moore, T., and Boahen, K. (2016). Selective modulation of cortical state during spatial attention. *Science*, 354(6316):1140–1144.

Erisken, S., Vaiceliunaite, A., Jurjut, O., Fiorini, M., Katzner, S., and Busse, L. (2014). Effects of locomotion extend throughout the mouse early visual system. *Curr Biol*, 24(24):2899–2907.

Ferezou, I., Haiss, F., Gentet, L. J., Aronoff, R., Weber, B., and Petersen, C. C. H. (2007). Spatiotemporal dynamics of cortical sensorimotor integration in behaving mice. *Neuron*, 56(5):907–923.

Frankel, W. N., Taylor, L., Beyer, B., Tempel, B. L., and White, H. S. (2001). Electroconvulsive thresholds of inbred mouse strains. *Genomics*, 74(3):306–312.

Fries, P., Reynolds, J. H., Rorie, A. E., and Desimone, R. (2001). Modulation of oscillatory neuronal synchronization by selective visual attention. *Science*, 291(5508):1560–1563.

Fries, P., Schroder, J.-H., Roelfsema, P. R., Singer, W., and Engel, A. K. (2002). Oscillatory neuronal synchronization in primary visual cortex as a correlate of stimulus selection. *J Neurosci*, 22(9):3739–3754.

Goard, M. and Dan, Y. (2009). Basal forebrain activation enhances cortical coding of natural scenes. *Nat Neurosci*, 12(11):1444–1449.

Grinvald, A. and Hildesheim, R. (2004). VSDI: a new era in functional imaging of cortical dynamics. *Nat Rev Neurosci*, 5(11):874–885.

Grinvald, A., Shoham, D., Shmuel, A., Glaser, D., Vanzetta, I., Shtoyerman, E., Slovin, H., Wijnbergen, C., Hildesheim, R., and Arieli, A. (1999). In-vivo optical imaging of cortical architecture and dynamics. In Windhorst, U. and Johansson, H., editors, *Modern techniques in neuroscience research*, pages 893–969. Springer Berlin Heidelberg, Berlin, Heidelberg.

Hackley, S. A., Woldorf, M., and Hillyard, S. A. (1990). Cross-modal selective attention effects on retinal, myogenic, brainstem, and cerebral evoked potentials. *Psychophysiology*, 27(2):195–208.

Haider, B. and McCormick, D. A. (2009). Rapid neocortical dynamics: cellular and network mechanisms. *Neuron*, 62(2):171–189.

Hallanger, A., Levey, A., Lee, H., and Rye, D. (1987). The origins of cholinergic and other subcortical afferents to the thalamus in the rat. *J Comp Neurol*, 262:105–124.

Han, H. J., Allen, C. C., Buchovecky, C. M., Yetman, M. J., Born, H. A., Marin, M. A., Rodgers, S. P., Song, B. J., Lu, H.-C., Justice, M. J., Probst, F. J., and Jankowsky, J. L. (2012). Strain background influences neurotoxicity and behavioral abnormalities in mice expressing the tetracycline transactivator. *J Neurosci*, 32(31):10574–10586.

Harris, C. D. (2005). Neurophysiology of sleep and wakefulness. *Respir Care Clin N Am*, 11(4):567–586.

Harris, K. D. and Thiele, A. (2011). Cortical state and attention. *Nat Rev Neurosci*, 12(9):509–523.

Hirata, A. and Castro-Alamancos, M. A. (2010). Neocortex network activation and deactivation states controlled by the thalamus. *J Neurophysiol*, 103(3):1147–1157.

Huang, Z. J. and Zeng, H. (2013). Genetic approaches to neural circuits in the mouse. *Annu Rev Neurosci*, 36:183–215.

Ison, J. R., Allen, P. D., and O'Neill, W. E. (2007). Age-related hearing loss in C57BL/6J mice has both frequency-specific and non-frequency-specific components that produce a hyperacusis-like exaggeration of the acoustic startle reflex. *J Assoc Res Otolaryngol*, 8(4):539–550.

Issa, J. B., Haeffele, B. D., Agarwal, A., Bergles, D. E., Young, E. D., and Yue, D. T. (2014). Multiscale optical ca2+ imaging of tonal organization in mouse auditory cortex. *Neuron*, 83(4):944–959.

Johnson, J. A. and Zatorre, R. J. (2006). Neural substrates for dividing and focusing attention between simultaneous auditory and visual events. *Neuroimage*, 31(4):1673–1681.

Kahneman, D. and Beatty, J. (1966). Pupil diameter and load on memory. *Science*, 154(3756):1583–1585.

Kawashima, R., Osullivan, B., and Rol, P. (1995). Positron-emission tomography studies of cross-modality inhibition. *Proc Natl Acad Sci USA*, 92:5969–5972.

Keller, G. B., Bonhoeffer, T., and Hobener, M. (2012). Sensorimotor mismatch signals in primary visual cortex of the behaving mouse. *Neuron*, 74(5):809–815.

Kleiner, M., Brainard, D., Pelli, D., Ingling, A., Murray, R., and Broussard, C. (2007). What's new in psychtoolbox-3. *Perception*.

Krauzlis, R. J., Bollimunta, A., Arcizet, F., and Wang, L. (2014). Attention as an effect not a cause. *Trends Cogn Sci (Regul Ed)*, 18(9):457–464.

Kurt, S. and Ehret, G. (2010). Auditory discrimination learning and knowledge transfer in mice depends on task difficulty. *Proc Natl Acad Sci USA*, 107(18):8481–8485.

Lakatos, P., Barczak, A., Neymotin, S. A., McGinnis, T., Ross, D., Javitt, D. C., and O'Connell, M. N. (2016). Global dynamics of selective attention and its lapses in primary auditory cortex. *Nat Neurosci*, 19(12):1707–1717.

Lakatos, P., Karmos, G., Mehta, A. D., Ulbert, I., and Schroeder, C. E. (2008). Entrainment of neuronal oscillations as a mechanism of attentional selection. *Science*, 320(5872):110–113.

Lakatos, P., Musacchia, G., O'Connel, M. N., Falchier, A. Y., Javitt, D. C., and Schroeder, C. E. (2013). The spectrotemporal filter mechanism of auditory selective attention. *Neuron*, 77(4):750–761.

Lakatos, P., O'Connell, M. N., Barczak, A., Mills, A., Javitt, D. C., and Schroeder, C. E. (2009). The leading sense: supramodal control of neurophysiological context by attention. *Neuron*, 64(3):419–430.

Lee, A. M., Hoy, J. L., Bonci, A., Wilbrecht, L., Stryker, M. P., and Niell, C. M. (2014). Identification of a brainstem circuit regulating visual cortical state in parallel with locomotion. *Neuron*, 83(2):455–466.

Lee, S., Carvell, G. E., and Simons, D. J. (2008). Motor modulation of afferent somatosensory circuits. *Nat Neurosci*, 11(12):1430–1438.

Ma, Y., Shaik, M. A., Kim, S. H., Kozberg, M. G., Thibodeaux, D. N., Zhao, H. T., Yu, H., and Hillman, E. M. C. (2016). Wide-field optical mapping of neural activity and brain haemodynamics: considerations and novel approaches. *Philos Trans R Soc Lond, B, Biol Sci*, 371(1705).

Madisen, L., Garner, A. R., Shimaoka, D., Chuong, A. S., Klapoetke, N. C., Li, L., van der Bourg, A., Niino, Y., Egolf, L., Monetti, C., Gu, H., Mills, M., Cheng, A., Tasic, B., Nguyen, T. N., Sunkin, S. M., Benucci, A., Nagy, A., Miyawaki, A., Helmchen, F., Empson, R. M., Knopfel, T., Boyden, E. S., Reid, R. C., Carandini, M., and Zeng, H. (2015). Transgenic mice for intersectional targeting of neural sensors and effectors with high specificity and performance. *Neuron*, 85(5):942–958.

Madisen, L., Zwingman, T. A., Sunkin, S. M., Oh, S. W., Zariwala, H. A., Gu, H., Ng, L. L., Palmiter, R. D., Hawrylycz, M. J., Jones, A. R., Lein, E. S., and Zeng, H. (2010). A robust and high-throughput cre reporting

and characterization system for the whole mouse brain. *Nat Neurosci*, 13(1):133–140.

Makino, H., Ren, C., Liu, H., Kim, A. N., Kondapaneni, N., Liu, X., Kuzum, D., and Komiyama, T. (2017). Transformation of cortex-wide emergent properties during motor learning. *Neuron*, 94(4):880–890.e8.

McAdams, C. J. and Maunsell, J. H. (1999). Effects of attention on the reliability of individual neurons in monkey visual cortex. *Neuron*, 23(4):765–773.

McAdams, C. J. and Maunsell, J. H. (2000). Attention to both space and feature modulates neuronal responses in macaque area v4. *J Neurophysiol*, 83(3):1751–1755.

McCormick, D. A. and Bal, T. (1997). Sleep and arousal: thalamocortical mechanisms. *Annu Rev Neurosci*, 20:185–215.

McGinley, M. J., Vinck, M., Reimer, J., Batista-Brito, R., Zagha, E., Cadwell, C. R., Tolias, A. S., Cardin, J. A., and McCormick, D. A. (2015). Waking state: rapid variations modulate neural and behavioral responses. *Neuron*, 87(6):1143–1161.

Mitchell, J. F., Sundberg, K. A., and Reynolds, J. H. (2009). Spatial attention decorrelates intrinsic activity fluctuations in macaque area v4. *Neuron*, 63(6):879–888.

Mohajerani, M. H., Chan, A. W., Mohsenvand, M., LeDue, J., Liu, R., McVea, D. A., Boyd, J. D., Wang, Y. T., Reimers, M., and Murphy, T. H. (2013). Spontaneous cortical activity alternates between motifs defined by regional axonal projections. *Nat Neurosci*, 16(10):1426–1435.

Mohajerani, M. H., McVea, D. A., Fingas, M., and Murphy, T. H. (2010). Mirrored bilateral slow-wave cortical activity within local circuits revealed by fast bihemispheric voltage-sensitive dye imaging in anesthetized and awake mice. *J Neurosci*, 30(10):3745–3751.

Monti, J. and Jantos, H. (2008). The roles of dopamine and serotonin, and of their receptors, in regulating sleep and waking. In *Serotonin dopamine*

interaction: experimental evidence and therapeutic relevance, pages 625–646. Elsevier.

Moran, J. (1985). Selective attention gates visual processing in extrastriate cortex. *Science*, 229:782–784.

Moruzzi, G. and Magoun, H. W. (1949). Brain stem reticular formation and activation of the EEG. *Electroencephalogr Clin Neurophysiol*, 1(4):455–473.

Murphy, T. H., Boyd, J. D., Bolanos, F., Vanni, M. P., Silasi, G., Haupt, D., and LeDue, J. M. (2016). High-throughput automated home-cage mesoscopic functional imaging of mouse cortex. *Nat Commun*, 7:11611.

Musall, S., Kaufman, M. T., Gluf, S., and Churchland, A. (2018). Movement-related activity dominates cortex during sensory-guided decision making. *BioRxiv*.

Nakai, J., Ohkura, M., and Imoto, K. (2001). A high signal-to-noise ca(2+) probe composed of a single green fluorescent protein. *Nat Biotechnol*, 19(2):137–141.

Niell, C. M. and Stryker, M. P. (2010). Modulation of visual responses by behavioral state in mouse visual cortex. *Neuron*, 65(4):472–479.

O'Connell, M. N., Barczak, A., Ross, D., McGinnis, T., Schroeder, C. E., and Lakatos, P. (2015). Multi-scale entrainment of coupled neuronal oscillations in primary auditory cortex. *Front Hum Neurosci*, 9:655.

O'Connell, M. N., Barczak, A., Schroeder, C. E., and Lakatos, P. (2014). Layer specific sharpening of frequency tuning by selective attention in primary auditory cortex. *J Neurosci*, 34(49):16496–16508.

Ongini, E., Caporali, M. G., and Massotti, M. (1985). Stimulation of dopamine d-1 receptors by SKF 38393 induces EEG desynchronization and behavioral arousal. *Life Sci*, 37(24):2327–2333.

Ongini, E. and Longo, V. G. (1989). Dopamine receptor subtypes and arousal. volume 31 of *International review of neurobiology*, pages 239–255. Elsevier.

Pare, D., Smith, Y., Parent, A., and Steriade, M. (1988). Projections of brainstem core cholinergic and non-cholinergic neurons of cat to intralaminar and reticular thalamic nuclei. *Neuroscience*, 25(1):69–86.

Parent, A., Pare, D., Smith, Y., and Steriade, M. (1988). Basal forebrain cholinergic and noncholinergic projections to the thalamus and brainstem in cats and monkeys. *J Comp Neurol*, 277(2):281–301.

Parvizi, J. and Damasio, A. (2001). Consciousness and the brainstem. *Cognition*, 79(1-2):135–160.

Pelli, D. G. (1997). The video toolbox software for visual psychophysics: transforming numbers into movies. *Spat Vis*, 10(4):437–442.

Petersen, C. C. H., Grinvald, A., and Sakmann, B. (2003a). Spatiotemporal dynamics of sensory responses in layer 2/3 of rat barrel cortex measured in vivo by voltage-sensitive dye imaging combined with whole-cell voltage recordings and neuron reconstructions. *J Neurosci*, 23(4):1298–1309.

Petersen, C. C. H., Hahn, T. T. G., Mehta, M., Grinvald, A., and Sakmann, B. (2003b). Interaction of sensory responses with spontaneous depolarization in layer 2/3 barrel cortex. *Proc Natl Acad Sci USA*, 100(23):13638–13643.

Petkov, C. I., Kang, X., Alho, K., Bertrand, O., Yund, E. W., and Woods, D. L. (2004). Attentional modulation of human auditory cortex. *Nat Neurosci*, 7(6):658–663.

Pinto, D., Tank, D., Brody, C., and Thiberge, S. (2018). Widespread cortical involvement in evidence-based navigation. Short Talk, Cosyne, Denver, CO.

Pinto, L., Goard, M. J., Estandian, D., Xu, M., Kwan, A. C., Lee, S.-H., Harrison, T. C., Feng, G., and Dan, Y. (2013). Fast modulation of visual perception by basal forebrain cholinergic neurons. *Nat Neurosci*, 16(12):1857–1863.

Pisauro, M. A., Dhruv, N. T., Carandini, M., and Benucci, A. (2013). Fast hemodynamic responses in the visual cortex of the awake mouse. *J Neurosci*, 33(46):18343–18351.

Polack, P.-O., Friedman, J., and Golshani, P. (2013). Cellular mechanisms of brain state-dependent gain modulation in visual cortex. *Nat Neurosci*, 16(9):1331–1339.

Poort, J., Khan, A. G., Pachitariu, M., Nemri, A., Orsolic, I., Krupic, J., Bauza, M., Sahani, M., Keller, G. B., Mrsic-Flogel, T. D., and Hofer, S. B. (2015). Learning enhances sensory and multiple non-sensory representations in primary visual cortex. *Neuron*, 86(6):1478–1490.

Poulet, J. F. A., Fernandez, L. M. J., Crochet, S., and Petersen, C. C. H. (2012). Thalamic control of cortical states. *Nat Neurosci*, 15(3):370–372.

Poulet, J. F. A. and Petersen, C. C. H. (2008). Internal brain state regulates membrane potential synchrony in barrel cortex of behaving mice. *Nature*, 454(7206):881–885.

Reimer, J., Froudarakis, E., Cadwell, C. R., Yatsenko, D., Denfield, G. H., and Tolias, A. S. (2014). Pupil fluctuations track fast switching of cortical states during quiet wakefulness. *Neuron*, 84(2):355–362.

Reimer, J., McGinley, M. J., Liu, Y., Rodenkirch, C., Wang, Q., McCormick, D. A., and Tolias, A. S. (2016). Pupil fluctuations track rapid changes in adrenergic and cholinergic activity in cortex. *Nat Commun*, 7:13289.

Rodin, E., Constantino, T., Rampp, S., and Wong, P. K. (2009). Spikes and epilepsy. *Clin EEG Neurosci*, 40(4):288–299.

Rossi, L. F., Wykes, R. C., Kullmann, D. M., and Carandini, M. (2017). Focal cortical seizures start as standing waves and propagate respecting homotopic connectivity. *Nat Commun*, 8(1):217.

Rougeul-Buser, A., Bouyer, J. J., and Buser, P. (1975). From attentiveness to sleep. a topographical analysis of localized "synchronized" activities on the cortex of normal cat and monkey. *Acta Neurobiol Exp (Wars)*, 35(5-6):805–819.

Sachidhanandam, S., Sreenivasan, V., Kyriakatos, A., Kremer, Y., and Petersen, C. C. H. (2013). Membrane potential correlates of sensory perception in mouse barrel cortex. *Nat Neurosci*, 16(11):1671–1677.

Schmidt-Supprian, M. and Rajewsky, K. (2007). Vagaries of conditional gene targeting. *Nat Immunol*, 8(7):665–668.

Schneider, D. (2018). A sensory motor interface for learning and predicting self-generated sounds. Workshop Talk, Cosyne, Denver, CO.

Schneider, D. M., Nelson, A., and Mooney, R. (2014). A synaptic and circuit basis for corollary discharge in the auditory cortex. *Nature*, 513(7517):189–194.

Scholvinck, M. L., Saleem, A. B., Benucci, A., Harris, K. D., and Carandini, M. (2015). Cortical state determines global variability and correlations in visual cortex. *J Neurosci*, 35(1):170–178.

Schroeder, C. E. and Lakatos, P. (2009). Low-frequency neuronal oscillations as instruments of sensory selection. *Trends Neurosci*, 32(1):9–18.

Schultz, W. (2016). Reward functions of the basal ganglia. *J Neural Transm*, 123(7):679–693.

Schultz, W., Dayan, P., and Montague, P. (1997). A neural substrate of prediction and reward. *Science*, 275(5306):1593–1599.

Shen, J.-x. and Yakel, J. L. (2009). Nicotinic acetylcholine receptor-mediated calcium signaling in the nervous system. *Acta Pharmacol Sin*, 30(6):673–680.

Sherman, S. M. and Guillery, R. W. (1996). Functional organization of thalamocortical relays. *J Neurophysiol*, 76(3):1367–1395.

Shimaoka, D., Harris, K. D., and Carandini, M. (2018). Effects of arousal on mouse sensory cortex depend on modality. *Cell Rep*, 22(12):3160–3167.

Shoham, D., Glaser, D. E., Arieli, A., Kenet, T., Wijnbergen, C., Toledo, Y., Hildesheim, R., and Grinvald, A. (1999). Imaging cortical dynamics at high spatial and temporal resolution with novel blue voltage-sensitive dyes. *Neuron*, 24(4):791–802.

Shuler, M. G. and Bear, M. F. (2006). Reward timing in the primary visual cortex. *Science*, 311(5767):1606–1609.

Silasi, G., Xiao, D., Vanni, M. P., Chen, A. C. N., and Murphy, T. H. (2016). Intact skull chronic windows for mesoscopic wide-field imaging in awake mice. *J Neurosci Methods*, 267:141–149.

Smiley, J. F., Subramanian, M., and Mesulam, M. M. (1999). Monoaminergic-cholinergic interactions in the primate basal forebrain. *Neuroscience*, 93(3):817–829.

Spitzer, H., Desimone, R., and Moran, J. (1988). Increased attention enhances both behavioral and neuronal performance. *Science*, 240(4850):338–340.

Spong, P., Haider, M., and Lindsley, D. B. (1965). Selective attentiveness and cortical evoked responses to visual and auditory stimuli. *Science*, 148(3668):395–397.

Sreenivasan, V., Esmaeili, V., Kiritani, T., Galan, K., Crochet, S., and Petersen, C. C. H. (2016). Movement initiation signals in mouse whisker motor cortex. *Neuron*, 92(6):1368–1382.

Starzl, T. E., Taylor, C. W., and Magoun, H. W. (1951). Ascending conduction in reticular activating system, with special reference to the diencephalon. *J Neurophysiol*, 14(6):461–477.

Steinmetz, N. A., Buetfering, C., Lecoq, J., Lee, C. R., Peters, A. J., Jacobs, E. A. K., Coen, P., Ollerenshaw, D. R., Valley, M. T., de Vries, S. E. J., Garrett, M., Zhuang, J., Groblewski, P. A., Manavi, S., Miles, J., White, C., Lee, E., Griffin, F., Larkin, J. D., Roll, K., Cross, S., Nguyen, T. V., Larsen, R., Pendergraft, J., Daigle, T., Tasic, B., Thompson, C. L., Waters, J., Olsen, S., Margolis, D. J., Zeng, H., Hausser, M., Carandini, M., and Harris, K. D. (2017). Aberrant cortical activity in multiple GCaMP6-expressing transgenic mouse lines. *Eneuro*, 4(5).

Steriade, M. (2000). Corticothalamic resonance, states of vigilance and mentation. *Neuroscience*, 101(2):243–276.

Steriade, M. (2003). The corticothalamic system in sleep. *Front Biosci*, 8:d878–99.

Steriade, M., McCormick, D. A., and Sejnowski, T. J. (1993). Thalamocortical oscillations in the sleeping and aroused brain. *Science*, 262(5134):679–685.

Steriade, M. and Timofeev, I. (2003). Neuronal plasticity in thalamocortical networks during sleep and waking oscillations. *Neuron*, 37(4):563–576.

Stringer, C., Pachitariu, M., Steinmetz, N., Bai Reddy, C., Carandini, M., and Harris, K. D. (2018). Spontaneous behaviors drive multidimensional, brain-wide population activity. *BioRxiv*.

Taub, A. H., Lampl, I., and Okun, M. (2013). Local field potential, relationship to membrane synaptic potentials. In Jaeger, D. and Jung, R., editors, *Encyclopedia of Computational Neuroscience*, pages 1–8. Springer New York, New York, NY.

Vanderwolf, C. H. (2003). *An odyssey through the brain, behavior and the mind*. Springer US, Boston, MA.

Vanni, M. P. and Murphy, T. H. (2014). Mesoscale transcranial spontaneous activity mapping in GCaMP3 transgenic mice reveals extensive reciprocal connections between areas of somatomotor cortex. *J Neurosci*, 34(48):15931–15946.

Vinck, M., Batista-Brito, R., Knoblich, U., and Cardin, J. A. (2015). Arousal and locomotion make distinct contributions to cortical activity patterns and visual encoding. *Neuron*, 86(3):740–754.

Vyazovskiy, V. V., Olcese, U., Hanlon, E. C., Nir, Y., Cirelli, C., and Tononi, G. (2011). Local sleep in awake rats. *Nature*, 472(7344):443–447.

Wang, L. and Krauzlis, R. J. (2018). Visual selective attention in mice. *Curr Biol*, 28(5):676–685.e4.

Wekselblatt, J. B., Flister, E. D., Piscopo, D. M., and Niell, C. M. (2016). Large-scale imaging of cortical dynamics during sensory perception and behavior. *J Neurophysiol*, 115(6):2852–2866.

Wimmer, R. D., Schmitt, L. I., Davidson, T. J., Nakajima, M., Deisseroth, K., and Halassa, M. M. (2015). Thalamic control of sensory selection in divided attention. *Nature*, 526(7575):705–709.

Xiao, D., Vanni, M. P., Mitelut, C. C., Chan, A. W., LeDue, J. M., Xie, Y., Chen, A. C., Swindale, N. V., and Murphy, T. H. (2017). Mapping cortical mesoscopic networks of single spiking cortical or sub-cortical neurons. *elife*, 6.

Zaborszky, L., Csordas, A., Mosca, K., Kim, J., Gielow, M. R., Vadasz, C., and Nadasdy, Z. (2015). Neurons in the basal forebrain project to the cortex in a complex topographic organization that reflects corticocortical connectivity patterns: an experimental study based on retrograde tracing and 3D reconstruction. *Cereb Cortex*, 25(1):118–137.

Zagha, E., Casale, A. E., Sachdev, R. N. S., McGinley, M. J., and McCormick, D. A. (2013). Motor cortex feedback influences sensory processing by modulating network state. *Neuron*, 79(3):567–578.

Zagha, E. and McCormick, D. A. (2014). Neural control of brain state. *Curr Opin Neurobiol*, 29:178–186.

Zerlaut, Y., Zucca, S., Panzeri, S., and Fellinn, T. (2018). The spectrum of asynchronous dynamics in spiking networks: A theory for the diversity of non-rhythmic waking neocortical states. Poster presentation, Cosyne, Denver, CO.

Zheng, Q. Y., Johnson, K. R., and Erway, L. C. (1999). Assessment of hearing in 80 inbred strains of mice by ABR threshold analyses. *Hear Res*, 130(1-2):94–107.

Zhou, M., Liang, F., Xiong, X. R., Li, L., Li, H., Xiao, Z., Tao, H. W., and Zhang, L. I. (2014). Scaling down of balanced excitation and inhibition by active behavioral states in auditory cortex. *Nat Neurosci*, 17(6):841–850.

Appendix A

Methods

Sound Calibration

Sound calibrations were performed using a GRAS 40BF (1/4" free field) microphone placed at the position of the animal's head in the training and imaging rigs, connected to a 26AC 1/4" preamplifier with lemo 1B7 pin and amplifier, which was connected to a NI-DAQ board (National Instruments). Acquisition was performed using Matlab's Data Acquisition Toolbox for NI-DAQ devices. Pure tones ranging from 4-32kHz in 100Hz steps were randomly played using PsychToolBox (Brainard, 1997; Pelli, 1997; Kleiner et al., 2007).

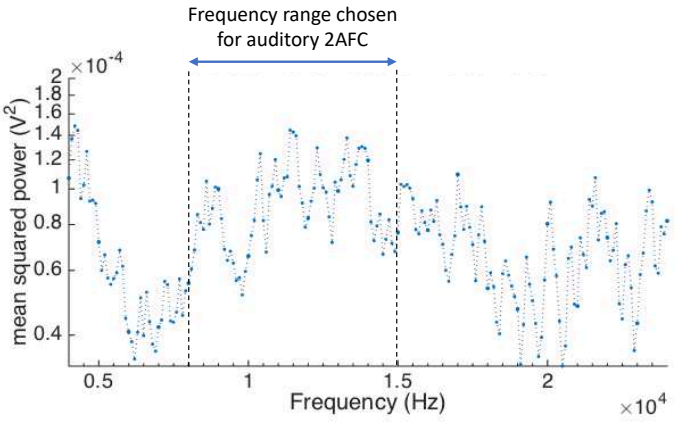

Figure A.1: Example sound calibration from the imaging rig.

SVD patial smoothing illustration

Relating to Section 2.5.2.

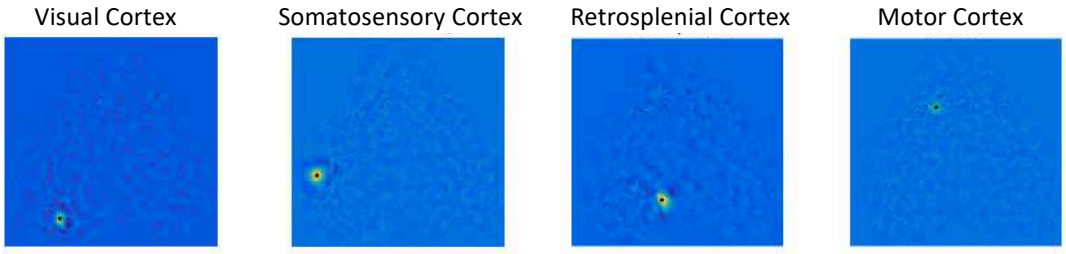

Figure A.2: Illustration of spatial smoothing resulting from the SVD dimensionality reduction.
The black dot denotes the pixel within each cortical region that was selected as the ROI. The maps represent the main spatial variability correlating with the selected pixel, which mostly comes from the pixels immediately surrounding the ROI pixel.

Appendix B

Main Results

Power difference computation using dff

Relating to Figure 4.13 in Section *Cortical state fluctuations are mostly global*.

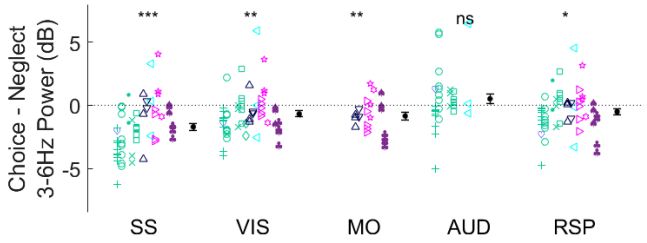

Figure B.1: Summary 3-6Hz power differences between choice and neglect trials in the visual task.

Signal amplitude does not have a multiplicative effect

Relating to Sections 4.1.2, 4.1.3 and 5.1.

If the effect of biggest difference in 3-6Hz power in somatosensory cortex was caused by increased signal amplitude in that cortical region, then the fluorescence would have to have a multiplicative rather than an additive effect on power. If the effect was additive, then even if there was more fluorescence in SS than in the other ROIs, this effect would be cancelled out during the power ratio computation. If the fluorescence has a multiplicative effect on power, than this effect should manifest across frequency bands and should not be specific to the frequency band I looked at.

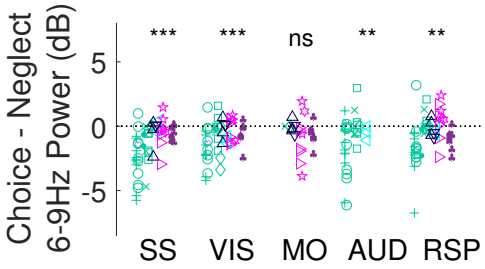

Figure B.2: Summary 6-9Hz power differences between choice and neglect trials in the visual task during the quiescent period.

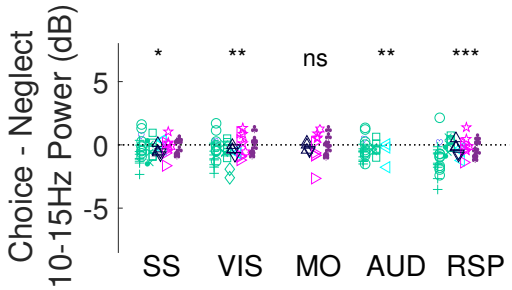

Figure B.3: Summary 10-15Hz power differences between choice and neglect trials in the visual task during the quiescent periods.

In contrast to the 3-6Hz frequency band, there were no significant differences between the ROIs in the 6-9Hz and 10-15Hz frequency bands (one-way ANOVA, p=0.14 & p=0.37, respectively; Figures B.2 and B.3). This suggests that there was no multiplicative effect of signal amplitude on power. Therefore, the effect in somatosensory cortex in the 3-6Hz band was unlikely to be caused by a difference in signal amplitude.